WATER AND ENERGY FLUXES FROM A PERMAFROST PEAT PLATEAU: EXAMINING THE CONTROLS ON RUNOFF GENERATION

by

Nicole Wright
B.Sc. with Honours, State University of New York at Buffalo, 2001
M.Sc. with Distinction, Bournemouth University, 2003

THESIS SUBMITTED IN PARTIAL FULFILLMENT OF
THE REQUIREMENTS FOR THE DEGREE OF

DOCTOR OF PHILOSOPHY

In the
Department of Geography

SIMON FRASER UNIVERSITY

Summer 2009

Approval

Name: **Nicole Wright**

Degree: **Doctor of Philosophy**

Title of Thesis: **Water and energy fluxes from a permafrost peat plateau: examining the controls on runoff generation**

Examining Committee:

Chair: **Ilja Tromp-van Meerveld**, Assistant Professor

Dr. William L. Quinton, Associate Professor
Senior Supervisor
Cold Regions Research Centre, Wilfrid Laurier University

Dr. Masaki Hayashi, Associate Professor
Supervisor
Department of Geoscience, University of Calgary

Dr. Lance F.W. Lesack, Associate Professor
Committee member
Departments of Geography and Biological Sciences, SFU

Dr. Garth van der Kamp, Research Scientist
Committee member
National Hydrology Research Centre

Paul H. Whitfield, M.Sc., Hydrologist and Adjunct Professor
Internal Examiner
Environment Canada, and Earth Sciences Department, SFU

Dr. Chris Spence, Research Scientist and Adjunct Professor
External Examiner
National Hydrology Research Centre, and Department of Geography, University of Saskatchewan

Date Defended/Approved: April 23, 2009

Declaration of
Partial Copyright Licence

Abstract

Water and energy fluxes from a treed peat plateau in a wetland-dominated discontinuous permafrost basin near Fort Simpson, NWT, Canada, were examined to determine the factors controlling runoff generation from peat-covered permafrost slopes. A water balance approach and the Dupuit-Forchheimer equation were used to quantify subsurface runoff from the peat plateau during spring. These two computations yielded similar results in both years of study (2004-2005), and showed that runoff accounted for approximately half of the moisture loss from the peat plateau, most of which occurred in response to snowmelt inputs. The melt of ground ice was also a significant source of water, which was largely detained in soil storage. The timing and magnitude of runoff was found to be dependant on the amount of water input, antecedent moisture conditions, the saturated hydraulic conductivity of the soil, and frost-table depth.

The distribution of frost-table depths on the peat plateau was examined over four consecutive years (2003-2006) at a variety of spatial scales, to elucidate the role of active-layer development on runoff generation. Frost-table depths were highly variable over relatively short distances (0.25 - 1 m), and the spatial variability was strongly correlated to soil moisture distribution, which was partly influenced by lateral flow converging to frost-table depressions. On an inter-annual basis, thaw rates were temporally correlated to air temperature and the amount of precipitation input. Simple simulations show that lateral subsurface flow is governed by the frost-table topography

having spatially variable storage that has to be filled before water can spill over to generate flow downslope.

The annual surface energy balance and thermal regimes of the peat plateau and an adjacent permafrost-free wetland were compared to identify the site characteristics that control ground surface energy input rates. The plateau tree canopy reduced the amount of energy available for ground thaw by 14% in summer, when compared to the tree-less wetland. The ground heat flux (*Qg*) was 54% greater than at the bog, largely because the plateau had a much steeper soil temperature gradient than the bog, and the bog released a large fraction of *Q** as latent heat of evaporation (*Qe*).

Keywords: hillslope hydrology, subsurface runoff, water balance, frost table, ground heat flux, surface energy balance, radiation budget, permafrost, organic soils

This research is dedicated to my soul mate, Jim

"*A soul mate is someone who has locks that fit our keys, and keys to fit our locks. When we feel safe enough to open the locks, our truest selves step out and we can be completely and honestly who we are; we can be loved for who we are….. Each unveils the best part of the other. No matter what else goes wrong around us, with that one person we're safe in our own paradise. Our soul mate is someone who shares our deepest longings, our sense of direction…. Our soul mate is the one who makes life come to life.*"

~ Richard Bach

Acknowledgements

I wish to express my deepest gratitude to my senior supervisor, and friend, Dr. Bill Quinton for his encouragement and guidance throughout my studies, his unwavering faith in my abilities, for the long hours and patience spent helping me prepare for my comprehensive exam and editing my papers, for his advice in the field, financial support, and for giving me the opportunity to work in Canada's northern peatlands. I am also indebted to Dr. Masaki Hayashi for his guidance, intellectual support and friendship. I appreciate his vast knowledge and expertise, his attention to detail and ability to focus my ideas and papers, and for his patience and time in teaching and helping me to become a better scientist.

I would also like to thank my other committee members: Dr. Garth van der Kamp for his interest and encouragement in my research, our yearly inspirational conversations at CGU, and helping me to keep everything in perspective; Dr. Lance Lesack for taking the time to be on the committee, for allowing me to use his lab to process water samples, and for helping me to organize the thesis defence; and the late Dr. Bill Bailey for his exceptional teachings and guidance at the start of my Ph.D. programme. I am thankful to Dr. Chris Spence and Mr. Paul Whitfield for taking time out from their busy schedules to serve as my external and internal readers, and for their insightful comments at my thesis defence. I would also like to thank Dr. Ilja Tromp-van Meerveld for her interest in my research and taking the time to chair my defence.

A special thank you goes to Gerry Wright and Roger Pilling of Water Survey of Canada, and Al Pietroniro of Environment Canada for logistical support and data collection, but also for their enjoyable conversations on Fort Simpson and life in general. My first and most memorable trip to Fort Simpson was a road trip from Saskatoon with Cuyler Onclin and Jessica L'Heureux of Environment Canada. I wish to thank them both for an incredibly fun experience, for their advice in the field, and for introducing me to Timbits. I would also like to thank Dr. Steven Robinson, and the many other

hydrologists/climatologists that have taken an interest in my work, inspired, and influenced me over the last few years.

The generous field assistance, fabulous cooking, and companionship of Michael Toews, Gregory Langston, Zayed Mohammed, Jaclyn Schmidt and Kimberley Blais were greatly appreciated. I also thank Pete Whittington and Trevor Meyers for an enjoyable trip up north. My gratitude goes to Jolie Gareis, Craig Emmerton and Jim Roy for their assistance in processing water samples. I thank Jaime Hogan and Jaclyn Schmidt for their friendships. To my colleagues past and present in the Geography Department at SFU, thanks for the memories (Jolie Garcies, James Morely, Neil Goeller, Taskin Shirazi, Kimberly Blais, Craig Emmerton and Cathy Febria …to name a few). Thanks to Marcia Crease, Hilary Jones, B-Jae Kelly, Marion Walter and the rest of the Geography Department staff.

This thesis is dedicated to my husband and best friend, Jim whose unconditional love, encouragement, patience, advice, and humour makes me the luckiest woman, and every day better than the last. I thank Jim's parents, Dave and Jean, for their love, support and encouragement. I also thank my parents for believing that I could do anything I put my heart and mind to. A special thank you goes to our soon-to-be-born son, Jack, for if it were not for him I would still be working on the thesis – thanks for giving me the kicks I needed to finish!

In conclusion, I recognize that this research would not have been possible without the financial assistance provided by the Canadian Foundation for Climate and Atmospheric Sciences (IP3 Research Network), the Natural Sciences and Engineering Research Council, Environment Canada Science Horizons Program, and the Northern Scientific Training Program, and the International Polar Year.

Table of Contents

List of Figures

List of Tables

Chapter 1
General Introduction

1.1 Background

Canadian wetlands are categorized as bogs, fens, swamps, marshes and shallow open water, and comprise 14% of Canada's land area (NWWG, 1988). Peatlands represent over 90% of Canadian wetlands (Tarnocai, 1998), most of which (97% by area) occur in the boreal (64%) and subarctic (33%) wetland regions (Tarnocai, 2006), where climate and land morphology are conducive to water-logged soils and low plant decomposition rates that result in the accumulation of organic matter (i.e. peat) over time (Zoltai *et al*., 1988). Approximately 30% of the peatland area in northern boreal Canada is underlain by permafrost (Zoltai, 1972; Seppälä, 1988; Aylsworth *et al*., 1993). Peat soils promote the aggradation and maintenance of permafrost due to their strong control on the surface energy balance (McFadden *et al*., 1998; Beilman, 2001), so that where permafrost is discontinuous in spatial extent, it is almost always restricted to ombrotrophic peatlands (Brown, 1968; Zoltai *et al.*, 1988). Discontinuous permafrost in the peatlands of northern boreal Canada commonly takes the form of treed peat plateaus, which are elevated up to 2 m above the surrounding landscape, and can be expansive in spatial extent, covering up to several square kilometres (Zoltai, 1972).

Runoff generation in northern boreal basins is strongly influenced by the presence or absence of peatlands and permafrost. Organic soils can provide significant water storage (Boelter, 1966), which attenuates stream-flow response to rainfall and snowmelt

runoff. However, the magnitude of the runoff response from peatland-dominated basins increases as the storage capacity in the soil and in lakes and wetlands decreases (Branfireun and Roulet, 1998; Woo and Young, 1998); thus peatlands have little effect in modifying spring high flows because of their low storage capacity when frozen. Likewise, the main source of runoff (i.e. soil water or event water) is dependant on antecedent moisture conditions in the soil and in topographic depressions (Hayashi *et al.*, 2004). The presence of permafrost plateaus in these basins tends to quicken the hydrological response of streams to rain and snowmelt (Woo, 1986), increase the magnitude of runoff, and control flow pathways (Quinton *et al.*, 2003). For example, the relatively high topographic position of peat plateaus, in combination with the very low permeability of the frozen, saturated peat that underlies them, suggests that these features (1) may act as 'permafrost dams' that obstruct and re-direct drainage in the surrounding wetlands, and (2) provide a major source of basin runoff (Quinton and Hayashi, 2005). Quinton *et al*. (2003) found that in the wetland-dominated zone of discontinuous permafrost, drainage basins with a greater percentage of peat plateaus had greater total annual runoff than basins with a smaller percentage.

The dominant runoff mechanism from peat-covered, permafrost slopes is subsurface flow via the saturated layer between the water table and frost table (Slaughter and Kane, 1979; Quinton and Marsh, 1999; Hayashi *et al*., 2004), as ice-rich permafrost confines the water flow to a relatively shallow, seasonally-thawed active layer. Thus, runoff generation from these slopes is largely controlled by the depth and lateral distribution of the frost table (Woo and Steer, 1982; Woo and Heron, 1987). Active layer thaw is strongly linked to the surface energy balance, and small additional ground heating

can cause substantial changes to the hydrology of peat plateaus and the basins in which they occupy (Rouse, 2000). Increases in shallow ground temperature and active layer thickness in the discontinuous permafrost zone have been observed in recent decades (Brown *et al*., 2000; Osterkamp, 2005), indicating degradation of warmer permafrost. The implications of these changes on the future runoff production from the basins of this region are poorly understood. The measurement, and ultimately modelling, of the water and energy balance of permafrost plateaus provides the means of predicting the hydrological impact of climate change on these peatlands and the basins in which they occur (Rouse, 2000).

1.2 Research Objectives

Although peat plateaus are common in Canadian peatlands of the discontinuous permafrost zone (Zoltai *et al.*, 1988; Metcalfe and Buttle, 1999), very few studies have examined the physical processes relating to runoff generation from peat plateaus. This study was conducted to examine the hydrological response of a peat plateau to water and energy inputs, to better understand their role in basin runoff generation, as well as to elucidate the basin response to hydrological changes brought on by permafrost thaw.

The specific objectives of this study are to

1) determine the rate and volume of runoff from a peat plateau during spring melt, and in doing so, evaluate the relative importance of various components of the plateau hydrologic system in determining the amount of water available for runoff;

2) document the spatial and temporal distribution of frost-table depths on a plateau hillslope, and examine the factors controlling its variability, in order to elucidate the role of active-layer development on runoff generation from peat plateaus;
3) compare the ground surface energy balance and thermal regimes of a treed peat plateau underlain by permafrost and an adjacent flat bog that is permafrost-free, in order to evaluate the factors that control soil thaw rates (e.g. radiation input and output, soil temperature and moisture, canopy cover), as they influence the presence and maintenance of perennially frozen peat plateaus, and therefore impact runoff generation.

1.3 Study region

The Mackenzie River Basin in northwestern Canada is among the largest peatland complexes in the world (Vitt *et al*., 2005), and the second largest in North America to the Hudson Bay Lowlands; forming one of the principal water and carbon storage reservoirs in the northern hemisphere (Vitt *et al*., 2005). In the central part of the Mackenzie River basin (60-64^{o}N) lies the wetland-dominated lower Liard River valley, a 55,100 km^{2} region of flat terrain located in the Continental High Boreal Wetland Eco-Climatic Region, [as defined by Zoltai *et al*. (1988)], and the zone of discontinuous permafrost (Hegginbottom and Radburn, 1992). Peatlands are estimated to occupy 30% of this region (Wright *et al*., 2003; Tarnocai *et al*., 2005), which provide 20% percent of the drainage area and 7% of the cumulative annual runoff to the Liard River, a major tributary of the Mackenzie River. Peatland complexes composed of perennially-frozen

peat plateaus, and seasonally-frozen flat bogs and channel fens are typical of the discontinuous permafrost zone, and such complexes account for approximately 33% of peatland area in the lower Liard valley (Wright *et al*., 2003; Tarnocai *et al*., 2005). Physical characteristics of the major peatlands of the region are described in Quinton *et al*. (2003) and Quinton and Hayashi (2005).

Field studies were conducted in a peatland complex located in the upper two-thirds of the Scotty Creek drainage basin (Figure 1-1). Scotty Creek is a 152 km^2 wetland-dominated basin located in the lower Liard River valley (61°18'N, 121°18'W), 50-km south of Fort Simpson, Northwest Territories, Canada (Figure 1-1). Natural surface drainage is northward to the Liard River Basin, and is composed of interconnected wetlands (channel fens), open stream channels, and intervening lakes (Quinton *et al*., 2003). The mean annual runoff pattern of Scotty Creek is typical of northern rivers in discontinuous permafrost basins (Church, 1974). Peak runoff occurs during spring in response to snowmelt, and usually coincides with the ice break-up on the Liard and Mackenzie Rivers. Secondary peaks in runoff sometimes occur during summer in response to rainfall, while in other years only minimal runoff occurs in summer. During freeze-up, there is a transfer of in-stream water from discharge into ice storage, and thus flow ceases during winter months.

The peatland complex in Scotty Creek was selected for study because it contained the major ground cover types within the region (i.e. channel fens, bogs, peat plateaus), and was logistically manageable given its close proximity to Fort Simpson. This region was chosen because it is situated in the southern fringe of the discontinuous permafrost zone with a 30-year mean annual air temperature of -2.8^{o}C, where permafrost is

particularly vulnerable to degradation (Burgess *et al*., 2000). Climate stations throughout the Mackenzie Basin exhibit statistically significant warming trends of up to 0.9^{o}C per decade since 1950, and a significant warming trend in April (Woo and Thorne, 2003). Slight shifts in temperature can alter the status of the ground from frozen to unfrozen, and some observations suggest this has already occurred in the Fort Simpson region (Chatwin, 1981; Kwong and Gan, 1994; Robinson and Moore 2000; Beilman and Robinson, 2003). Climate change scenarios indicate that the warming under a doubling of CO_2 conditions is likely to cause complete degradation of permafrost in the Fort Simpson region within 50 years or less (Burgess *et al*., 2000). This highlights the urgency in understanding the factors controlling runoff generation from peat plateaus, which is essential in the prediction of future responses and feedbacks in the land surface–climate system of wetland-dominated basins in this region, and to reduce uncertainties regarding the influence of climate warming on the future availability of Canada's northern water resources.

1.4 Thesis organization and role of co-authors

This thesis consists of a series of manuscripts for publication in peer-reviewed journals, together with an introduction (Chapter 1) and conclusion (Chapter 5). These manuscripts are reproduced here in a format consistent with thesis requirements. In accordance with the Simon Fraser University Faculty of Graduate Studies and Research guidelines, I declare here that the research presented in these papers is work of my conception and execution undertaken with the input and assistance of the listed co-authors. The role of these co-authors is listed below.

Chapter 2: Is a modified version of Wright, N., Quinton, W.L., and Hayashi, M., 2008. Hillslope runoff from an ice-cored peat plateau in a discontinuous permafrost basin, Northwest Territories, Canada. *Hydrological Processes* 22: 2816-2828. Both Dr. Bill Quinton and Dr. Masaki Hayashi contributed to the overall paper development through discussions with me and provided intellectual comments on drafts of the manuscript. Dr. Masaki Hayashi developed the methodology used in computing the Dupuit-Forchheimer approximation of hillslope flow, which is outlined in Appendix 1. Dr. Nigel Roulet, Dr. Mike Waddington, and an anonymous reviewer provided helpful comments that improved the manuscript.

Chapter 3: Wright, N., Hayashi, M., and Quinton, W.L., 2009. Spatial and temporal variations in active-layer thawing and their implication on runoff generation in peat-covered permafrost terrain. *Water Resources Research* 45: W05414, doi:10.1029/2008WR006880. Dr. Masaki Hayashi developed the coupled flow and heat simulation model (Simple Fill and Spill Hydrology, SFASH) presented in this paper. Both Dr. Bill Quinton and Dr. Masaki Hayashi provided intellectual comments on drafts of the manuscript. Four anonymous reviewers provided helpful comments that improved the manuscript.

Chapter 4: An extended version of this chapter will be submitted to a Special Issue in the *Journal of Hydrology and Earth System Sciences* for IP3 (Improved Processes and

Parameterisation for Prediction in Cold Regions). Both Dr. Bill Quinton and Dr. Masaki Hayashi contributed to the overall paper development through discussions with me, and provided intellectual comments on drafts of the chapter.

1.5 Figures

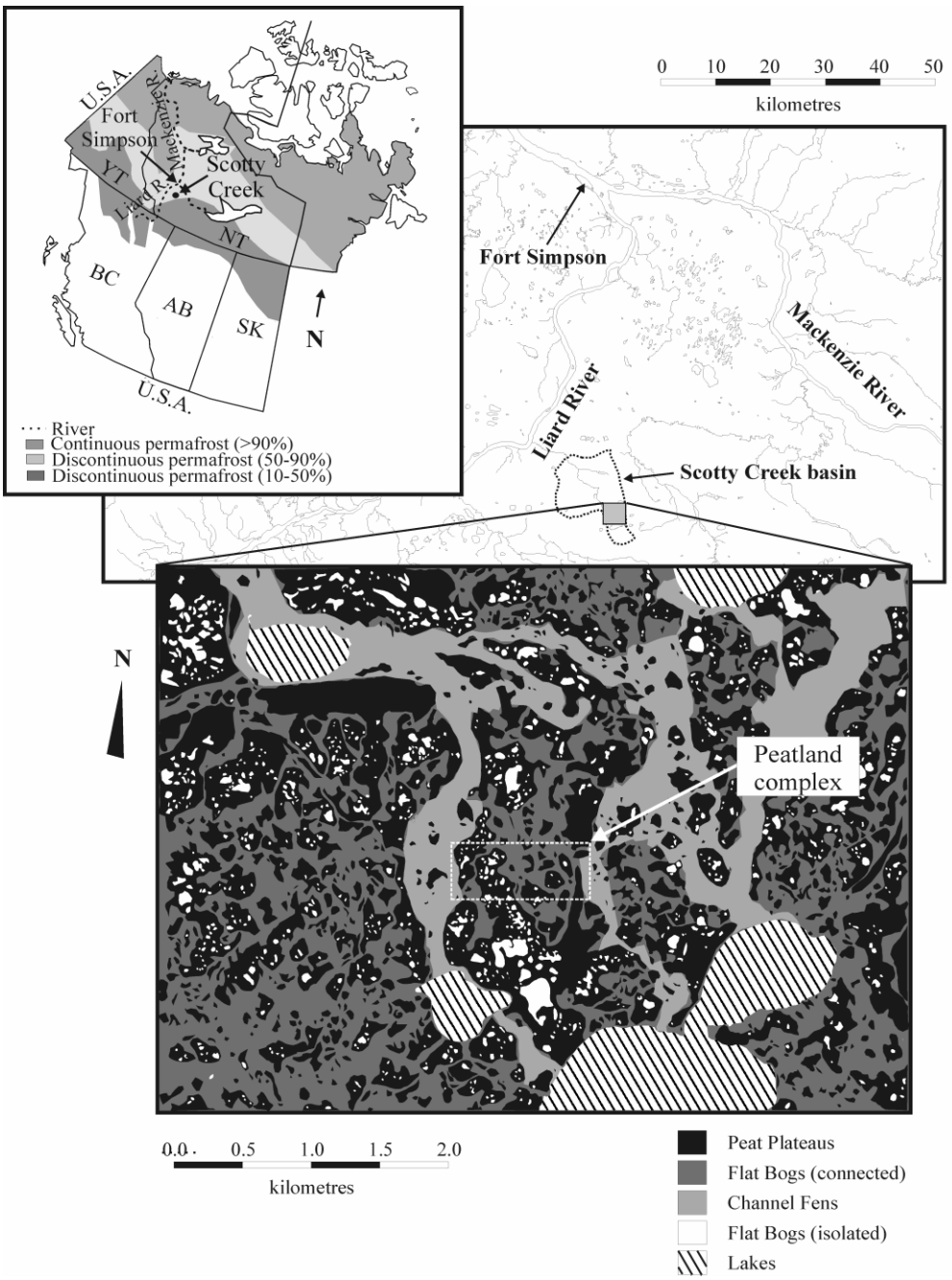

Figure 1-1 Location of the Scotty Creek drainage basin within the Lower Liard River Valley, Northwest Territories, Canada, and a schematic of the upper two-thirds of the basin, depicting the peatland complex and the different ground cover types within it.

1.6 Reference List

Aylsworth, J.M., Kettles, I.M. and Todd, B.J. 1993. Peatland distribution in the Fort Simpson area, Northwest Territories with a geophysical study of peatland-permafrost relationships at Antoine Lake. *Current Research, Geological Survey of Canada Paper* 93-1E: 141-148.

Beilman, D.W. 2001. Plant community and diversity change due to localized permafrost dynamics in bogs of western Canada. *Canadian Journal of Botany* 79: 983-993.

Beilman, D.W. and Robinson, S.D. 2003. Peatland permafrost thaw and landform type along a climatic gradient. In *Permafrost*, M. Phillips, S.M. Springman, and L.U. Arenson (eds). Swets and Zeilinger, Liesse, 61-64.

Boetler, H. 1966. Hydrological characteristics of organic soils in Lake States Watersheds. *Journal of Soil and Water Conservation* 21: 50-53.

Branfireun, B. and Roulet, N. 1998. The baseflow and stormflow hydrology of a Precambrian shield headwater peatland. *Hydrological Processes* 12: 57–72.

Brown, J., Hinkel, K. M. and Nelson, F. E. 2000. The Circumpolar Active Layer Monitoring (CALM) program: Research designs and initial results. *Polar Geogr*aphy 24: 165–258.

Brown, R.J.E. 1968. Occurrence of permafrost in Canadian peatlands. In *Proceeding of the Third International Peat Congress*, C. Lafleur and J. Butler (eds.). Ottawa: National Research Council of Canada, 174-181.

Burgess, M.M., Smith, S.L., Brown, J., Romanovsky, V. and Hinkel, K. 2000. Global Terrestrial Network for Permafrost (GTNet-P): Permafrost monitoring contributing to global climate observations. *Geological Survey of Canada, Current Research 2000-E14*, 8 pp.

Chatwin, S. 1981. Permafrost aggradation and degradation in a sub-arctic peatland. M.Sc. thesis, University of Alberta, Edmonton, 176 pp.

Church, M. 1974. Hydrology and Permafrost with Reference to Northern North America. In *Proceedings Workshop Seminar on Permafrost Hydrology*. Ottawa: Canadian National Committee, International Hydrological Decade (IHD), 7-20.

Hayashi, M., Quinton, W.L., Pietroniro, A. and Gibson, J.J. 2004. Hydrologic functions of wetlands in a discontinuous permafrost basin indicated by isotopic and chemical signatures. *Journal of Hydrology* 216: 81-97.

Heginbottom, J.A. and Radburn, L.K. 1992. Permafrost and ground ice conditions of Northwestern Canada. *Geological Survey of Canada, Map 1691A*, scale 1:1 000 000.

Kwong, J. and Gan, T.Y. 1994. Northward migration of permafrost along the Mackenzie Highway and climatic warming. *Climate Change* 26(4): 399-419.

McFadden, J.P., Chapin, F.S. and Hollinger, D.Y. 1998. Subgrid-scale variaibility in the surface energy balance of arctic tundra. *Journal of Geophysical Research-Atmospheres* 103: 28947-28961.

Metcalfe, R.A. and Buttle, J.M. 1999. Semi-distributed water balance dynamics in a small boreal forest basin. *Journal of Hydrology* 226: 66-87.

Osterkamp, T. E. 2005. The recent warming of permafrost in Alaska. *Global and Planetary Change* 49 (3-4): 187-202.

Quinton, W.L. and Hayashi, M. 2005. The flow and storage of water in the wetland-dominated central Mackenzie River basin: Recent advances and future directions. In: *Prediction in ungauged basins: Approaches for Canada's cold regions*, C. Spence, J.W. Pomeroy and A. Pietroniro (eds). Canadian Water Resources Association, Cambridge Ontario; pp. 45-66.

Quinton, W.L., Hayashi, M. and Pietroniro, A. 2003. Connectivity and storage functions of channel fens and flat bogs in northern basins. *Hydrological Processes* 17: 3665-3684.

Quinton, W.L. and Marsh, P. 1999. A conceptual framework for runoff generation in a permafrost environment. *Hydrological Processes* 13: 2563-2581.

Robinson, S.D. and Moore, T.R. 2000. The influence of permafrost and fire upon carbon accumulation in high boreal peatlands, Northwest Territories, Canada. *Arctic, Antarctic and Alpine Research* 32(2): 155-166.

Rouse, W.R. 2000. The energy and water balance of high-latitude wetlands: controls and extrapolation. *Global Change Biology* 6(1): 59-68.

Seppälä, M. 1988. Palsas and related forms. In *Advances in Periglacial Geomorphology*, M. J. Clark (ed.). Wiley, Chichester, 247-278.

Slaughter, C.W. and Kane, D.L. 1979. Hydrologic role of shallow organic soils in cold climates. In *Canadian Hydrology Symposium: Cold Climate Hydrology Proceedings*. Ottawa, Ontario: National Research Council of Canada, 380-389.

Tarnocai, C. 1998. The amount of organic carbon in various soil orders and ecological provinces in Canada. In *Soil Processes and the Carbon Cycle,* Lal R., J.M. Kimble, R.F. Follet, and B.A. Stewart BA (eds). The Pensylvania Academy of Science: Pittsburgh, 168-398.

Tarnocai, C. 2006. The effect of climate change on carbon in Canadian peatlands. Global Planetary Change 53: 222-232.

Tarnocai, C., Kettles, I.M. and Lacelle, B. 2005. Peatlands of Canada Database. Research Branch, Agriculture and Agri-Food Canada, Ottawa, Ontario, Canada. digital database.

Vitt, D. H., Halsey, L. A . and Nicholson, B. J . 2005. The Mackenzie River basin. In *The World's Largest Wetlands: Their Ecology and Conservation*, L. H. Fraser and P. A. Keddy (eds.). Cambridge University Press, Cambridge, 166-202.

Woo, M-K. 1986. Permafrost hydrology in North America. *Atmosphere-Ocean* 24: 201-234.

Woo, M-K. and Heron, R. 1987. Effects of forests on wetland runoff during spring. In *Forest Hydrology and Watershed Management*, Swanson RH, Bernier PY and Woodard PD (eds). IAHS Publication No. 167, IAHS Press, Wallingford; 297-307.

Woo, M-K. and Steer, P. 1983. Slope hydrology as influenced by thawing of the active layer, Resolute, N.W.T. *Canadian Journal of Earth Sciences* 20(6): 978-986.

Woo, M-K. and Thorne, R. 2003. Streamflow in the Mackenzie Basin, Canada. *Arctic* 56: 328-340.

Woo, M-K. and Young, K.L. 1998. Hydrogeomorphology of patchy wetlands in the High Arctic, polar desert environment. *Wetlands* 23(2): 291-309.

Wright, J.F., Duchesne, C. and Côté, M.M. 2003. Digital compilation of vegetation types of the Mackenzie Valley transportation corridor. *Geological Survey of Canada, Open File 1614*.

Zoltai, S.C. 1972. Palsas and peat plateaus in central Manitoba and Saskatchewan. *Canadian Journal of Forest Research* 2:291-302.

Zoltai, S.C., Tarnocai, C., Mills, G.F. and Velduis, H. 1988. Wetlands of Canada. Ecological Land Classification Series No. 24. Environment Canada, Ottawa, and Polyscience Publications Inc., Montreal, Quebec, 452 pp.

Preface to Chapter 2

Understanding the factors that control runoff generation from peat plateaus is the essential first step toward developing methods of accurately predicting basin runoff from wetland-dominated basins in the region of discontinuous permafrost, as well as understanding the basin response to hydrological changes brought on by the thermal degradation and thaw of permafrost peatlands. In the following chapter, a water balance approach and the Dupuit-Forchheimer equation were used to quantify subsurface runoff from a forested peat plateau at Scotty Creek during the spring field seasons of 2004 and 2005. The results give insight into the relative contributions of snowmelt, ground ice melt, and soil storage to runoff generation, and the major factors controlling the timing and magnitude of runoff from the hillslope. The chapter also evaluates the use of the Dupuit-Forchheimer equation in quantifying subsurface runoff from peat plateaus.

Chapter 2
Hillslope runoff from an ice-cored peat plateau in a discontinuous permafrost basin, Northwest Territories, Canada[1]

2.1 Introduction

Permafrost underlies approximately 25% of the land surface in the Northern Hemisphere (Zhang *et al*., 2000), and plays an important role in the northern hydrological cycle (Woo and Winter, 1993). A large portion of the permafrost regions of the world are covered by peatlands; as an example, one-half of the peatlands in Canada are found in permafrost-affected regions (Robinson *et al*., 2003). The spatial extent of permafrost is discontinuous (covering 10-90% of the land surface) in the peatlands of western subarctic and northern boreal Canada, and the northern taiga of Europe and Russia. Permafrost in these regions often takes the form of large expansive areas of peatland, completely underlain by a perennially frozen core. These features are called peat plateaus in Canada (Zoltai, 1971; Zoltai and Tarnocai, 1975), and are similar to flat palsas in Russia and palsa plateaus in northern Norway (NWWG, 1988). Peat plateaus are treed in the discontinuous permafrost region of northwestern Canada, whereas peat plateaus are commonly treeless in colder areas further north. This distinction is hydrologically important, as the presence of trees affects the amount of snow accumulation, evapotranspiration and runoff of peat plateaus.

[1] The following chapter has been published in *Hydrological Processes* (vol. 22, pp. 2816-2828, 2008) under the co-authorship of Wright, N., Quinton, W.L., and Hayashi, M.

This paper focuses on treed peat plateaus. The surface of these peat plateaus rise 1–2 m above the regional water table because of the volumetric expansion of frozen peat, and are dominated almost exclusively by *Picea mariana* (in North America) (Camill, 1999; Quinton *et al*., 2003). Their relatively high topographic position means that they are ombrotrophic, and as the hydraulic gradient is directed away from the plateaus, a high proportion of the hydrological inputs runs off to adjacent wetlands (Woo and Heron, 1987; Quinton *et al*., 2003; Hayashi *et al*., 2004). Surface flow is thought to be negligible due to the large water holding capacity (Dingman, 1971), high porosity (>0.7) (Hinzman *et al*., 1991; Quinton and Gray, 2001) and high frozen and unfrozen infiltration rates of peat soils (Dingman, 1973; Slaughter and Kane, 1979). Thus, the dominant runoff mechanism from peat plateaus is subsurface flow via the saturated layer between the water table and frost table (Hayashi *et al*., 2004), as ice-rich permafrost confines the water flow to a relatively shallow, seasonally thawed active layer (Dingman, 1970; Roulet and Woo, 1988; McNamara *et al*., 1997). The depth of the frost table controls the magnitude and timing of hillslope drainage to stream channels, given the depth-dependency of saturated hydraulic conductivity (Quinton *et al*. 2000) and the relative impermeability of the upper boundary of the frozen saturated layer.

Hillslopes in permafrost regions, such as peat plateaus, are hydrologically important to basin runoff, because they accumulate a large proportion of the basin snow water prior to spring melt (Woo and Marsh, 1978; Woo and Heron, 1987; Metcalfe and Buttle, 1999), and contribute to streamflow generation long after they have become depleted of snow cover (Marsh and Pomeroy, 1996; Quinton and Marsh 1998), even into the summer months (Woo and Heron, 1987). Quinton *et al*. (2003) found that in the

wetland-dominated zone of discontinuous permafrost, drainage basins with a greater percentage of peat plateaus had greater total annual runoff than basins with a smaller percentage of peat plateaus. The role of treed peat plateaus as runoff producers is particularly pronounced during the annual spring melt event, as there is a large amount of water input in a short amount of time, and flow during spring is restricted by shallow ground thaw (because the frozen soil is relatively impervious to water movement and storage), which results in a large amount of runoff to adjacent wetlands (Glenn and Woo, 1987).

Although peat plateaus are common in peatlands of the discontinuous permafrost zone (e.g. Zoltai and Tarnocai, 1975; NWWG, 1988; Metcalfe and Buttle, 1999; Tarnocai *et al*., 2000), and appear to play an important role in basin runoff of these regions, very few studies have examined how runoff is generated from peat plateaus. As a result, there is a lack of knowledge on basin water cycling in a region that is undergoing rapid change due to climate warming, increased industrial development, and permafrost degradation (Rouse *et al*., 1997; Serreze *et al*., 2000). Increases in shallow ground temperature and active layer thickness in the southern boundary of discontinuous permafrost, and thermokarst development in recent decades, have been observed in North America (Brown *et al*., 2000; Osterkamp, 2005), Europe (Harris *et al*., 2003) and Russia (Frauenfeld *et al*., 2004), indicating degradation of warmer permafrost. In continental western Canada, there is evidence of extensive degradation and widespread disappearance of peat plateaus for some time (Robinson and Moore 2000; Jorgensen *et al*. 2001; Beilman and Robinson, 2003; Camill, 2005). The implications of these changes on the future runoff production from the basins of this region are poorly understood.

Understanding the factors that control the volume and timing of runoff from peat plateaus is the essential first step toward developing methods of accurately predicting basin runoff from wetland-dominated basins in the region of discontinuous permafrost, as well as understanding the basin response to hydrological changes brought on by the thermal degradation and thaw of permafrost peatlands. Thus, the objective of this study was to determine the timing and volume of runoff from a peat plateau hillslope during spring melt. A water balance approach was used to determine the magnitude of runoff, and to assess the relative contributions of snowmelt, ground ice melt, and soil storage to runoff generation from a permafrost peatland. A second estimation of runoff was also computed from hydraulic conductivity and gradient to corroborate the results from the water balance approach. Data sets such as these are useful in assessing the predictions of hydrological models, but are rare due to the logistics of northern research.

2.2 Site description

Scotty Creek is a 152 km^2 wetland-dominated drainage basin located in the lower Liard River valley (61°18'N, 121°18'W), 50-km south of Fort Simpson, Northwest Territories, Canada (Figure 2-1a)). The stratigraphy of the region includes an organic layer of varying thickness (*ca*. 0.5 m to 8 m) that overlays a silt-sand layer, below which lies a thick (several meters) clay to silt-clay deposit of low permeability (Aylesworth *et al*., 1993). The Fort Simpson area is in the continental high boreal wetland region of Canada, slightly south of the transition to low subarctic (NWWG, 1988), and lies within the southern fringe of discontinuous permafrost (Hegginbottom and Radburn, 1992). The region is characterised by a dry continental climate, with short, dry summers, and long

cold winters. The 1964-2005 mean annual air temperature at Fort Simpson airport (169 m a.s.l.) is -3.2^{o} C, and the mean January and July temperatures are -25.9 and 17.1 °C, respectively (MSC, 2005). The region receives an average of 363 mm of precipitation annually, of which 45 % falls as snow (MSC, 2005). Snowmelt usually commences in late March and continues throughout April, with small amounts of snow typically remaining on the ground during the early weeks of May.

The upper two-thirds of the Scotty Creek drainage basin is a peatland complex composed of peat plateaus, flat bogs and channel fens (Figure 2-1b). Spatial analysis of a *ca.* 22 km^2 representative sample of this complex (Figure 2-1 b), indicated that peat plateaus occupy the largest areal portion (43%), followed by flat bogs, and then channel fens. Most field measurements were made near the centre of this complex at the Study plateau (61°18'48.9"N, 121°18'22.7"W).

The Study plateau rises 0.9 m above the surrounding wetlands, and its active layer, measured over four consecutive years (2003-2006) extends to an average depth of 0.64 m ± 0.18 m. The upper layer typically extends to an approximate depth of 0.2 m, and is composed of living vegetation and lightly decomposed fibric peat; while the lower layer contains denser, more decomposed sylvic peat with dark, woody material, and the remains of lichen, rootlets and needles[2] (Quinton *et al*., 2003). This two-layered peat profile is similar to that found in wetlands possessing acrotelm and catotelm layers (Ivanov, 1981). However, unlike a catotelm, the lower peat layer is not permanently

[2] The von Post H-values were not estimated for the plateau peat soils, because this method is not recommended for relatively dry peat materials, upper peat layers of drained organic soils, and sedge and woody peat, since the degree of humification of these less compressible materials is easily underestimated (Grosse-Brauckmann, 1976).

saturated (water drains away from the peat profile as the soil thaws). The active layer mantles permafrost that is between 5 to 10 m in thickness (Burgess and Smith, 2000).

The Study plateau supports an open tree canopy, composed predominantly of black spruce (*Picea mariana*). Maximum measured tree height is 9.3 m, and the mean tree height is 3.1 ± 2.2 m. Mean tree density is approximately 1 stem m^{-2}. Shrubs occupy 56 % of the plateau and are dominated by Labrador tea (*Ledum groenlandicum*), small bog cranberry, Leatherleaf (*Chamaedaphne calyculata*) and bog birch (*Betula glandulosa*). *Cladina mitis, C. rangiferina* and other lichen species cover 65% of the forest floor, while the remaining 35% is occupied by *Sphagnum fuscum*, *S.capillifolium* and other moss species. The microtopographic variation on the ground surface of the peat plateau ranges from less than 10 cm to a few tens of centimetres per square metre[3]. Although standing water occupied up to one-fifth of the plateau during the spring melt period, it accounted for <1% of the plateau ground surface during summer.

2.3 Methods

2.3.1 Water balance equation

Field study was conducted in the spring of 2004 and 2005, to estimate the amount of spring runoff, and to assess the relative importance of the major hydrological elements of the Study plateau. The daily net runoff (R_1) was computed from the water balance:

$$R_1 = M + I_M + P - ET - \Delta S \qquad (2.1)$$

where snow melt (M), melt of ice in the active layer (I_M), rainfall (P), evapotranspiration

[3] Note that the depth below the peat plateau surface is defined in this thesis as the depth below the average ground surface elevation, which is fixed (i.e. it does not change in elevation).

(ET), and active layer moisture storage (ΔS) all have units of mm day^{-1}. Although some localized surface flows were discernable once the snow cover on the plateau had melted, surface discharge on the plateau, measured from the velocity-area method, was relatively small (< 1%). Thus, R_1 essentially represents subsurface runoff, and will be treated as such in this study. Each of the terms in the right hand side of Eq. (2.1) were measured or estimated as follows.

2.3.2 Snow measurements and site instrumentation

Snow depth and snow water equivalent (SWE) measurements commenced at the height of the snow-accumulation season, and were made daily using an Eastern Snow Conference snow sampler (ESC-30) (Goodison, 1978) and calibrated (to ± 3 mm) scale. Snow depth was measured at 1 m, and SWE at 5 m intervals along a 41 m transect (T1) that traversed the Study plateau from channel fen to flat bog (Figure 2-1 c). In 2005, a 28 m long transect (T2) was added, and like T1, was used for snow depth and SWE measurements following the same measurement intervals. The depth of ablation M, which is comprised of both snow sublimation and melt, was calculated from the difference in successive daily measurements of snow water equivalent averaged along each transect. To determine the relative proportion of sublimation to ablation, sublimation of the snowpack was estimated over 12 days in 2005, by measuring the change in snow surface elevation from an arbitrary datum, at 1 m intervals along T2. During this measurement period, an average of 18 mm of snow sublimated along T2, which was 11% of the average 156 mm of snow that ablated along the same transect, over the same time period. This indicates that the majority (89%) of the plateau

snowpack is removed via melt processes during spring melt, and thus, *M* is hereafter [and in equation (2.1)] referred to as the depth of melt rather than the depth of ablation.

Parallel to T1, were two polyvinyl chloride (PVC) observation wells (0.05 m i.d.), located 2.7 m (West well) and 15.9 m (Centre well) from the edge of a channel fen (Figure 2-1 c). Each well was instrumented with a Global Water WL15 pressure transducer that measured water table depth every minute, and averaged and recorded these measurements every 30 minutes. The water table depth at each of the wells was also measured manually with a water level sounder and ruler on a daily basis, to ensure the accuracy of the continuous measurements. The Centre and West wells were each installed in a soil pit (described in detail by Hayashi *et al*., 2007) that was excavated to the frost table (a depth of 0.7 m) on August 20, 2001. Approximate locations of the two pits are shown in Figure 2-1 c), though only the data from the Centre pit were used in this study. The Centre pit was instrumented with calibrated soil temperature sensors (Campbell Scientific 107B) at 0.05, 0.1, 0.15, 0.2, 0.25, 0.3, 0.4, 0.5, 0.6, and 0.7 m depths, and soil moisture sensors (Campbell Scientific CS615) at 0.1, 0.2, 0.3 and 0.4 m depths. A 92 cm^3 soil sample was taken next to each of the CS615 water content reflectometers (WCR) at the time the sensors were installed, in order to calibrate the soil sensors, and measure the soil porosity and bulk density in the laboratory following the approach of Quinton *et al*. (2000).

At a meteorological station located between the Centre and West wells, upward and downward-directed short and long wave radiation at 2 m (Kipp & Zonen, CNR1), wind speed at 2.7 m (Met One 014A), relative humidity and air temperature at 2 m (Vaisala, HMP45C) and snow depth (Campbell Scientific, SR50) were measured above a

moss-covered ground surface. A tipping-bucket rain gauge (0.2 m diameter, 0.35 m height) calibrated to 0.26 mm per tip was located next to the meteorological station. All sensors were connected to Campbell Scientific, CR10X dataloggers, programmed to measure every minute, and average and record every 30 minutes.

2.3.3 Evapotranspiration

In 2005, five identical evaporation pans (colourless, plastic pails of 0.19 m diameter and depth) were installed in meltwater pools on the plateau to measure the evaporation rate of the standing water on the plateau. The rims of the pans were between 10 and 20 mm above the surrounding water surface. The decrease in pan water level below a fixed mark was recorded every 24 hours. Daily evaporation was obtained by measuring the volume of water required to restore the water level to a fixed mark. Following the daily readings, water was added to each pan so that their water levels were brought back to that of the fixed marks. In addition, 10 soil lysimeters (0.19 m diameter; same as the evaporation pans) were used to measure the daily evapotranspiration from lichen and moss surfaces gravimetrically following the method of Lafleur and Schreader (1994). Because drainage was not permitted, the monolith of soil and the surface vegetation in the lysimeters were carefully replaced after large rain events. During extended periods without rain, the near surface soil moisture (0-0.2 m) inside and outside of the lysimeters was measured every few days with a portable soil water content probe that was calibrated for peat soils (Campbell Scientific Inc., HydroSense). This was done to ensure the soil in the lysimeters had not dried out, relative to the surrounding soil, because they were cut off from the vertical and lateral transport of water within the soil

matrix. When the difference in volumetric water content (VWC) inside the lysimeter was more than 10% of the VWC outside, the soil monoliths were replaced. The daily rate of evapotranspiration from each of the moss and lichen soil-filled lysimeters (ET_{LM} in mm day^{-1}) was computed from:

$$ET_{LM} = [(\Delta W_w/\rho_w)/A] \cdot 1000, \quad (2.2)$$

where ΔW_w is the daily change in weight of the soil-filled lysimeter (kg day^{-1}), ρ_w is the density of water (kg m^{-3}), and A is the cross-sectional area of the lysimeters (m^2). The total daily evapotranspiration for the plateau was computed as a weighted average based on the measured evaporation and percent cover of moss, lichen and pools on the plateau. The percent cover of each was estimated from the relative proportion of the three ground cover types measured in a 1 × 1 m grid, every metre along transects T1 and T2 (Figure 2-1 c) on a weekly basis.

For 2004, and for the 18 days in 2005 when the lysimeter data were unreliable due to rainfall, evapotranspiration (ET in mm day^{-1}) from the plateau ground surface was estimated using the Priestley and Taylor (1972) method[4]:

$$ET = \alpha E_{eq} = \alpha \left[\frac{s}{s+\gamma} \right] \frac{\lambda}{\rho_w} \left[Q^* - Q_g \right] \ 1000 \quad (2.3)$$

where E_{eq} (mm day^{-1}) is equilibrium evaporation, α is a dimensionless coefficient to be determined (see below), s is the slope of the saturation vapour pressure – temperature curve (Pa ^{o}C^{-1}), γ is the psychrometric constant (0.066 kPa ^{o}C^{-1} at 20^{o} C), λ is the latent heat of vaporisation (J kg $^{-1}$), ρ_w is the density of water (kg m^{-3}), Q^* (J m^{-2} day $^{-1}$) is the

[4] The Priestley and Taylor (1972) method was used to compute daily ET in this study, because the results were found to be more comparable to actual ET measurements than the Granger and Gray (1989) method.

available energy from net radiation, and Q_g (J m^{-2} day^{-1}) is the ground heat flux. All meteorological variables were supplied by the measurements made at the meteorological tower. Ground heat flux was computed from the thermocalimetric method described in Quinton *et al*. (2005), using the temperature and moisture measurements at the Centre pit. Direct measurements of evapotranspiration from the pans and lysimeters in 2005 were plotted against E_{eq} to determine α for each of the three ground cover types (Table 2-3); α computations in 2004 were also verified with actual data in 2005.

The methods used in this study account only for evapotranspiration losses from the ground surface of the peat plateau. Although Eq. (2.1) does not include the water loss evaporated from trees, omission of this is not thought to be significant to the water balance calculation, considering the relatively low water loss from black spruce stands in the boreal forest reported in the previous literature (e.g. Pattey *et al*., 1997; Nijssen *et al*., 1997; Kimball *et al*., 1997; Arain *et al*., 2003). Based on the evapotranspiration rates of the black spruce stands published in these studies (which ranged from an average of 1.4 mm day^{-1} to 2.6 mm day^{-1}), total *ET* could be underestimated by as much as 50 mm in this study; however, the error is expected to be much less, because the peat plateau has an open canopy with a much lower stand density than those studied in the southern and northern boreal forest.

2.3.4 Active layer melt and soil water storage

The partitioning of snowmelt and rainfall input into soil storage and runoff is strongly affected by the soil moisture condition prior to freeze-up in the previous autumn, and by late winter moisture gains (Kane, 1980; and Kane and Stein, 1983; Gray and

Granger, 1986). The available soil storage capacity (S_c) prior to freeze-up at the Centre pit was computed from the product of the thickness d_{uz}, and air-filled porosity of the unsaturated zone:

$$S_c = d_{uz} \cdot (\phi - \theta_L) \tag{2.4}$$

where ϕ is average porosity (= 0.8) of d_{uz}, derived from the single-valued function of porosity with respect to depth reported by Quinton and Hayashi (2005), and θ_L is the average liquid water content measured with all the CS615 sensors located above the water table.

The daily melt rate of ice in the active layer, I_M (mm day^{-1}) at the Centre pit was computed from:

$$I_M = (\theta_T - \theta_L) \cdot \frac{\Delta z_f}{\Delta t} \cdot 0.9 \tag{2.5}$$

where θ_T is total volumetric moisture content (ice + water) below the cryofront, 0.9 accounts for the density difference between ice and water, and $\Delta z_f / \Delta t$ is the daily change in the depth, z_f (m) to the cryofront (i.e. the top of the frozen layer, which was measured with a graduated steel rod). The values of θ_T were not measured in this study, and hence had to be estimated from the liquid water content measured prior to freeze up in the following manner. The water content profile at the Centre pit was measured in the fall of 2002 immediately before the freeze-up, and two 0.7 m deep frozen peat core samples were obtained near the Centre pit on April 6, 2003 for another study (Hayashi *et al*., 2007). We assumed the difference between pre-freezing θ_L (=θ_T) measured in 2002 and the average of θ_T of the two frozen peat cores in 2003 gave the over-winter addition of

water to the peat profile, presumably due to mid-winter melt of snowpack and the capillary-driven, upward flow of water to the freezing front advancing from the surface. Assuming that the meteorological conditions in 2003-2004 and 2004-2005 winters were similar to 2002-2003 winters, we added the over-winter change of θ_T observed in 2002-2003 to the fall 2003 values of θ_L to estimate the spring 2004 values of θ_T, and to the fall 2004 values of θ_L to estimate the spring 2005 values of θ_T. The total amount of over-winter increase in θ_T was 99 mm over the 0.7 m peat profile. Hayashi *et al*. (2004) examined the electrical conductivity and isotopic composition of water in the active layer during snowmelt, and found that much of the water was old or pre-event water, suggesting that the over-winter increase in θ_T is likely due to liquid and vapour transfer processes during freeze-up. Early snowmelt water may have also infiltrated into the still frozen, but partially saturated peat near the surface (i.e. upper 10 cm) (Hayashi *et al*., 2004) to contribute to the increase in θ_T.

To determine ΔS in Eq. (2.1) the Centre pit was divided into soil layers, the boundaries of which were set at the mid-point between the moisture sensors. The moisture content in each layer was assumed to be equal to the value measured by the sensor it contained. For each day, the liquid moisture content of the active layer was estimated as the sum of the liquid moisture in all layers. To determine how well the Centre pit represented the average soil moisture conditions on the Study plateau, ΔS estimations were also made daily (over 25 days) at 15 sampling points in 2005. Soil moisture was measured gravimetrically at 0.05 m depth increments to the water table at each of the 15 flagged sampling points (exact measurement locations changed to avoid destructive sampling, although all measurements were within 1 m of the flagged point),

seven of which were over moss and eight over lichen (Figure 2-1c), using 162 cm^3 soil sample tins. The depth to the water table and frost table were also measured daily at each sampling point, with a ruler and graduated steel rod. The liquid moisture content of the thawed, saturated portion of the active layer at each flagged point was computed as the product of the thickness of layer between the frost and water tables, and the average porosity of the saturated layer, where the latter was derived from the single-valued function of porosity with respect to depth reported by Quinton and Hayashi (2005). For each day, the liquid moisture content of the thawed, saturated and unsaturated portions of the active layer at each sampling point were summed. As the soils beneath moss exhibited a significantly (p=0.001**)** greater volumetric water content at depths to 0.15 m compared to lichen soils, the daily liquid moisture content of the plateau was obtained by averaging the liquid moisture content found at the two cover types of moss and lichen, and then weighting these average values by the proportion of moss (35%) and lichen (65%) found on the plateau.

2.3.5 Runoff computed from hydraulic conductivity and gradient (R_2)

To corroborate the runoff calculation based on the water balance (R_1), subsurface runoff was independently estimated from the hydraulic gradient and conductivity using the Dupuit-Forchheimer approximation (Childs, 1971). The main assumptions for this method are: 1) subsurface runoff occurs only in the thawed, saturated zone between the water table and the impermeable frost table, 2) the subsurface flow rate is equal to the amount of water added to the water table by snowmelt, precipitation minus evaporation, and storage release (see Eq. 2.1), and 3) the flow is one dimensional and parallel to the

slope. Our field observations indicate that these assumptions are justified as a first approximation. If the hydraulic conductivity, K (m day^{-1}) is constant, the rate of subsurface runoff generation, r (m day^{-1}) on a hillslope can be estimated from the hydraulic head measured in two wells (Eq. 1.A6 in Appendix 1):

$$r = -Ky_m\,[(h_2 - h_1)/(x_2 - x_1)] / x_m \tag{2.6}$$

where y_m is the average thickness of the saturated zone between the two wells, $(h_2 - h_1)/(x_2 - x_1)$ is the hydraulic gradient between the two wells, and x_m (m) is the distance from the drainage divide ($x = 0$) to the mid point between the two wells. On the peat plateau in this study, the first well is located at Centre pit, the second well is at West pit (Figure 2-1c) and $x_m = 18$ m.

In reality hydraulic conductivity is not constant on the hillslope, requiring that K in Eq. (2.6) be replaced by an average value representing the heterogeneous peat on the hillslope. Among many possible methods to calculate an average value, we chose the following because the depth-dependence of hydraulic conductivity is believed to be the most important factor controlling the hillslope flow in this environment (Quinton *et al*., 2000). First, saturated hydraulic conductivity, K_{sat} (m day^{-1}) was defined as a function of depth, z (m) below the ground surface, based on the local data measured at various locations on the peat plateau by several methods (Figure 2-2), including *in situ* water tracing, constant-head well permeameter tests, and laboratory measurements (Quinton *et al*., 2008). The solid line in Figure 2-2 indicates the best-fit $K_{sat}(z)$ function representing the peat plateau (Quinton *et al*., 2008):

$$\log K_{sat}(z) = 0.15 + 2.41 / [1 + (z/0.15)^{4.3}]. \tag{2.7}$$

The function was integrated with respect to z to compute the vertically-averaged conductivity, $\overline{K_{sat}}$ (m day^{-1}) of the thawed, saturated zone at the Centre well and the West well:

$$\overline{K_{sat}} = \frac{\int_{zw}^{zf} K_{sat}(z)dz}{z_f - z_w} \tag{2.8}$$

where z_w is the water table depth and z_f is the frost table depth. Daily values of $\overline{K_{sat}}$ were computed from measured z_f and z_w. To represent the average conductivity of the hillslope between the two wells, a geometric mean $\overline{K_g}$ of the two $\overline{K_{sat}}$ values were computed daily. The geometric mean, rather than an arithmetic mean, was used because K_{sat} of peat soils is highly heterogeneous (e.g. Chason and Siegel, 1986) varying by orders of magnitude even within the peat plateau (Figure 2-2). Replacing K in Eq. (2.6) by $\overline{K_g}$, the subsurface runoff from the peat plateau (R_2) was computed from:

$$R_2 = -\overline{K_g}\, y_{\text{m}} [(h_2 - h_1)/(x_2 - x_1)] / x_{m.} \tag{2.9}$$

2.4 Results and discussion

2.4.1 Snowmelt (*M*), rainfall (*P*), and evapotranspiration (*ET*)

The water balance (Eq. 2.1) was computed for the spring melt regime, from March 29 to June 4, 2004 and April 19 to June 8, 2005. The computations were split into two periods: the snowmelt runoff period, defined in this study as time from maximum SWE to when the snowpack completely disappeared from the Study plateau (period 1); and the following 3-4 week period from the day the Study plateau became snow free to

the end of the field campaign, during which time the spring freshet had ended (period 2) (Table 2-1).

During the two years of study, the late winter snowpack contributed 63% (in 2004) and 46 % (in 2005) of the total precipitation input to the Study plateau from late March to September. The SWE reached a maximum and the main phase of snowmelt started on March 29 in 2004, which was 20 days earlier than the maximum SWE in 2005 (Table 2-1). The average daily air temperature during snowmelt was 0.67 ^{o}C in 2004 (Figure 2-3(a)) compared with 2.1 ^{o}C in 2005 (Figure 2-4(a)). This reflects the more intensive melt pattern of 2005 (Figure 2-4(b)) compared to a relatively gradual melt, interspersed with sub-0 ^{o}C temperatures and additional snowfall events, in the preceding year (Figure 2-3(b)). So, although the snow pack yielded similar amounts of water in both years (202 mm in 2004 and 206 mm in 2005), it melted in about half the time in 2005 (Figure 2-3(b), 2-4(b)). An additional 20 mm SWE fell after the plateau became snow free in 2004, which resulted in 16 mm more melt water input to the plateau in 2004 relative to 2005 (Table 2-2).

Both study years had a higher than normal (from 1964-2005) amount of spring rainfall (MSC, 2005). In 2004, 53 mm of rain fell during the 68-day measurement period for the water balance computations, 91% of which was deposited in the three-day event of May 25-27 (Figure 2-3(c)). In 2005, 63 mm fell during the 51-day measurement period (Figure 2-4(c)).

Evapotranspiration from snow-free surfaces commenced on April 25 in 2004 and April 24 in 2005. The mean daily evapotranspiration rates varied dramatically between

the three different cover types of moss, lichen, and melt water pools (Figure 2-5), with moss surfaces evaporating at much higher rates than lichen surfaces and pools located in low-lying areas (Table 2-3). The greater evaporative loss from moss soils relative to those underlain by lichen was mostly due the differences in near-surface moisture availability (as detailed in the following section). The difference in evaporation rates between moss and melt water pools was most likely due to the water wicking capability of moss species (Vitt, 2000), their greater aerodynamic roughness compared to pools, and to their higher landscape position relative to the pools (Lafleur and Schreader, 1994). Mean daily evapotranspiration for the plateau weighted according to the proportion of moss, lichen and pools was 1.4 ± 0.5 mm for the 2004 study period, and 1.5 ± 0.5 mm for the 2005 study period. The cumulative weighted evapotranspiration by the end of spring melt on June 4, 2004 was 56 mm, and 67 mm on June 8, 2005 (Table 2-2).

2.4.2 Active layer melt (I_M) and soil water storage (ΔS)

Rainfall recorded at the Study plateau from August to November of 2003 was 140 mm, approximately two and a half times the depth that fell over the same period in 2004 (55 mm). As a result, pre-freeze-up value of available soil storage capacity (S_c) was 53 mm smaller in the autumn of 2003 compared to the drier autumn of 2004. If it is assumed that over-winter changes in soil moisture storage are similar in both years, then the capacity of the active layer to absorb melt and rainfall inputs would have been proportionately higher in the melt period of 2005 than during the same period of 2004. This seems reasonable given the relatively small increase in soil water content prior to melt in 2005, as described below.

In 2005, the WCR at 0.1 m indicated an increase in water content on 11 April (Figure 2-4(d)), likely in response to meltwater infiltration from an early snow melt event (Figure 2-4(b)), as the soils were still largely frozen (Figure 2-4(e)) (Stein and Kane, 1983). By 27 April, when soil thaw began in 2005, the liquid water content at this depth had increased by approximately 0.15 since 11 April (Figure 2-4(d)). This 15 mm increase in water content at 0.1 m potentially reduced the difference in the S_c, estimated at soil freeze-up between the two years, from 53 mm to 38 mm, as no similar increase in water content was indicated by the WCR at 0.1 m in 2004 until 4 May (Figure 2-3(d)), two days after soil thaw began (Figure 2-3(e)).

The timing of soil thaw initiation also played a role in the amount of active layer ice melt that occurred during the snowmelt runoff period (period 1) in both years. Active layer ice melt during this period was 26 mm higher in 2005 than in 2004, mostly due to the warmer air and soil temperatures (Figures 2-3(a), (c) and 2-4(a) and (c)) and the earlier initiation of ice melt in 2005 (Figure 2-3(e) and 2-4(e)); while during period 2, 25 mm more ice melt was produced in 2004 relative to 2005 (Table 2-2). The cumulative input of water from ice melt in the active layer at the Centre pit was 162 mm in the 34-day measurement period of 2004 and 163 mm in the 43-day period of 2005 (Table 2-2), or 37% and 38% of the total water budget inputs during spring melt in 2004 and 2005, respectively.

Soil moisture conditions at the Centre pit, like ice melt, were similar in both years. Soil moisture storage at the Centre pit was computed from the day soil thaw was initiated to the end of the study period: May 2 to June 4, 2004 and April 27 to June 8, 2005. During this time, the total change in liquid water content ΔS at the Centre pit was 9

mm greater in 2005 than 2004 (Table 2-2). ΔS was also measured at 15 sampling points for comparison with ΔS measured at the Centre pit. The daily standard deviation of soil moisture measured at the 15 sampling points varied from 31 mm to 96 mm, indicating a high spatial variability in moisture conditions on the peat plateau. When the average ΔS values of the 15 points are added for the 25 days when the data were available, the total ΔS was 47 mm, while the total ΔS for the Centre pit for the same 25 days was 44 mm. Thus, the total ΔS measured at the Centre pit was thought to represent the average moisture conditions on the Study plateau during spring melt reasonably well.

2.4.3 Runoff computed from the water balance (R_1)

The total runoff computed over the entire study period was 238 mm in 2004 and 213 mm in 2005 (Table 2-2). As soil thaw at the Centre pit did not occur until May 2 in 2004 and April 27 in 2005, it can not be concluded that all of the runoff computed from equation (2.1) was indeed subsurface runoff. Much of the runoff (84% in 2004 and 70% in 2005) had occurred before the soil began to thaw. However, many authors have found that snow meltwater can enter, percolate, and laterally drain through the organic layer, even under frozen conditions (Woo and Heron, 1987; Quinton and Marsh, 1999; Carey and Woo, 2000), as the near-surface soil layer is typically made porous by an upward flux of moisture to the overlying snowpack during winter (Smith and Burn, 1987). Snow meltwater may have also been stored in surface depressions beneath the snowpack for a short period of time before infiltrating into the soil or draining laterally through the organic layer.

A comparison of the water balances (Table 2-2), showed that both years had significantly larger runoff totals and flow rates during snowmelt (period 1), compared to the weeks following (period 2). During the snowmelt period, the difference in runoff timing between the two years was mostly due to differences in the initiation of snowmelt and soil thaw. Subsurface drainage rates decreased after the snowmelt runoff period (period 2), as ET and ΔS increased (Table 2-2). The melt of ground ice resulted in a large source of water to the peat plateau; however, most of this input (88-93%) was detained in the soil as ΔS (Table 2-2). The ratios of runoff to precipitation computed for the snowmelt runoff period (Table 2-2) are similar to those published for other permafrost environments (Kuchment *et al*., 2000).

2.4.4 Uncertainty in the water balance calculation

To estimate the accuracy of M in equation (2.1), the standard deviation of all SWE measurements was calculated daily. The average of all daily SWE standard deviations was 11% of the maximum SWE in 2004 and 15% in 2005. The potential error in measuring evapotranspiration, taken to be equal to the areally weighted, mean daily standard error of the five pool evaporation pans, and the five moss and five lichen lysimeters, was 0.15 mm day^{-1}, or 9% of the mean daily evapotranspiration for the 28 days in which ET was measured in 2005. For those days in which ET had to be estimated from equation (2.3), errors could be as high as 15% (Shuttleworth, 1993).

The accuracy of the computations of the melt of ice in the active layer is difficult to assess owing to the uncertainty of the performance of the CS615 water content meters in frozen conditions, which is not well known. For unfrozen conditions, their accuracy is

expected to be ± 2%, as they were calibrated for the peat soils at the Study plateau. The time domain reflectometry (TDR) calibration equations of Spaans and Baker (1996) cannot be applied directly to CS615 data (Seyfried and Murdock, 1996). The use of TDR probes in measuring the dielectric permittivity to determine the liquid water content of unfrozen soils has been found to be highly accurate and relatively similar to CS615 WCR results under the same moisture conditions (Seyfried and Murdock, 2001; Yoshikawa *et al*., 2004). Thus, the potential error of using the CS615 to measure the liquid water content in frozen soils is assumed to be 0.02 m^3 m^{-3} based on the relative errors published for TDR sensors (Spaans and Baker, 1995). It is difficult to estimate the magnitude of errors associated with the estimate of the total water content (θ_T) prior to snowmelt, however, we feel that an error of 10-20% is appropriate for this parameter based on the inter-annual variability in the fall water content.

Although equation 2.1 includes all readily measurable water balance terms, it does not include a term that accounts for runoff inputs from upslope areas. These lateral inputs appeared to have an influence on the calculation of R_1 from equation (2.1). For example, several instances were noted where the increase in soil moisture following a rain event exceeded the depth of rainfall. Ponding occurred at the Centre pit during snowmelt and following heavy rain, suggesting that the Centre pit was susceptible to runoff inputs. Consequently, Figure 2-6 shows instances of negative runoff, indicating that the subsurface drainage to the soil pit was greater than the runoff from the pit. If it is assumed that the sum of the negative runoff computed for the study period was caused only by lateral inputs to soil storage, then the potential error of ΔS would be 13% in 2004 and 24% in 2005.

Based on the error estimates of individual water balance components, and noting that some errors may cancel each other over the entire period, we expect that the computed runoff (R_1) in Table 2-2 may have an error margin of 20-30%, although this only provides a rough estimate.

2.4.5 Runoff computed from hydraulic conductivity and gradient (R_2)

Subsurface runoff computations commenced (when the water table was measurable in both the West and Centre wells) on April 26 in 2004, 28 days after maximum SWE (and the start of R_1 computations), and on April 22, three days after maximum SWE, in 2005 (Figure 2-7). The total R_2 during spring melt was 175 mm in 2004 and 196 mm in 2005, whereas the total R_1 was 238 mm in 2004 and 213 mm in 2005. Thus, the two methods used to compute runoff (R_1 and R_2) from the Study plateau produced relatively similar runoff totals for the spring melt in 2005; given the relative errors of the water balance approach (Table 2-2; section 2.4.4) and an estimated 20% margin of error in R_2, which is largely based on the high heterogeneity of K_{sat} found on the plateau (Figure 2-2). To explain the difference between R_1 and R_2 for 2004, we note that sub-0 ^{o}C air temperatures occurred throughout the melt season in 2004 (Figure 2-3(a)), which may have caused the snowmelt water to re-freeze in the upper soil (depth < 10 cm) and melt again at a later date, when air temperatures increased. The re-freezing of melt water was not accounted for in equation (2.1) because the shallowest WCR was at 10 cm, and also because the WCR was insensitive to the change in ice content. Temporary surface ponding of snowmelt water beneath the snowpack was also not accounted for. Therefore, equation (2.1) may have overestimated runoff during the early

snowmelt period, prior to April 26, 2004. It is also important to note that the R_2 computation missed 28 days of the snowmelt period in 2004, because of a delay in the water table formation in the wells, possibly due to the sub-0 ^{o}C air temperatures that occurred throughout the melt season (Figure 2-3(a)). Although the peat normally transmits water readily when thawed, frozen icy peat may have inhibited lateral flow to the wells, which may have also caused some of the 63 mm difference in runoff amounts computed from the two methods (R_1 and R_2) in 2004.

The hydrographs for flows computed from the water balance and the hydraulic method are illustrated in Figure 2-7 for both years. The hydrographs for both years follow a similar pattern, with high flows in response to snowmelt when the water and frost tables were near the ground surface, followed by a general decline as the saturated layer became deeper with time and there were smaller water inputs to the Study plateau. The slow runoff recession of R_2 relative to snowmelt in 2005 implies that there was temporary storage in the soil (which is consistent with the larger pre-melt S_c in 2005, relative to S_c in 2004). The minimal lag between rain events and hydrograph response of R_2 in both years suggests that much of the runoff produced from rain events is rapidly transported to the adjacent wetlands. For example, in 2004, the largest peak flow was in response to a 49 mm rain event that occurred from May 25-28 (Figure 2-7). This event produced a relatively rapid (same day) runoff response from the hillslope. Early rain events in 2005, such as the 22 mm rain event that occurred on May 18-19, also produced a rapid and relatively large runoff response (Figure 2-7). However, there was a 2-day delay in runoff from the plateau during the larger (34 mm) rain event on June 2-4, 2005. This delay,

coupled with the smaller runoff amount relative to the May 18-19 rain event, suggests that much of the water went to soil storage.

2.5 Conclusion

Melting snow water constitutes a significant portion of the annual water input to the peat plateau, and was the largest contributor to runoff during spring melt. In both years, flow rates were significantly larger during the snowmelt runoff period, when there was more available water and frost table depths were shallow, than in the subsequent 3-4 weeks. During snowmelt, over half of the water inputs to the hillslope went to runoff. A major influence on the volume of runoff from the peat plateau during snowmelt was the soil storage deficit of the thawed layer, which had to be satisfied before water inputs could be transmitted downslope. After the snowmelt runoff period, subsurface drainage rates declined dramatically, as the majority of water inputs went to soil storage. The minimal lag between rain events and hydrograph response in both years suggests that much of the runoff produced from rain events is rapidly transported to the adjacent wetlands. The melt of ground ice was a significant source of water to the peat plateau during the study periods; however, most of this water was detained in soil storage. Evapotranspiration from the plateau was relatively low and was of roughly equal magnitude to precipitation inputs. The results show the importance of correctly accounting for changing storage and storage capacity in hydrological models that are applied to permafrost hillslopes; specifically to accurately account for snow melt inputs and antecedent moisture conditions, as they are important in determining the runoff response of peat plateaus during spring melt.

Two methods (a water balance and Dupuit-Forchheimer approximation) were used to estimate spring runoff in this study, both of which yielded similar results. This suggests that the Dupuit-Forchheimer approximation may provide a simpler approach to accurately estimating the amount of runoff from peat plateaus compared to the field-intensive water balance approach; this assumes that an average K_{sat} value, representing the heterogeneous peat on the hillslope, can be obtained.

2.6 Figures

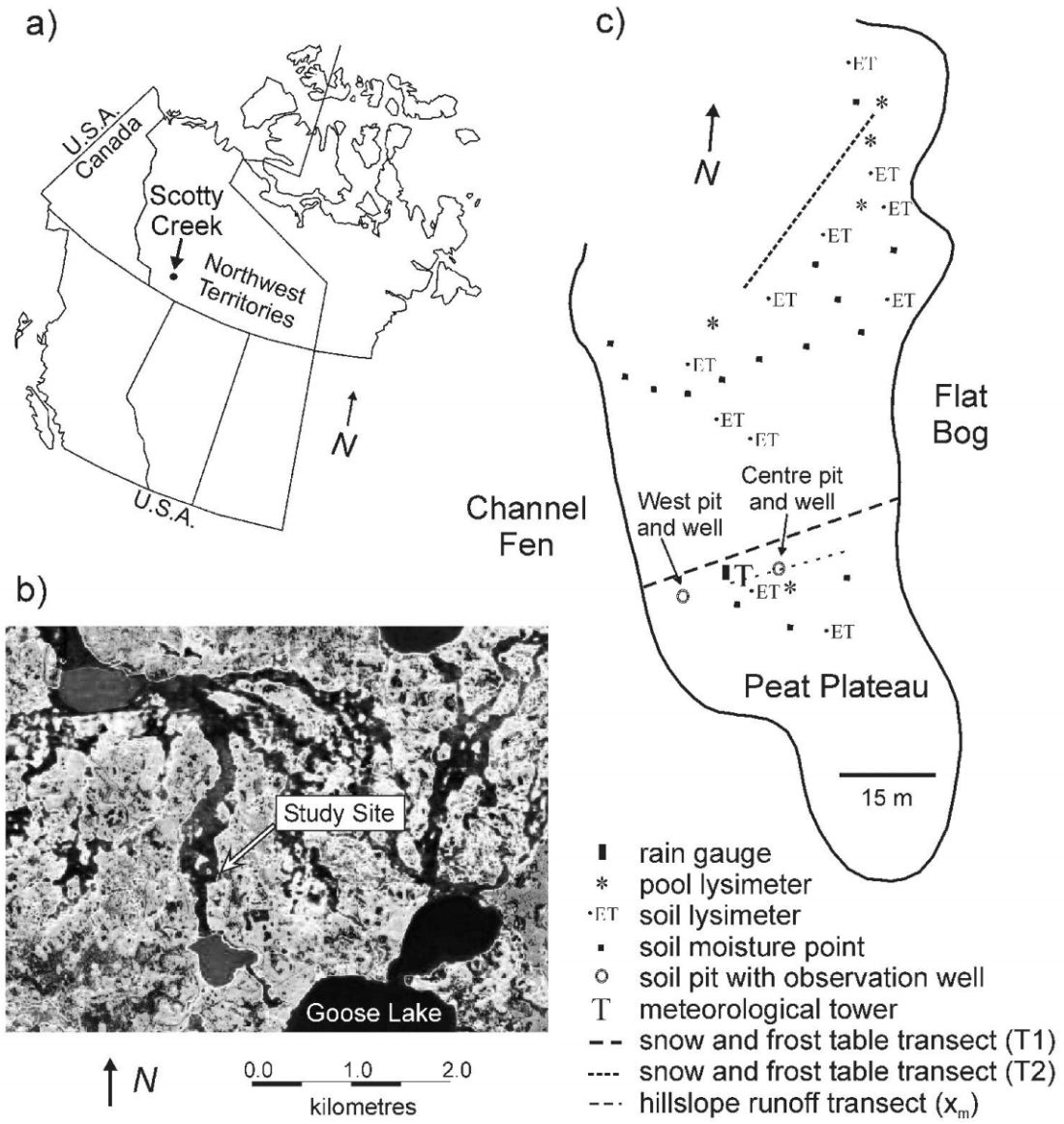

Figure 2-1 a) The location of the Scotty Creek basin within north-western Canada. b) A sample of the high-resolution (4 m × 4 m) IKONOS image showing a 22 km^2 section in the southern part of Scotty Creek basin where field studies are concentrated. The unclassified image has been converted from false-colour to a grey scale. Channel fens appear relatively dark compared with the surrounding areas composed of flat bogs and peat plateaus. c) The peat plateau study site with the location of instrumentation.

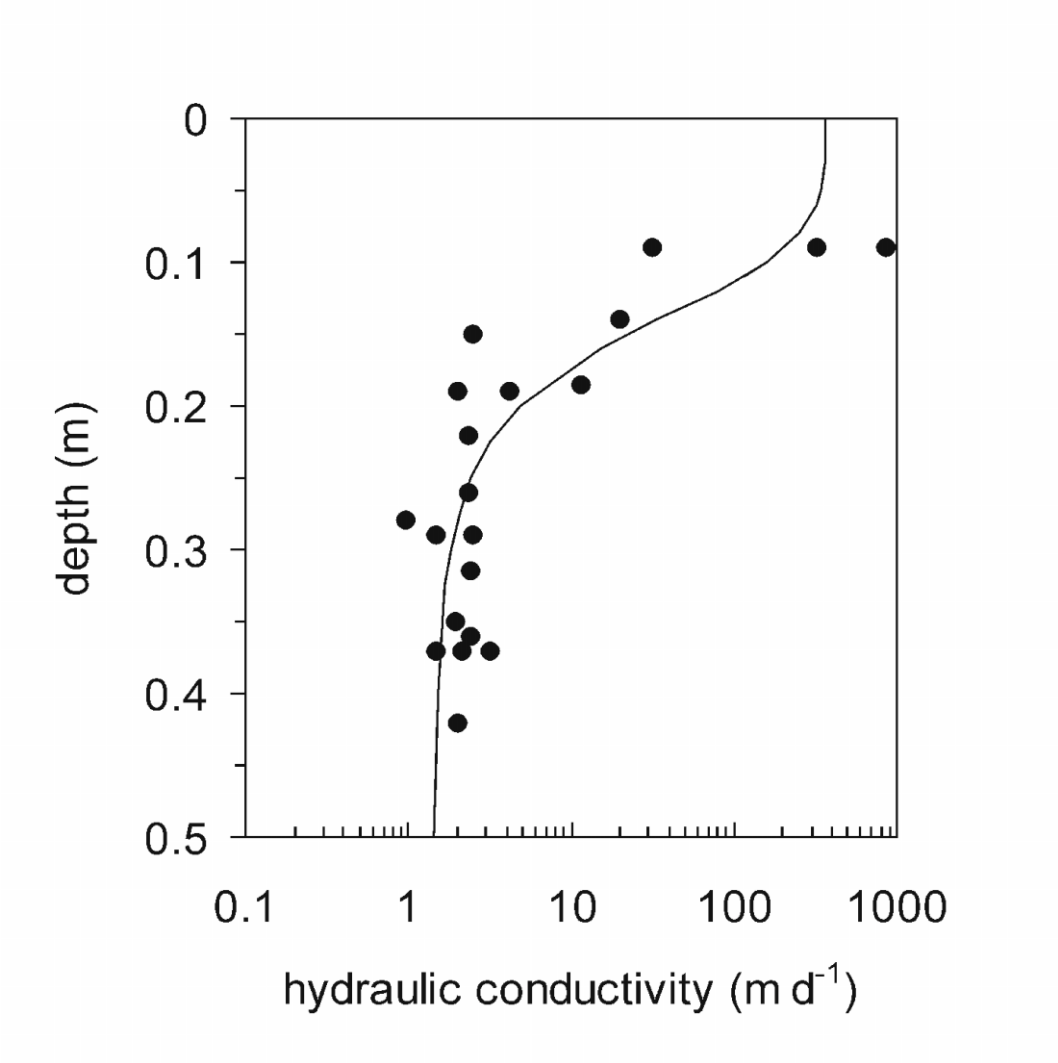

Figure 2-2 Saturated hydraulic conductivity with depth from the ground surface, measured at the peat plateau in Scotty Creek using various field and laboratory methods. The sold line indicates the best-fit function determined by Quinton *et al.* (2008) from non-linear, least-squared regression.

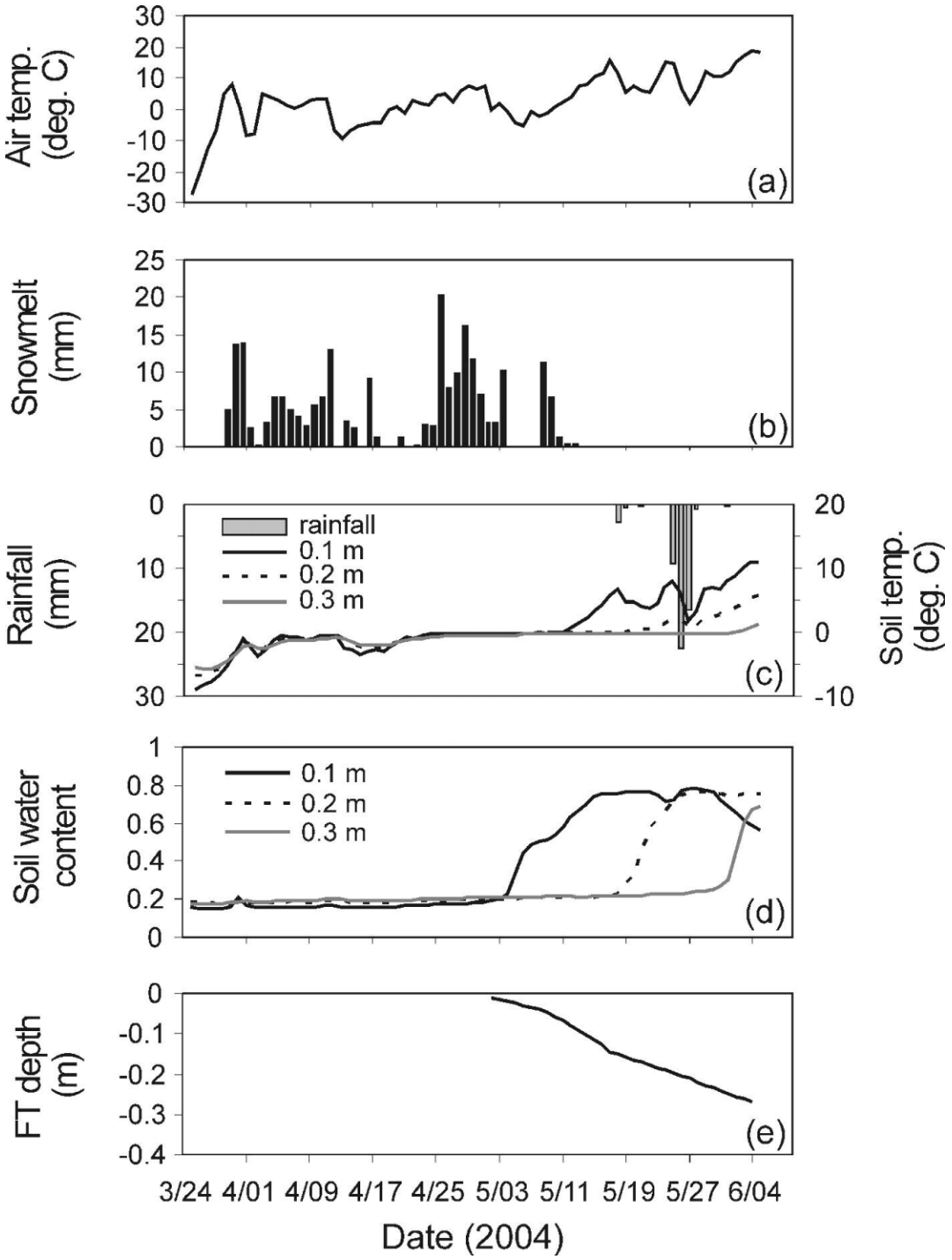

Figure 2-3 2004 (a) air temperatures (Air temp.); (b) daily snow melt plotted from the day of maximum SWE; (c) rainfall depth plotted with soil temperatures (Soil temp.) measured at the Centre pit; (d) soil volumetric water content measured at the Centre pit; and (e) frost table (FT) depth relative to the ground surface, measured manually at the Centre pit with a graduated steel rod.

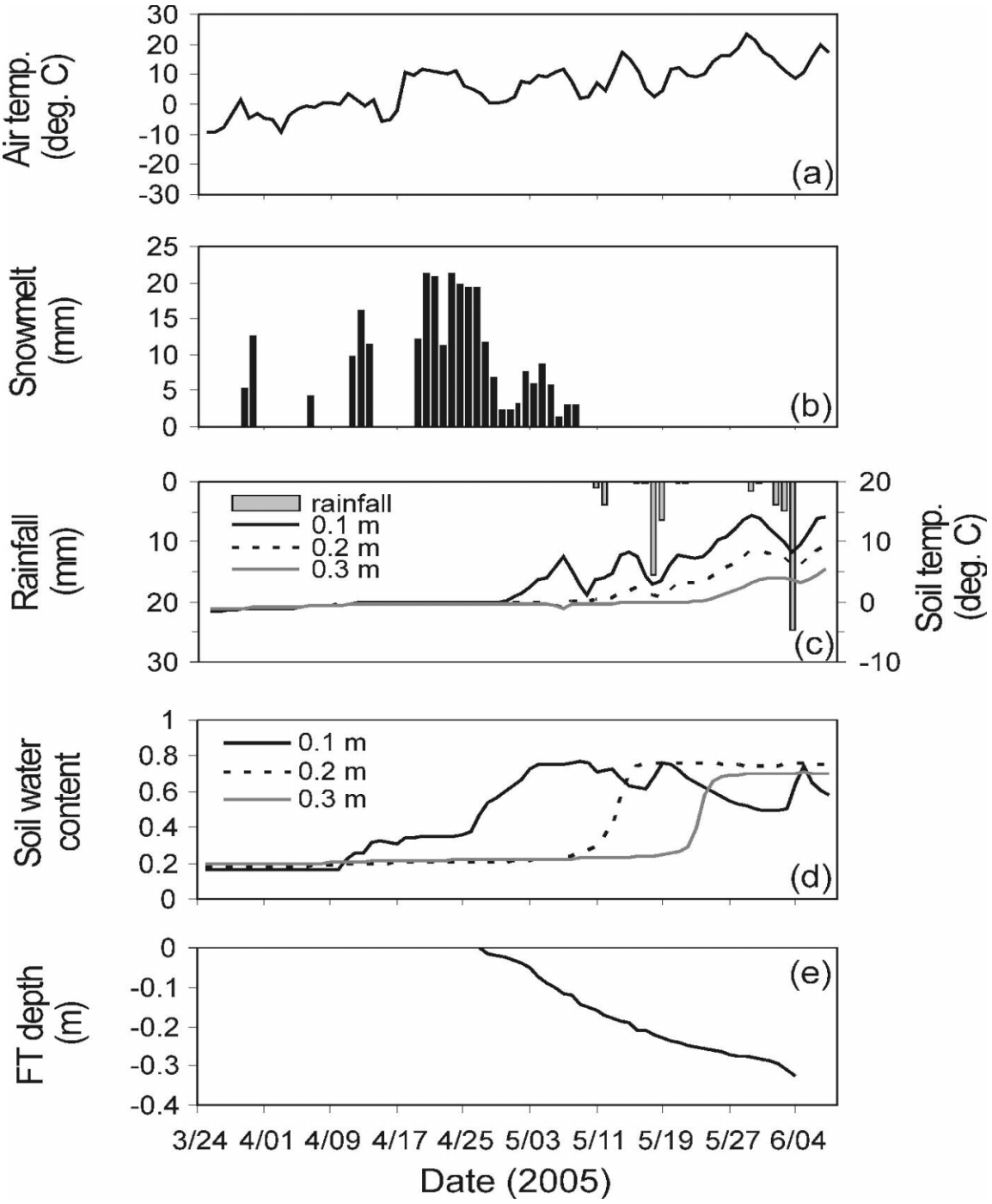

Figure 2-4 2005 (a) air temperatures (Air temp.); (b) daily snow melt (note: water balance computations begin on the day of maximum SWE, April 19); (c) rainfall depth plotted with soil temperatures (Soil temp.) measured at the Centre pit; (d) soil volumetric water content measured at the Centre pit; and (e) frost table (FT) depth relative to the ground surface, measured manually at the Centre pit with a graduated steel rod.

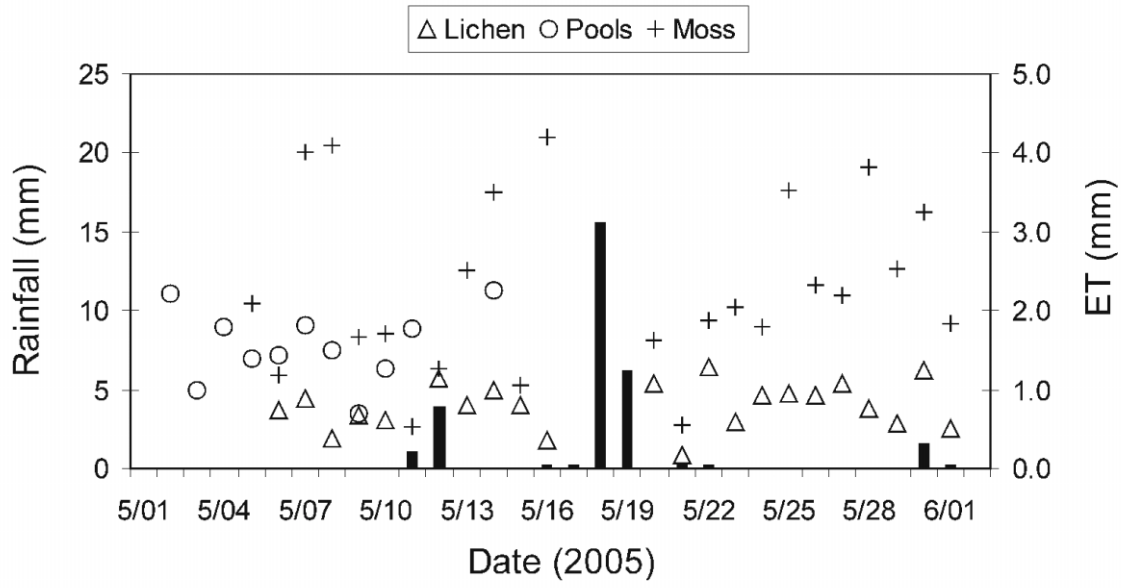

Figure 2-5 Daily evapotranspiration (ET) from moss and lichen-covered ground surfaces, and evaporation from melt water pools, measured on the Study plateau from May 2 to June 1, 2005, plotted with rainfall depth. Days not shown were computed from the Priestley and Taylor (1972) method. Note that melt water pools were too shallow for measurement after May 14, as much of the standing water had drained and/or evaporated.

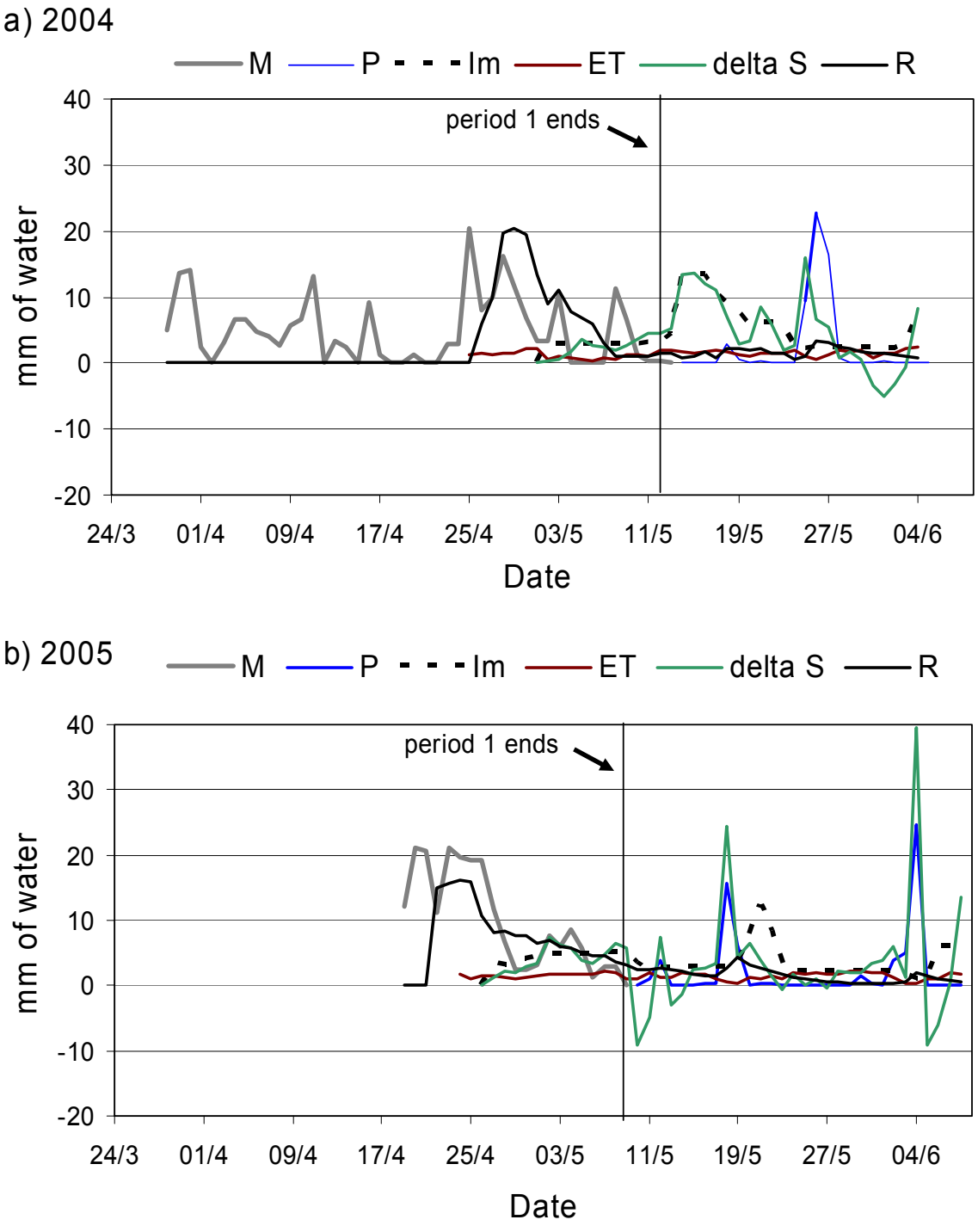

Figure 2-6 Daily values (in mm) of the water balance components, where M is snowmelt, P is rainfall, Im is active layer ice melt, ET is evapotranspiration, delta S is change in soil storage, and R is runoff computed using soil moisture measurements at the Centre pit in a) 2004 and b) 2005.

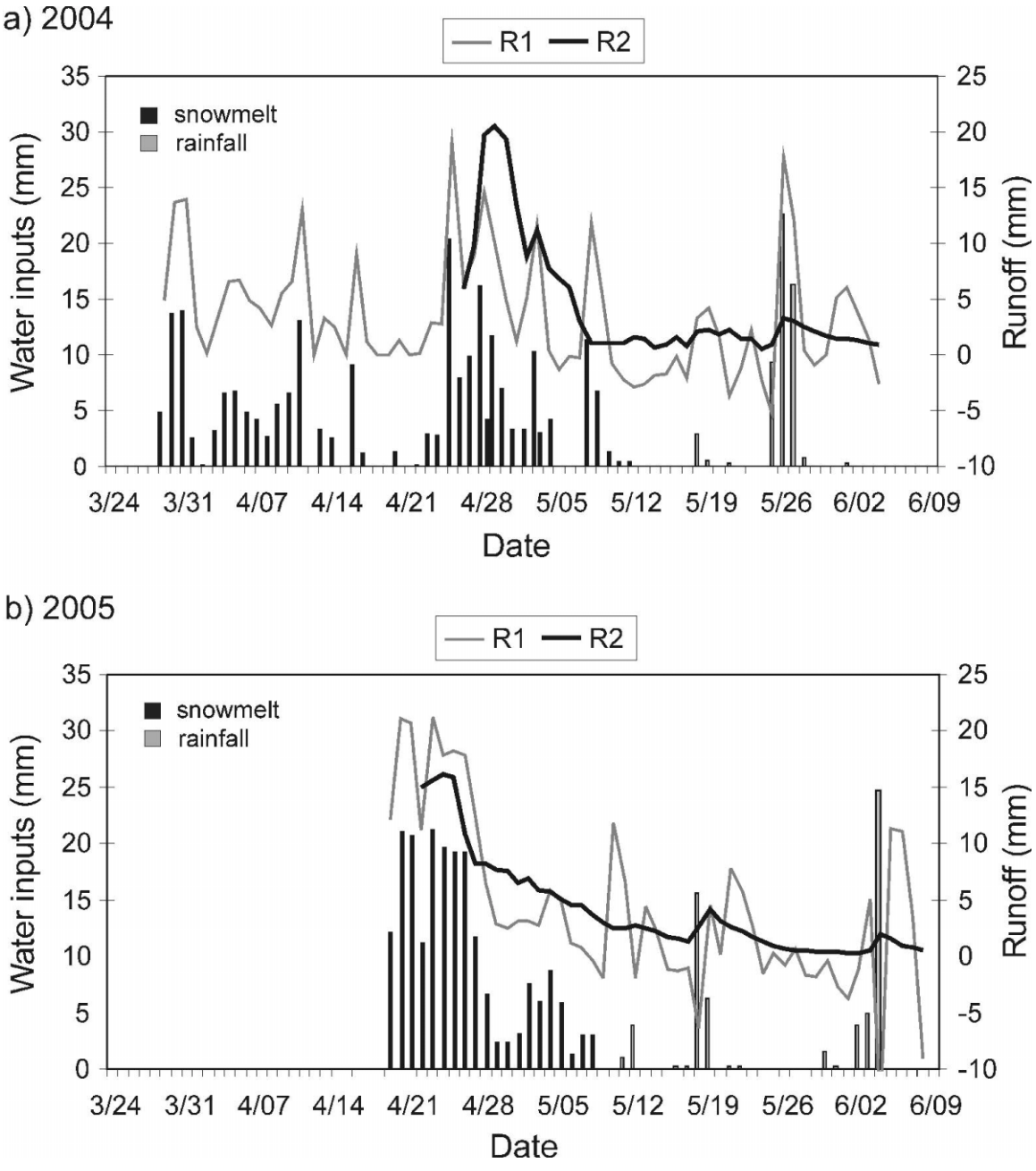

Figure 2-7 Daily snowmelt and rainfall depth, plotted with subsurface runoff computed from the water balance (R_1) and from the hydraulic method (R_2) during the a) 2004 and b) 2005 study periods. Note that R_2 computed from Eq. (2-9) was converted from m day^{-1} to mm day^{-1} for comparison with R_1.

2.7 Tables

Table 2-1 Measurement periods for the water balance computations. Period 1 represents the snowmelt runoff period, during which time the plateau was snow covered, and period 2 represents the 3-4 weeks from the day the plateau became snow free to the end of the field campaign. Not all measurements started on the same day, due to frozen soils and/or snow cover; a summary of the start dates for various measurements of the water balance computations is listed in italics.

	2004	**2005**
Period 1	March 29 - May 12	April 19 - May 9
Period 2	May 13 - June 4	May 10 - June 8
Ice melt	*May 2*	*April 27*
Soil moisture	*May 2*	*April 27*
Evaporation	*April 25*	*April 24*

Table 2-2 Water balance computations for the 2004 and 2005 spring melt regime (period 1+2): March 29 to June 4, 2004 and April 19 to June 8, 2005, broken up into the snowmelt runoff period (period 1), and the following 3-4 weeks, during which time the Study plateau was snow-free and the spring freshet had ended (period 2). The runoff ratio in this instance is equal to R_1/ (M + P). The runoff rate (mm day^{-1}) is the average daily rate of runoff computed from R_1 over the specified time period. All other values are expressed in mm. Error estimates recorded in the table are the highest estimates noted in section 2.4.4.

2004	Snowmelt M	Precipitation P	Active Layer Melt I_M	Evaporation ET	Soil moisture change ΔS	Computed runoff R_1	Runoff ratio	Runoff rate
Period 1	202 ± 22	0	32 ± 6	21 ± 3	29 ± 4	204 ± 61	0.92	4.5
Period 2	20 ± 2	53 ± 1	130 ± 26	35 ± 5	114 ± 15	34 ± 10	0.64	1.5
Period 1 + 2	222 ± 24	53 ± 1	162 ± 32	56 ± 8	143 ± 19	238 ± 71	0.87	3.5

2005	Snowmelt M	Precipitation P	Active Layer Melt I_M	Evaporation ET	Soil moisture change ΔS	Computed runoff R_1	Runoff ratio	Runoff rate
Period 1	206 ± 31	0	58 ± 12	25 ± 2	55 ± 13	184 ± 55	0.89	8.8
Period 2	0	63 ± 1	105 ± 21	42 ± 4	97 ± 23	29 ± 9	0.46	1.0
Period 1 + 2	206 ± 31	63 ± 1	163 ± 33	67 ± 6	152 ± 36	213 ± 64	0.79	4.2

Table 2-3 Mean daily evapotranspiration and standard deviation (mm) for the dominant ground covers of moss and lichen on the plateau measured from May 2 to June 1, 2005, and the mean daily evaporation from meltwater pools from May 2 to May 14 (after which time the standing water had drained and/or evaporated). Average α represents the ratio of actual (lysimeter) to equilibrium evapotranspiration (mm) (Eq. (2.3)). The average α of the peat plateau ground surface, based on the percent coverage of the three cover types, ranged from 0.68-0.91.

	Moss	Lichen	Water
Mean ET:	2.3 ± 1.1	0.79 ± 0.3	1.56 ± 0.48
average α:	1.19 ± 0.61	0.42[†] ± 0.23	1.11 ± 0.4

[†]Relatively low near-surface soil moisture was the primary reason that lichen soils had an average α value less than 1.

2.8 Reference List

Arain, M.A., Black, T.A., Barr, A.G., Griffis, T.J., Morgenstern, K. and Nesic, Z. 2003. Year-round observations of the energy and water vapour fluxes above a boreal black spruce forest. *Hydrological Processes* 17: 3581-3600.

Aylsworth, J.M., Kettles, I.M. and Todd, B.J. 1993. Peatland distribution in the Fort Simpson area, Northwest Territories with a geophysical study of peatland-permafrost relationships at Antoine Lake. *Current Research, Geological Survey of Canada Paper* 93-1E: 141-148.

Beilman, D.W. and Robinson, S.D. 2003. Recent discontinuous permafrost melt in peatlands along a climatic gradient in western Canada: large-scale peatland mapping. *Proceedings of the 8th International Conference on Permafrost*, Zurich, Switzerland, Vol. 1, 61-65.

Brown, J., Hinkel, K. M. and Nelson, F. E. 2000. The Circumpolar Active Layer Monitoring (CALM) program: Research designs and initial results. *Polar Geogr*. 24: 165– 258.

Burgess, M.M. and Smith, S.L. 2000. Shallow ground temperatures. In *The physical environment of the Mackenzie Valley, Northwest Territories: a base line for the assessment of environmental change*, Dyke LD, Brooks GR (eds). Geological Survey of Canada Bulletin 547: 89-103.

Camill, P. 1999. Patterns of boreal permafrost peatland vegetation across environmental gradients sensitive to climate warming. *Canadian Journal of Botany* 77(5): 721-733.

Camill, P. 2005. Permafrost thaw accelerates in boreal peatlands during late-20th century climate warming. *Climate Change* 68: 135-152.

Carey, S.K. and Woo, M.-K. 2000. The role of soil pipes as a slope runoff mechanism, SubarcticYukon, Canada. *Journal of Hydrology* 233: 206-222.

Chason, D.B. and Siegel, D.I. 1986. Hydraulic conductivity and related physical properties of peat, Lost River Peatland, northern Minnesota. *Soil Science* 142: 91-99.

Childs, E.C. 1971. Drainage of groundwater resting on a sloping bed. *Water Resources Research* 7: 1256-1263.

Dingman, S.L. 1970. Hydrology of the Glenn Creek watershed, Tanana River basin, central Alaska. U.S. Army *CRREL Research Report 297*; 111 p.

Dingman, S.L. 1971. Hydrology of the Glen Creek Watershed in central Alaska. U.S. Army *CRREL Research Report 279*; 112 p.

Dingman, S.L. 1973. Effects of permafrost on streamflow characteristics in the discontinuous permafrost zone of central Alaska. In *Permafrost: the North American contribution to the Second International Conference, Yakutsk, U.S.S.R*. Washington, National Academy of Sciences; 447-453.

Frauendeld, O.W., Zhang, T., Barry, R.G. and Gilichinsky, D. 2004. Intedecadal changes in seasonal freeze and thaw depths in Russia. *J. Geophys. Res.* 109: D05101.

Glenn, M.S. and Woo, M-K. 1987. Spring and summer hydrology of a valley-bottom wetland, Ellesmere Island, Northwest Territories, Canada. *Wetlands* 17: 321-329.

Goodison, B.E. 1978. Accuracy of snow samplers for measurement of shallow snowpacks: An Update. In *Proceedings of the 34th Eastern Snow Conference*, Hanover, New Hampshire, 36-49.

Gray, D.M. and Granger, R.J. 1986. In situ measurements of moisture and salt movement in freezing soils. *Canadian Journal of Earth Sciences* 23(5): 696 704.

Gray, D.M. and Granger, R.J. 1989. Evaporation from natural non-saturated surfaces. *Journal of Hydrology* 111: 21-29.

Grosse-Brauckman, G. 1976. In *Mooor- und Torfkunde*, E. Scheizerbart'sche Verlag, Nagele und Obermiller, Stuttgart. Quoted in: Parent, L.E. and Caron, J. 1993. Physical Properties of Organic Soils. In *Soil sampling and methods of analysis*, M.R. Carter (ed). Canadian Society of Soil Science, Lewis Publishers, p.442

Harris, C., Vonder Mühll, D., Isaksen, K., Haeberli, W., Sollid, J.L., King, L., Holmlund, P., Dramis, F., Guglielmin, M. and Palacios, D. 2003. Warming permafrost in European mountains. *Global and Planetary Change* 39: 215–225.

Hayashi, M., Quinton, W.L., Pietroniro, A. and Gibson, J.J. 2004. Hydrologic functions of wetlands in a discontinuous permafrost basin indicated by isotopic and chemical signatures. *Journal of Hydrology* 216: 81-97.

Hayashi, M., Goeller, N., Quinton, W.L. and Wright, N. 2007. A simple heat-conduction method for simulating frost table depth in hydrological models. *Hydrological Processes* 21: 2610-2622.

Heginbottom, J.A. and Radburn, L.K. 1992. Permafrost and ground ice conditions of Northwestern Canada. *Geological Survey of Canada, Map 1691A*, scale 1:1 000 000.

Hinzman, L. D., Kane, D. L., Gieck, R. E. and Everett, K. R. 1991. Hydrologic and thermal properties of the active layer in the Alaskan Arctic, *Cold Regions Science and Technology* 19: 95–110, 1991.

Ivanov, K.E., 1981. Water movement in mirelands, translated by A. Thomson and H.A.P. Ingram. Academic Press, Toronto (p. 276).

Jorgenson, M.T., Racine, C.H., Walters, J.C. and Osterkamp, T.E. 2001. Permafrost degradation and ecological changes associated with a warming climate in central Alaska. *Climatic Change* 48: 551-579.

Kane, D.L. 1980. Snowmelt infiltration into seasonally frozen soils. *Cold Regions Science and Technology* 3: 153-161.

Kane, D.L. and Stein, J. 1983. Water movement into seasonally frozen soils. *Water Resources Research* 19: 1547-1557.

Kimball, J.S., White, M.A. and Running, S.W. 1997. BIOME-BGC simulations of stand hydrologic processes for BOREAS. *Journal of Geophysical Research* 102(D24): 29,043-29,051.

Kuchment, L.S., Gelfan, A.N. and Demidov, V.N. 2000. A distributed model of runoff generation in the permafrost regions. *Journal of Hydrology* 240:1-22.

Lafleur, P.M. and Schreader, C.P. 1994. Water loss from the floor of a subarctic forest. *Arctic Alpine Research*, 26: 152–158.

Marsh, P. and Pomeroy, J.W. 1996. Meltwater fluxes at an arctic forest-tundra site. *Hydrological Processes* 10: 1383-1400.

McEnroe, B.M. 1993. Maximum saturated depth over landfill liner. *Journal of Environmental Engineering* 109: 262-270.

McNamara, J.P., Kane, D. L. and Hinzman, L. D. 1997. Hydrograph separations in an Arctic watershed using mixing model and graphical techniques. *Water Resources Research* 33(7): 1707-1719.

Metcalfe, R.A. and Buttle, J.M. 1999. Semi-distributed water balance dynamics in a small boreal forest basin. *Journal of Hydrology* 226: 66-87.

National Wetlands Working Group (NWWG) 1988. *Wetlands of Canada: Ecological Land Classification Series, no. 24*. Sustainable Development Branch, Environment Canada, Ottawa, Ontario, and Polyscience Publications Inc., Montreal, Quebec; 452 pp.

Nijssen, B., Haddeland, I. and Lettenmaier, D. 1997. Point evaluation of a surface hydrology model for BOREAS. *Journal of Geophysical Research* 102(D24): 29,367-29,378.

Pattey, E., Desjardins, R.L. and St-Amour, G. 1997. Mass and energy fluxes over a black spruce forest during key periods of BOREAS 1994. *Journal of Geophysical Research* 102(D24): 28,967-28,975.

Priestley, C.H.B and Taylor, R.J. 1972. On the assessment of surface heat flux and evaporation using large-scale parameters. *Monthly Weather Review* 100(2): 81-92.

Quinton, W.L. and Gray, D.M. 2001. Estimating subsurface drainage from organic-covered hillslopes underlain by permafrost: toward a combined heat and mass flux model. Soil-Vegetation-Atmosphere Transfer Schemes and Large-Scale Hydrological Models. *Sixth IAHS Scientific Assembly*, Maastricht, Netherlands; 333-341.

Quinton, W.L., Gray, D.M. and Marsh, P. 2000. Subsurface drainage from hummock-covered hillslope in the Arctic tundra. *Journal of Hydrology* 237: 113-125.

Quinton, W.L. and Hayashi, M. 2005. The flow and storage of water in the wetland-dominated central Mackenzie River basin: Recent advances and future directions. In: *Prediction in ungauged basins: Approaches for Canada's cold regions*, C. Spence, J.W. Pomeroy and A. Pietroniro (eds). Canadian Water Resources Association, Cambridge Ontario; pp. 45-66.

Quinton, W.L., Hayashi, M. and Carey, S.K. 2008. Peat hydraulic conductivity in cold regions and its relation to pore size geometry. *Hydrological Processes* 22: 2829-2837.

Quinton, W.L., Hayashi, M. and Pietroniro, A. 2003. Connectivity and storage functions of channel fens and flat bogs in northern basins. *Hydrological Processes* 17: 3665-3684.

Quinton, W.L. and Marsh, P. 1998. Melt water fluxes, hillslope runoff and stream flow in an Arctic permafrost basin. In *Permafrost 7th International Conference*, Yellowknife, Canada, Lewkowicz AG, Allard M (eds), Laval University Press; 921-926.

Quinton, W.L. and Marsh, P. 1999. A conceptual framework for runoff generation in a permafrost environment. *Hydrological Processes* 13: 2563-2581.

Quinton, W.L., Shirazi, T., Carey, S.K. and Pomeroy, J.W. 2005. Soil water storage and active-layer development in a sub-alpine tundra hillslope, southern Yukon Territory, Canada. *Permafrost and Periglacial Processes* 16: 369-382.

Osterkamp, T. E. 2005. The recent warming of permafrost in Alaska. *Global and Planetary Change* 49 (3-4): 187-202.

Robinson, S.D. and Moore, T.R. 2000. The influence of permafrost and fire upon carbon accumulation in high boreal peatlands, Northwest Territories, Canada. *Arctic, Antarctic and Alpine Research* 32(2): 155-166.

Robinson, S.D., Turetsky, M.R., Kettles, I.M. and Wieder, R.K. 2003. Permafrost and peatland carbon sink capacity with increasing latitude. *Proceedings of the 8th international Conference on Permafrost*, Zurich, Switzerland, Balkema Publishers; Vol. 2: 965-970.

Roulet, N.T. and Woo, M.-K. 1988. Runoff generation in a low arctic drainage basin. *Journal of Hydrology* 101: 213-226.

Rouse, W.R., Douglas, M.S.V., Hecky, R.E., Hershey, A.E., Kling, G.W., Lesack, L., Marsh, P., McDonald, M., Nicholson, B.J., Roulet, N.T. and Smol, J.P. 1997. Effects of climate change on the freshwaters of arctic and subarctic North America. *Hydrological Processes* 11: 873-902.

Serreze, M.C., Walsh, J.E., Chapin III, F.S., Osterkamp, T., Dyurgerov, M.,Romanovsky, V., Oechel, W.C., Morison, J., Zhang, T. and Barry, R.G. 2000. Observational evidence of recent change in the northern high-latitude environment. *Climatic Change* 46: 159-207.

Seyfried, M.S. and Murdock, M.D. 1996. Calibration of time domain reflectometry for measurement of liquid water in frozen soils. *Soil Science* 161: 87–98.

Seyfried, M. S. and Murdock, M.D. 2001. Response of a new soil water sensor to variable soil water content and temperature. *Soil Science Society of America Journal* 65: 28-34.

Shuttleworth, W. J. 1993. Evaporation. In *Handbook of Hydrology*, Maidment DR (ed). McGraw-Hill, New York; 4.1-4.53.

Slaughter, C.W. and Kane, D.L. 1979. Hydrologic role of shallow organic soils in cold climates. In *Canadian hydrology symposium: Proceedings, 79- Cold climate hydrology*. Ottawa, Ontario: National Research Council of Canada; 380-389.

Smith, M.W. and Burn, C.R. 1987. Outward flux of vapour from frozen soils at Mayo, Yukon, Canada: results and interpretation. *Cold Reg. Sci. Tech*. 13, 143-152.

Spaans, E.J.A. and Baker, J.M. 1995. Examining the use of time domain reflectometry for measuring liquid water content in frozen soil. Water *Resources Research* 31: 2917–2925.

Spaans, E.J.A. and Baker, J.M. 1996. The soil freezing characteristic: Its measurement and similarity to the soil moisture characteristic. *Soil Science Society of America Journal* 60: 13-19.

Stein, J. and Kane, D.L. 1983. Monitoring the unfrozen water content of soil and snow using time domain reflectometry. *Water Resources Research* 19: 1573–1584.

Tarnocai, C., Kettles, I.M. and Lacelle, B. 2000. Peatlands of Canada digital database. *Geological Survey of Canada*, Ottawa, Open File 3834. (map and database)

Vitt, D.H. 2000. Peatlands: ecosystems dominated by bryophytes. *Bryophyte Biology*, Shaw J.R. and Goffinet B, (eds). Cambridge University Press, Cambridge; 312-343.

Woo, M-K. and Heron, R. 1987. Effects of forests on wetland runoff during spring. In *Forest Hydrology and Watershed Management*, Swanson RH, Bernier PY and Woodard PD (eds). IAHS Publication No. 167, IAHS Press, Wallingford; 297-307.

Woo, M-K. and Marsh, P. 1978. Analysis of error in the determination of snow storage for small High Arctic basins. *Journal of Applied Meterology* 17(10): 1537-1541.

Woo, M-K. and Winter, T.C. 1993. The role of permafrost and seasonal frost in the hydrology of northern wetlands in North America. *Journal of Hydrology* 141, 5-31.

Yoshikawa, K., Overduin, P.P. and Harden, J.W. 2004. Moisture content measurements of moss (*Sphagnum* spp.) using commercial sensors. *Permafrost and Periglacial Processes* 15: 309-318.

Tarnocai, C. 1998. The amount of organic carbon in various soil orders and ecological provinces in Canada. In *Soil Processes and the Carbon Cycle,* Lal R., J.M. Kimble, R.F. Follet, and B.A. Stewart BA (eds). The Pensylvania Academy of Science: Pittsburgh, 168-398.

Zhang, T., Heginbottom, J.A., Barry, R.G. and Brown, J. 2000. Further statistics of the distribution of permafrost and ground ice in the Northern Hemisphere. *Polar Geogr*aphy 24: 126–131.

Zoltai, S. C. 1971. Southern limit of permafrost features in peat landforms, Manitoba and Saskatchewan. *Geological Association of Canada*, Special Paper 9: 305-3 10.

Zoltai, S. C. and Tarnocai, C. 1975. Perennially frozen peatlands in the western arctic and subarctic of Canada. *Canadian Journal of Earth Sciences* 12: 2843.

Preface to Chapter 3

The last chapter identified the importance of a changing soil storage capacity in determining the runoff response from peat plateau hillslopes during spring melt. The following chapter attempts to further elucidate the role of active-layer development on runoff generation by examining the distribution of frost-table depths on a peat plateau over four consecutive years at a variety of spatial scales. The chapter examines how air temperature, rain and snowmelt inputs, soil moisture, vegetation, snow cover, and surface topography affect the variability of frost-table depth. A simple flow model was created to demonstrate how the frost-table variability might result in preferential flow pathways for subsurface runoff. The results of the simulation are compared to runoff generation in environments controlled by bedrock topography.

Chapter 3
Spatial and temporal variations in active-layer thawing and their implication on runoff generation in peat-covered permafrost terrain[5]

3.1 Introduction

Permafrost (lithospheric material that has a temperature at or below 0°C for a minimum of two consecutive years) and seasonally frozen soils play a significant role in slope runoff generation and the basin hydrology of cold regions (e.g. Dingman, 1973; Woo and Winter, 1993; Carey and Woo, 2001; Quinton and Hayashi, 2005). Permafrost in high latitude regions is often saturated or oversaturated with ice, and, therefore, acts as a confining layer, limiting the movement and storage of groundwater to a seasonally thawing active layer, below which the frozen ice-saturated soil is relatively impermeable (Dingman, 1975). Seasonal ice in the active layer decreases the hydraulic conductivity and available storage capacity of the soil, which significantly reduces water infiltration (Kane and Chacho, 1990), potentially increasing surface ponding and the magnitude of slope runoff during snowmelt and spring rainfall events. However, the occurrence of overland flow is rare on permafrost slopes covered by highly permeable, moist peat. On these slopes, the drainage of precipitation and meltwater inputs occurs primarily as subsurface flow through the thawed water-saturated layer perched above the frost table (Slaughter and Kane, 1979; Quinton and Marsh, 1999). In the context of subsurface flow, the frost table is the relatively impermeable upper surface of the frozen, ice-saturated soil

[5] The following chapter has been published in *Water Resources Research* (2009, vol. 45, W05414, doi:10.1029/2008WR006880) under the co-authorship of Wright, N., Hayashi, M., and Quinton, W.L.

that coincides closely with the zero-degree isotherm during soil thawing (Carey and Woo, 1998). The depth and distribution of the frost table indirectly controls the position of the zone of saturated water flow, which changes as the soil thaws (Woo, 1986). During soil thawing, the frost table and the water-saturated zone above it descend through the soil profile. Due to the large reduction of the saturated hydraulic conductivity of organic soils with depth (Quinton *et al*., 2000), lateral flow rates decrease as frost-table depths increase (Glenn and Woo, 1987; Wright *et al*., 2008).

Uneven soil thawing on frozen slopes also affects the mode and rate of water flow downslope (e.g. Woo and Steer, 1983; Stadler *et al*., 1996; Metcalfe and Buttle, 1999; Quinton *et al*., 2004). Therefore, knowledge of the spatial and temporal variation of thaw depths (i.e. frost-table depths) is essential to understanding how water flows downslope. These often complex variations in frost-table topography (Nelson *et al*., 1998, 1999) must be considered before point measurements are scaled-up for use in basin studies (Young *et al*., 1997). Furthermore, understanding the factors that control the distribution of frost-table depths is critical to hillslope runoff modelling in permafrost basins (Woo, 1986; Metcalfe and Buttle, 2001), particularly in wetland-dominated, discontinuous permafrost basins, where permafrost often exists only as scattered patches (ranging from 0.5 to 2 meters in height above the surrounding terrain and commonly extending to several square kilometres in area) that appear as islands amongst otherwise unfrozen, peat-covered, saturated terrain (NWWG, 1988). These slightly inclined permafrost slopes, called peat plateaus, are hydrologically important to basin drainage, as they generate a large amount of runoff for streamflow (Wright *et al*., 2008).

There have been numerous field measurement and modelling studies describing the spatial and temporal variation in frost-table depths for different landcover types, and attempts to ascertain the specific factors controlling the distribution (e.g. Smith, 1975; Nelson *et al*., 1997, 1999; Hinkel and Nelson, 2003). However, most of these studies are conducted at relatively large spatial scales (often ≥ 100 m measurement intervals) and are limited to end-of-summer or annual frost-table depths only. Hinkel and Nelson (2003) noted the need for specific small-scale studies to understand the causes of the significant intra-site variation in thaw depth and moisture conditions found at the larger scale. There is a lack of knowledge on the small-scale spatial and temporal variability of frost-table depths on permafrost slopes, including the factors controlling it, and more importantly, how it influences runoff generation. The overall goal of the present study is to close this knowledge gap and provide new scientific insights into the complex interplay between subsurface flow and active layer thawing on permafrost hillslopes. More specifically, this study will: (1) document the spatial variability of frost-table depth and its temporal evolution across a peat plateau during the thawing seasons of 2003-2006; (2) examine how the variability of frost-table depth is affected by air temperature, rain and snowmelt inputs, soil moisture, vegetation, snow cover, and surface topography; and (3) demonstrate how the frost-table variability may result in preferential flow pathways for subsurface runoff.

3.2 Study Area and Methods

3.2.1 Site description

Field studies were conducted on a peat plateau located in the 152-km^2 Scotty Creek basin (61°18'N, 121°18'W; 285 m above sea level), which lies in the lower Liard

River valley, Northwest Territories, Canada (Figure 3-1a). The study area is located in the zone of discontinuous permafrost (Hegginbottom and Radburn, 1992), and is in the continental high boreal wetland region of Canada, slightly south of the transition to the low subarctic wetland region (NWWG, 1988). Climate data are available from the nearest Environment Canada weather station at Fort Simpson airport (169 m above sea level), 50 km north of the study site. There, the mean (1964-2006) annual air temperature is -3.2°C, with a mean total annual precipitation of 363 mm, including the moisture equivalent of 163 mm of snow (MSC, 2006). Snowmelt usually commences in late March, and due to occasional periods of sub-0^{o}C air temperatures and additional snowfall events, generally lasts from two to six weeks. The stratigraphy of the region includes a peat layer of varying thickness (*ca*. 0.5 m to 8 m) that overlays a mineral silt-sand layer (up to 1 m thick), below which lies a thick (average thickness 6 m) clay to silt-clay deposit of low permeability (Rutter *et al*., 1973; Aylesworth *et al*., 1993). Permafrost thickness under peat-covered terrain in the Fort Simpson area has been reported to be 5-10 m (Burgess and Smith, 2000).

The ground surface of the peat plateau examined in this paper (Figure 3-1b) rises 0.9 m above the surrounding permafrost-free terrain, and has a considerable micro-relief (Figure 3-2; for measurement see section *3.2.3*). The plateau supports a sparse stand (1 stem m^{-2}) of relatively short (mean height 3.1 m) black spruce trees (*Picea mariana*), and a variety of shrubs, of which Labrador tea (*Ledum groenlandicum*) is the dominant. The ground cover is dominated by lichen (mostly *Cladina* spp.), covering 65% of the forest floor, while the remaining 35% is occupied by moss (mostly *Sphagnum* spp.). The top 0.15-0.2 m of active layer is composed of living vegetation and lightly decomposed fibric

peat, below which lies a layer containing denser, more decomposed sylvic peat with dark, woody material, and the remains of lichen and moss, rootlets and needles. Small ponds occupy up to one-fifth of the total plateau area during snowmelt, at which time some surface flows have been observed. However, normally the ground surface is relatively dry, and the lateral movement of water occurs as subsurface flow through the thawed, saturated zone between the water table and frost table.

3.2.2 Site instrumentation and soil moisture measurements

Table 3-1 provides a summary of the following field measurements in terms of their spatial and temporal resolution and methodology. Two soil pits (see Figure 3-1b for location) were excavated to the frost table on 20 August 2001 to install PVC observation wells (0.1 m inner diameter), and soil temperature and moisture sensors. The observation wells at the Centre and West pits were each instrumented with a pressure transducer (Global Water WL15) that measured the elevation of the water table every minute, and averaged and recorded these measurements every 30 minutes. The water-table depth at each of the wells was also measured daily with a water-level sounder and ruler during the spring field campaigns in 2004 and 2005, to ensure the accuracy of the transducer measurements.

Only the temperature and soil moisture data from the Centre pit were used in this study (data from the West pit were published in Hayashi *et al.*, 2007). The depth to the frost table in relation to the peat surface at the Centre pit was 0.7 m at the time of installation, and the groundcover was composed of both lichen and moss. The Centre pit was instrumented with thermistor probes (Campbell Scientific 107B) at depths of 0.05, 0.1, 0.15, 0.2, 0.25, 0.3, 0.4, 0.5, 0.6, and 0.7 m, and water content reflectometers

(Campbell Scientific CS615) at 0.1, 0.2, 0.3 and 0.4 m depths. The water content reflectometers were calibrated against the water content of 17 peat samples (sample volume = 92 cm^3) that were collected from the face of the soil pit at the time of installation. After the sensors were installed, the pits were backfilled with the excavated material, with care taken to preserve the original layering and groundcover. Using the water content reflectometer data, depth-integrated average water content was calculated for the unfrozen portion of the active layer at a daily interval.

Soil water content was also measured daily during the spring study period (3-31 May) in 2005 at 15 flagged points, indicated as "soil sampling points" in Figure 3-1b. Seven of the 15 points were under moss and eight under lichen. The exact sampling locations were varied on a daily basis to avoid disturbance, though all samples were taken within 1 m of the flagged point, and at the same ground cover type. Soil moisture was measured gravimetrically at 0.05-m depth increments to the water table at each of the 15 points, using 162-cm^3 soil sample tins, and depth-integrated average water content was calculated. Near-surface soil moisture (0-0.2 m depth) was also measured every 1 m along transect T1 (Figure 3-1b) on September 4 using time domain reflectometry (TDR) (Soil Moisture Equipment Corp., MiniTrase), with a 20-cm probe inserted vertically into the soil.

Air temperature (using a thermistor housed in a Gill radiation shield) and net radiation (using a Kipp and Zonen, CNR1 sensor) were measured 2 m above a moss-covered ground surface at a meteorological station located between the Centre and West pits (Figure 3-1b). Rainfall was measured with a tipping-bucket rain gauge (Jarek Manufacturing) that was located next to the meteorological station. All sensors were

connected to Campbell Scientific CR10X data loggers, programmed to measure every minute and record hourly or half-hourly averaged values. Rainfall data from the Fort Simpson weather station were used for analysis in 1999 and 2002, because the rain gauge was not installed on the peat plateau until 2003.

3.2.3 Frost-table depth and snow measurements

Snow depth and snow water equivalent (SWE) measurements commenced at the peak of the snow-accumulation season, and were made daily using a steel ruler and an Eastern Snow Conference snow sampler (ESC-30) (Goodison, 1978) and scale (calibrated to ± 3 mm). Snow depth was measured at 1 m, and SWE at 5 m intervals along a 36 m transect (T1) that traversed the width of the peat plateau (Figure 3-1b) in 2003-2006, and along an additional 28-m long transect (T2 in Figure 3-1b) in 2004 and 2005. The average snow depth and SWE of the peat plateau at the peak of snow accumulation in 1999 and 2002 was measured by Environment Canada (Carter and Onclin, 1999; Bastien *et al*., 2002), in the same fashion as in 2003-2006.

Depth to the frost table in relation to the peat surface[6] was measured every 2 m in 2003 and every 1 m in 2004-2006 along transect T1 at the end of the spring field season (early to mid June) and at the end of the summer field season (late August to mid September). Frost-table depths were also measured approximately every 2 m along T1 at the end of the summer field season in 1999 and 2002. In 2004 and 2005, the frost-table depth was measured along T1, T2, and an additional 10 m long transect (T3 in Figure 3-1b), every two days during the early soil thaw period (May to early June), at 1 m

[6] Note that the depth below the peat plateau surface is defined in this thesis as the depth below the average ground surface elevation, which is fixed (i.e. it does not change in elevation).

intervals. During the same time period, the frost-table depth was measured at least every two days at both soil pits in 2004 and 2005, and daily at each of the 15 soil sampling points in 2005. All frost-table measurements were made by probing the ground with a graduated steel rod, which clearly detected the top of the frozen layer. Subsurface temperature data at the Centre pit were used to examine the accuracy of the timing of frost probe measurements in relation to the spring and maximum annual thaw depth. The ground cover type (moss or lichen), and any micro-relief feature (depression or mound) relative to an arbitrary reference level, were recorded at each measurement point along the frost-table transects.

On 12 June 2006, the frost-table depth was measured in a 33.8-m^2 plot on the plateau, next to the channel fen (Figure 3-1b), with a frost probe, every 0.25 m along the 21 transects that ran south to north, in a 5 m x 6.75 m grid with a spatial resolution of 0.25 m. Each of the 21 transects had a taught wire tied from end to end, levelled using a bubble level, from which the distance between the wire and ground surface was measured with a ruler, at the same 0.25 m interval as the frost-table depth measurements. The elevation of the frost table, Z_{FT}, in relation to the elevation of the ground surface, Z_{GS}, was computed from the frost-table depths, d_{FT}, as:

$$Z_{FT} = Z_{GS} - d_{FT} \tag{3.1}$$

where Z_{GS} was computed by subtracting the distance between the taught wire and the ground surface from an arbitrary datum, such that Z_{GS} = 0.4 m at the fen water level. The ground surface and frost-table elevation data were interpolated by the kriging method

(Davis, 1973) to assign elevation on a 0.1 m grid using commercial software (Golden Software, Surfer).

3.3 Field Results

In this study, "spring" is defined as the period beginning at the onset of soil thaw and ending on the last day of frost-table measurements in early/mid June. The onset of soil thaw is indicated by the rise of soil temperature above 0^{o}C at 0.05-m depth at the Centre pit, which was 4 May in 2004 (Figure 3-2a) and 27 April in 2005 (Figure 3-2b). Figure 2c shows the daily depth to the frost table measured by the frost probe near the Centre pit as continuous lines, and the arrival of the thawing front at discrete depths, according to soil temperature data at the Centre pit, as symbols. There was relatively good agreement between the frost-probe data and soil temperature data in 2004 (Figure 3-2c). In 2005, the two data sets were consistent for the onset of soil thaw, but frost-table depth values had a difference of 0.05-0.1 m (Figure 3-2c). This difference was most likely due to the high variability of thaw depths found on the plateau (as described in section *3.3.1*), as the frost-probe measurements were made 0.5 m away from the soil temperature sensor array at the Centre pit to avoid disturbance to the instrumented pit. Frost-probe measurements were also made in late August to mid September; these measurements are referred to in the following as "end-of-summer" frost-table depths. Romanovsky and Osterkamp (1997) showed that the maximum frost-table depth occurs approximately two weeks prior to the start of soil freezing. Figure 3-2 (a, b) shows that the reversal of temperature gradient occurs around 26-30 September, therefore, the end-of-summer frost probe measurements may not be maximum, but were fairly close, giving confidence that the frost-table measurements are comparable in the different years.

3.3.1 Frost-table depth, spatial and seasonal variation

Figure 3-3a illustrates the variability of frost-table elevations along transect T1 over relatively short distances (1 m) and its seasonal and inter-annual consistency. The points that had lower frost-table elevation (i.e. deeper frost table) in June also had lower frost-table elevation in September, and the points with lower frost-table elevation in 2004 generally had lower frost-table elevation in other years. Mean frost-table depths measured in June of 2003-2006, were on average, 39% of the end-of-summer frost-table depths measured over the same four years (Table 3-2). The locations with a deeper frost-table in June tended to maintain higher thawing rates over the summer as well. This is illustrated in the frequency distributions of frost-table depths measured on T1, T2 and T3, which were skewed with a tail toward deeper frost-table depths; a pattern that persisted and became more pronounced during the thawing season (Figure 3-4). Taking the logarithm of the frost-table depths resulted in a normal distribution and thus, the logarithm of depth was used to calculate the geometric mean and standard deviation, as well as the observed level of significance (p) using two-tailed t-test. Frost-table depths were deeper beneath moss ground covers compared to lichen covers ($p \leq 0.04$, Table 3-3a); a trend that persisted seasonally and inter-annually (Table 3-3a).

3.3.2 Frost-table depth, inter-annual variation

The literature suggests that the two primary factors controlling frost-table depth are soil temperature (e.g. Gray *et al.*, 1988) and soil moisture (e.g. Kane *et al.*, 2001). Here we examine the influence of air temperature (used as a surrogate for near-surface

soil temperature as it governs inter-annual variations in ground temperature) and soil moisture on the inter-annual variation of frost-table depths measured at the peat plateau in spring and at the end of summer.

To determine the inter-annual relationship between air temperature and frost-table depth on the peat plateau, the accumulated degree days of thaw, *ADDT* (d ^{o}C) was computed by summing the daily average air temperatures for the period beginning at the onset of soil thaw and ending on the last day of frost-table measurements in early to mid June of 2003-2006 (see Table 3-2 for the actual dates). The *ADDT* was also computed for the end-of-summer period ending in late August to early September in 1999, 2002-2006 (Table 3-2). It is commonly observed that frost-table depths are strongly correlated with the square root of *ADDT* over a large scale (e.g. Nelson *et al*., 1997; Hinkel and Nelson, 2003). While frost-table depths in June had a relatively strong correlation with the square root of *ADDT* (r^2 = 0.80, Figure 3-5), the end-of-summer frost-table depths were poorly correlated (r^2 = 0.07) to the square root of *ADDT* (data and linear regression not shown), where r^2 is the coefficient of determination. The relatively low values of *ADDT* in the spring of 2004, compared to other years, was due to lower mean daily air temperatures and fewer days with above-freezing temperatures, which delayed the progression of the thawing front. For example, the average daily air temperature during the first 10 days of thaw in 2004 was -0.37 ^{o}C, compared to 2.9, 4.9 and 5.7 ^{o}C in 2003, 2005 and 2006, respectively. The data suggest that air temperature (and thus, soil-surface temperature) strongly affects thaw rates of the relatively shallow frost table in May-June when there is a greater temperature gradient between the ground surface and the frost table, but it likely has weaker effects on thaw rates in July-August, when the frost table is much deeper, as

the effects of air-temperature variation is dampened in the soil during downward heat conduction. Other studies have shown that snowpack can have a significant influence on soil freezing and thawing (Bayard *et al*., 2005; Iwata *et al*., 2008; Leutschg *et al*., 2008]. However, no clear relationship was found at this particular site during the four years of study.

To determine the inter-annual relationship between frost-table depths and moisture conditions on the peat plateau, frost-table depths were compared with the total water input (i.e. estimated snowmelt and rainfall) during the period between the peak of snow accumulation and early to mid June of 2003-2006, and between the peak snow accumulation and late August to early September of 1999, 2002-2006. The total amount of snowmelt water input was estimated from the average snow water equivalent (SWE) that was measured on the peat plateau at the peak of snow accumulation (late March or April depending on the year), as described in the methods. The average SWE was added to the cumulative rainfall, also from the peak of snow accumulation (to include rain on snow events), to the day when the frost-table depths were measured at the end of the spring (early to mid June) and summer (late August to early September) field seasons (Table 3-1). The relationship between average spring frost-table depths and total water input to the peat plateau was not strong over the four year period of 2003-2006 ($r^2 = 0.15$; Figure 3-6). Unlike the spring thaw depths, the average end-of-summer frost-table depths were significantly correlated ($r^2 = 0.978$, $p < 0.01$) to the total water input to the plateau over the seven years of measurement (Figure 3-6), with deeper frost table in years with greater water inputs, than in years with lower precipitation amounts.

To examine the correlation between total water inputs and the soil moisture condition on the peat plateau, the depth-integrated average liquid water content data at the Centre pit was used, which represents the average moisture conditions on the plateau reasonably well (Wright *et al*., 2008), even though this is only one point. Total water inputs were highly correlated to the seasonal mean of water content at the Centre pit over the same time period (to the end of summer) in 2003-2006 (r^2=0.911, data and linear regression not shown).

3.3.3 Spatial variability of soil moisture, snow depth and frost table

Having identified a significant effect of water input (and moisture condition) on the inter-annual variability of frost-table depths, the effect of soil moisture on the spatial variability of frost-table depths was investigated. Figure 3-7a illustrates the positive correlation between spring frost-table depth and depth-integrated average soil volumetric water content (VWC) at the 15 soil sampling points. Frost-table depth at the end of summer (3 September 2006) was also related to average soil water content in the 0-0.2 m depth interval measured by TDR on transect T1 (Figure 3-7b). This correlation was positive as well, though strongly influenced by one data point (Figure 3-7b). This measurement point was located at the bottom of the slope next to the fen (a wetland), which may have influenced the greater saturation and frost-table depth at this point.

Since the frost-table depths were correlated to soil moisture (Figure 3-7) and to ground-cover types (Table 3-3a), a significant correlation is expected between soil moisture and ground cover. This was true during spring 2005 to depths of 0.15 m, but not for end of summer 2006 (Table 3-3b). In spring, the frost table and water saturated zone are close to the ground cover. *Sphagnum* mosses have hyaline cells which allow them to

store water (up to 20 times their dry weight) (Vitt, 2000), and to retain capillary water far above the actual water table (Lafleur *et al*., 2005). Lichens on the other hand, have no such water retention capabilities, and thus, act as a mulch layer providing the underlying soil with thermal insulation by decoupling the moist subsurface from the atmosphere (Rouse and Kershaw, 1971), possibly due to mire breathing (Kellner, 2001). These differences control soil temperature and the rate of soil thaw in spring. However, at the end of summer the frost table and the water saturated zone are much deeper, and as neither mosses nor lichens have roots and are active in moisture exchange only when moist (Rouse, 2000), the correlation is weaker.

To examine the effect of snow cover and topography, Figure 3-3 (b and c) shows the progression of snow cover and frost-table depth along transect T1 from April to June 2005. Distances 11 m and 17-19 m are areas of relatively low ground surface elevation, and are hereafter referred to as d1 and d2, respectively. Both depressions had relatively similar snow depths on 10 April 2005 (Figure 3-3b). However, d1 became snow free on 24 April, and the frost table was among the deepest of all points on the transect on 6 May (Figure 3-3c); while d2 only became snow free on 5 May, and the frost table was very close to the ground surface on 6 May. The frost table depth at d2 reached a local minimum on 4 June despite the shallow frost table on 6 May (Figure 3-3c), indicating that the thawing rate at d2 was much greater than at d1, and most other points on T1. The main difference between d2 and the other points was that it was the only location where water was ponding above the ground surface (due to saturation of the soil) during snowmelt and for more than a week afterwards. This suggests that the high rate of soil thaw at d2 is related to the wetness of this location.

The relatively deep frost table measured near the edges of T1 (at distances of 1-3 m and 34-36 m in Figure 3-2c) on 4 June, were largely due to the lateral transfer of energy provided by relatively warm water flowing in the ditch that surrounds the peat plateau (visible in Figure 3-1b on the bog side). This ditch conveys fen water downstream, and bog water around the peat plateau to the fen (during snowmelt). This is consistent with larger scale studies that have found frost-table depths to be greater in wetlands than in drier uplands (Nelson *et al*., 1997; Hinkel and Nelson, 2003).

3.3.4 Physical link between soil moisture and thawing rates

The data above have shown that the spatial and temporal variability of frost-table depths is related to soil moisture conditions. This is consistent with the results of Hayashi *et al*. (2007), who used a heat conduction model with the soil temperature and moisture data from the Centre and West pits to show that the difference in thawing rates between the two pits was due to the difference in thermal conductivity, as the thermal conductivity of peat is strongly dependent on water content. The Centre pit is located in an area of relatively low ground surface elevation, while the opposite is the case for the West pit (Figure 3-3c). The frost table was 0.13 m deeper at the West pit than at the Centre pit in this study when the measurements began on 1 May, possibly because the snowcover melted much earlier at the West pit than at the Centre pit (Figure 3-3b). However, during the 35 day measurement period, the mean soil thaw rate at the Centre pit (9 mm/day) was much higher than that at the West pit (4 mm/day); so that by 4 June, the frost table at the Centre pit was deeper (Figure 3-8). The greater thaw rate observed at the Centre pit was largely due to the shallower water table measured at the Centre pit compared to that measured at the West pit (Figure 3-8). Given that both pits had similar vertical inputs of

snowmelt and rainwater, the difference in water table depths, and thus, soil thaw rates between the two sites, must be due to the convergence of lateral flow to the depression containing the Centre pit, as this process 1) maintains a high soil moisture (and thermal conductivity), thereby enhancing vertical heat conduction, and 2) provides additional energy for ground thaw by lateral advection.

There have been studies suggesting that the correlation between soil moisture and thawing rates is partially explained by the vertical advection of heat by infiltration of relatively warm rainwater (e.g. Hinkel *et al*., 1997) and snowmelt water (e.g. Rist and Phillips, 2005). We used the soil temperature and moisture data from the Centre pit to examine the influence of rainwater infiltration on soil thawing rates. The vertical infiltration of water during the spring rain events of 2004 and 2005 had little effect on soil thawing rates; if anything, soil thaw rates decreased during periods of rain, when both the air temperature and near-surface soil temperature decreased. This suggests that the effect of soil moisture on the ground thermal regime at the peat plateau is primarily due to its influence on thermal conductivity, while the advection by rainwater infiltration may play a secondary role.

3.3.5 Spatial variability in two dimensions

While the variability of the surface and frost-table topography is shown one-dimensionally at 1 m intervals across the plateau in Figure 3-3, the thickness of the thawed layer as a composite of the surface and frost-table topography is shown two-dimensionally at smaller measurement intervals of 0.25 m at the frost-table plot (Figure 3-1b) in Figure 3-9a. The overall slope of the ground surface was very small, 0.003 in the east-west direction (referenced distance into peat plateau) and -0.005 in the north-south

direction (referenced to as the distance along the fen). However, the ground surface and frost table had significant relief, with surface elevation ranging from 0.41 to 0.88 m above the survey datum, and frost-table elevation ranging from 0.04 to 0.64 m above the datum. The surface and frost-table topography were not spatially constant, suggesting large variability concerning the soil moisture and material composition of the frost-table plot, which has important implications for runoff generation from the plateau.

3.4 Simple flow model simulation

As soil hydraulic conductivity increases with increasing water content, water preferentially moves through areas of greater soil moisture (Woo and Steer, 1983; Kane *et al*., 2001). This has special implications for permafrost regions. Woo and Steer (1983) suggested that uneven thaw rates, which generates an irregularly-shaped frost-table (e.g. Figure 3-3 and 3-9a), could result in lateral preferential flow paths as described above (section *3.3.4*). This situation is similar to hillslopes studies conducted in temperate regions, where irregularly-shaped bedrock surfaces have a strong influence on flow (e.g. Freer *et al*., 2002). The hillslope flow controlled by the topography of a bedrock surface is referred to as "fill and spill" (Spence and Woo, 2003; Tromp-van Meerveld and McDonnell, 2006). Weiler and McDonnell (2004) demonstrated the usefulness of numerical experiments using a simple numerical flow model, HillVi, to investigate how the complex bedrock topography enhances the variability of subsurface runoff. A simple flow model, similar to HillVi, was developed in this study to demonstrate the effects of the frost-table (instead of the bedrock) topography on subsurface flow on the peat plateau.

The model SFASH (Simple Fill and Spill Hydrology) solves the two-dimensional Dupuit-Forschheimer flow equation (Wigmosta and Lettenmaier, 1999, Eq. 1) using the finite difference spatial discretization and implicit time scheme (Huyakorn and Pinder, 1983, p.56). Similar to HillVi, vertical water input is added directly to the water table. However, unlike HillVi, saturated hydraulic conductivity is independent of depth in the current version of SFASH, which is meant to be a simple demonstrative tool. Therefore, transmissivity in the Dupuit-Forchheimer equation is given by saturated hydraulic conductivity times the thickness of the saturated zone (i.e. distance between the water table and frost table). Transmissivity between two grid nodes is set to zero when the node on the up-gradient side is completely unsaturated. The non-linear flow equation is solved iteratively using a modified Picard method (Celia *et al*., 1990, Eq. 16) and a variable time step size to ensure the convergence of numerical solution.

The frost table in Figure 3-9a represents the physical boundary of the SFASH model domain on 12 June 2006. The values of saturated hydraulic conductivity (10^{-4} m/s) and drainable porosity (0.21) were chosen based on the soil properties measured at the peat plateau by Quinton and Hayashi (2005, Figure 3-3). For simplicity, it was assumed that (1) the peat was completely drained to field capacity prior to the input of water to the domain; (2) water inputs were directly delivered to the water table, and were not retained in the unsaturated zone, as peat soils are highly permeable when they are wet during infiltration events; and (3) there was no lateral input or output of water across the domain boundary (no-flow condition). The last assumption may not be representative of the field condition, but it was used to demonstrate the effects of fill and spill. In the simulation runs, a set amount of water was instantaneously added over the entire model domain at

time = 0, and allowed to flow laterally until the steady state was reached. The purpose of this exercise was to examine how the soil wetness of the domain affects the connectivity of saturated areas.

Figure 3-9b shows the simulated thickness of the saturated zone overlying the three-dimensional surface of the frost table, with 15 mm of water added to the domain. The simulated distribution of saturated areas suggests that it is largely controlled by the frost-table topography, as they followed the topographic lows; with deeper water tables in areas with lower frost-table elevation (i.e. deeper frost table). Simulations with different amounts of water input (5-30 mm) showed that the spatially variable frost-table topography results in highly convoluted, tortuous subsurface flow paths with small amounts of water input. As water input increases, the maximum extent of the saturated areas increases, as does subsurface channelling in the downslope direction, which increases the area contributing to runoff from the plateau.

In order to elucidate the effects of differential thawing on frost-table topography and subsurface flow, SFASH was coupled with a simple heat conduction algorithm of Hayashi *et al*. (2007, Eq. 3), in which the thermal conduction is driven by the temperature gradient between the ground surface and the frost table, and thermal conductivity is dependent on soil moisture content (Hayashi *et al*., 2007, Eq. 8). The thawing algorithm was applied at each time step and melt water was treated as water input in SFASH to simulate the simultaneous deepening of the frost table and the lateral redistribution of liquid water. Starting from the 15-mm input scenario presented in Figure 3-9b, the model simulated the thawing and flow for 30 days, assuming the no-flow boundary condition on all four sides of the model domain. In this simple simulation, surface temperature was

assumed constant and equal to the average air temperature (18 °C) during 12 June – 11 July, 2006. After the 30-day simulation was complete, all excess water (above the field capacity) was drained from the model domain to create the initial condition for the second rainfall experiment, in which 15 mm of rain was added and SFASH was run without the heat conduction algorithm until the steady state was reached.

Figure 3-9c shows the change in the frost-table elevation (gray-scale contours) resulting from the simulated 30-day thawing, overlaid on the original frost table topography. The largest change in frost-table elevation generally occurred in the wetter areas. Figure 3-9d shows the simulated frost-table topography and the thickness of the saturated zone, which resulted from 15-mm rainfall on the simulated frost table. Comparing Figures 3-9b and 3-9d, more areas are exposed above the water table in the simulated topography. This is because the valleys and depressions in the frost table, where the melt water converges, are more deeply incised in the simulated than in the original frost table due to differential thawing of the wet areas. As a result, a larger amount of rainfall would be required to connect the flow pathways on the simulated frost table.

A closer inspection of the individual transect cross-sections at 1 m (Figure 3-10a) and 2.6 m (Figure 3-10b) along the channel fen, gives further insight into how the spatial and temporal variability of frost-table depths affects the lateral flow of water downslope. Frost-table depressions located in the middle and upper reaches of the slope (shown at both transects) act as a barrier to the lateral drainage of water downslope to the channel fen. As the soil thaws and the depressions deepen, a larger amount of water is needed to fill them before the water stored upslope can connect to flow downslope. Thus, the

location and the volume of frost-table depressions on the plateau (and their evolution with thawing), and the amount of water input, determines the degree of saturated connectivity, and thus, affects the timing and magnitude of runoff. Therefore, differential thawing caused by the variability in soil wetness provides a feedback mechanism between the thermal and hydrological processes.

3.5 Discussion

The SFASH simulation showed that the frozen, saturated layer of the peat plateau affects the movement of water (by creating a barrier or conduit to lateral flow) in the same way (but maybe at a different scale) that the confining subsurface topography (e.g. bedrock) controls the flow from slopes in non-permafrost locations (e.g. Buttle and McDonald, 2002; Spence and Woo, 2003; Tromp-van Meerveld and McDonnell, 2006). A major difference between the hillslope studies highlighted above, and this study, is that the aquiclude of the peat plateau is ice-saturated, frozen ground (not bedrock or glacial till), which undergoes an annual freeze-thaw process. Thus, the association between the flux and storage of water evolves as the active layer thaws (Woo and Steer, 1983; Wright *et al*., 2008). As shown in the field and simulation results, when the lateral flow of water (from rain, snowmelt, and ground ice melt) converges to depressions in the frost table, the water table in the depressions is maintained close to the ground surface. This causes the rate of soil thaw at these points to increase, because wet peat has a higher thermal conductivity than dry peat. As depressions in the uneven frost table are able to store water, they are also an important source of runoff when the active layer is not saturated (particularly in summer); a water source that is "rapidly released when part of the frozen sill is breached by continual thawing" (Woo and Steer, 1983). Thus, the depth of water

input needed to produce a spill in the downslope direction increases as the frost table deepens and varies in topography.

High-resolution mapping of the frost table provided detailed information on the frost-table topography. Combined with a simple hillslope water flow and heat transfer model, this provided new scientific insights into the effects of the spatial and temporal variability of frost table on subsurface flow on the peat plateau. However, the parameterization of water storage and redistribution used in the current model is too simple for realistic flow simulations. To advance our understanding of the flow processes in the active layer, the model needs to incorporate depth-dependent hydraulic conductivity, which is the essential feature of peat-covered terrains in northern Canada (Quinton *et al*., 2000). Such a model will provide a valuable tool to explore the feedback between soil moisture and thaw, its effect on water transport and runoff from permafrost slopes, and eventually the response of the permafrost slopes to climatic fluctuations.

3.6 Conclusion

The frost-table depths measured on a forested peat plateau, located in the discontinuous permafrost region of northwestern Canada, exhibited high spatial variability over relatively short distances (0.25-1 m). There was a seasonal consistency in the frost-table depth distribution, as the locations with a deeper frost table in spring tended to have higher thawing rates over the summer; a pattern that persisted over four consecutive years. While the thaw rates in spring (late April to early June) were strongly correlated to air temperature, the correlation was weak during the summer months. In contrast, rain and snowmelt water inputs to the plateau had a significant effect on the inter-annual variability of frost-table depths in both spring and summer, with deeper

frost-table depths in years with greater water inputs, indicating the importance of the soil moisture condition in influencing the spatial variability of frost-table depths. As the thermal conductivity of peat increases with water content, deeper frost table in wetter areas is due to higher rates of thermal conduction providing melt energy to the frost table. The ground covers, lichen and moss, were found to have different controls on soil temperature and development of soil frost, due to their differences in moisture retention capabilities during spring.

Simple subsurface flow simulations illustrated that lateral subsurface flow on the peat plateau is governed by the frost-table topography having spatially variable storage that has to be filled before water can spill over to generate subsurface flow. This has important implications for the magnitude and timing of runoff from peat plateaus, as the relief of the frost table acting as aquiclude, and the amount of water input (apart from the soil's hydraulic conductivity), determine if and when water is exported from the slope. The field data and simulations also suggest that the soil moisture distribution is influenced by lateral flow converging to frost-table depressions. Coupling the flow simulations with a simple heat conduction algorithm helped elucidate the role of the evolving frost table and the feedback between thawing and lateral advection.

3.7 Figures

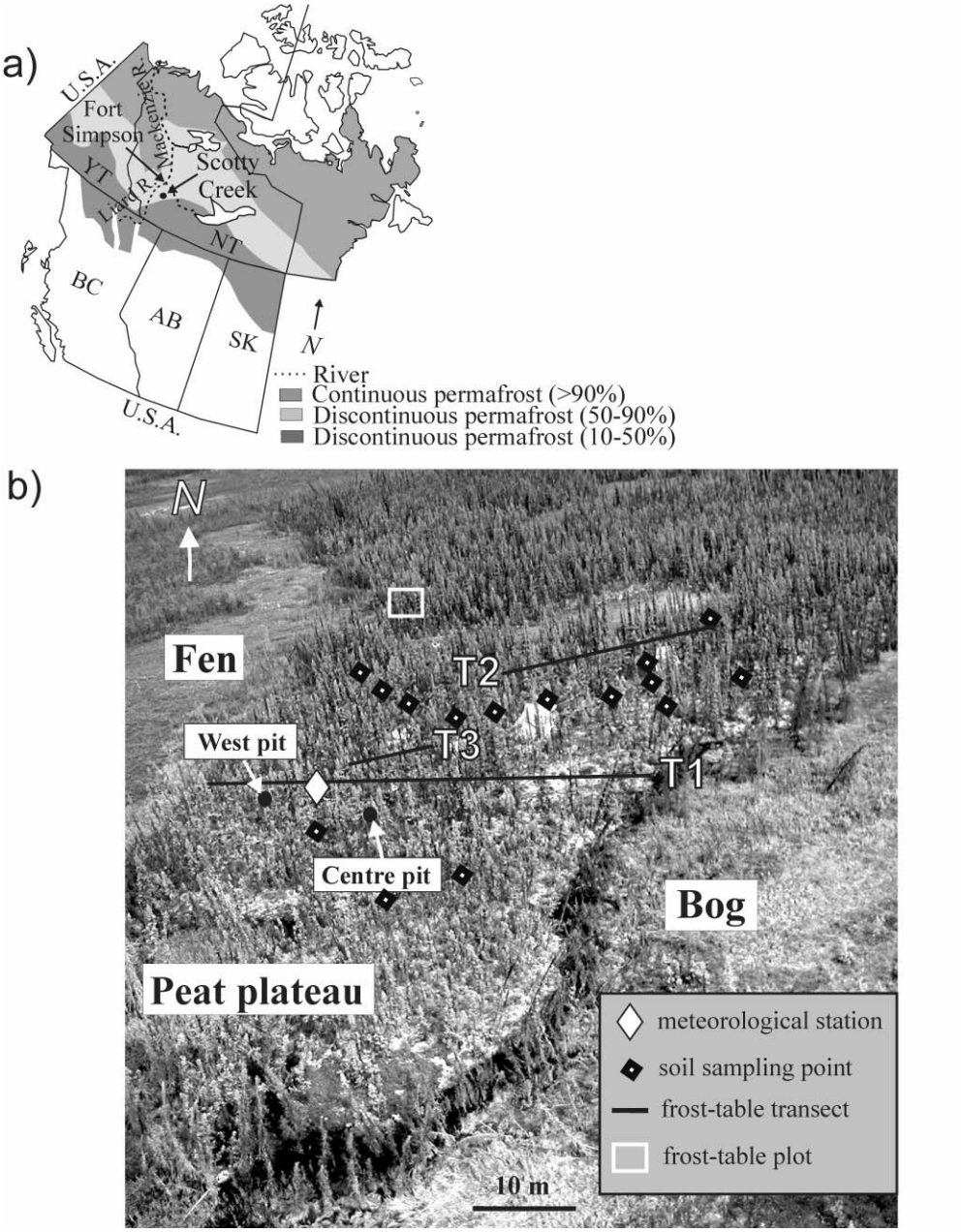

Figure 3-1 a) The location of Scotty Creek within north-western Canada. b) Photo of the peat plateau study site, positioned between two seasonally frozen wetlands (a fen and bog), and the location of the instrumentation and frost-table measurement transects (T1, T2 and T3).

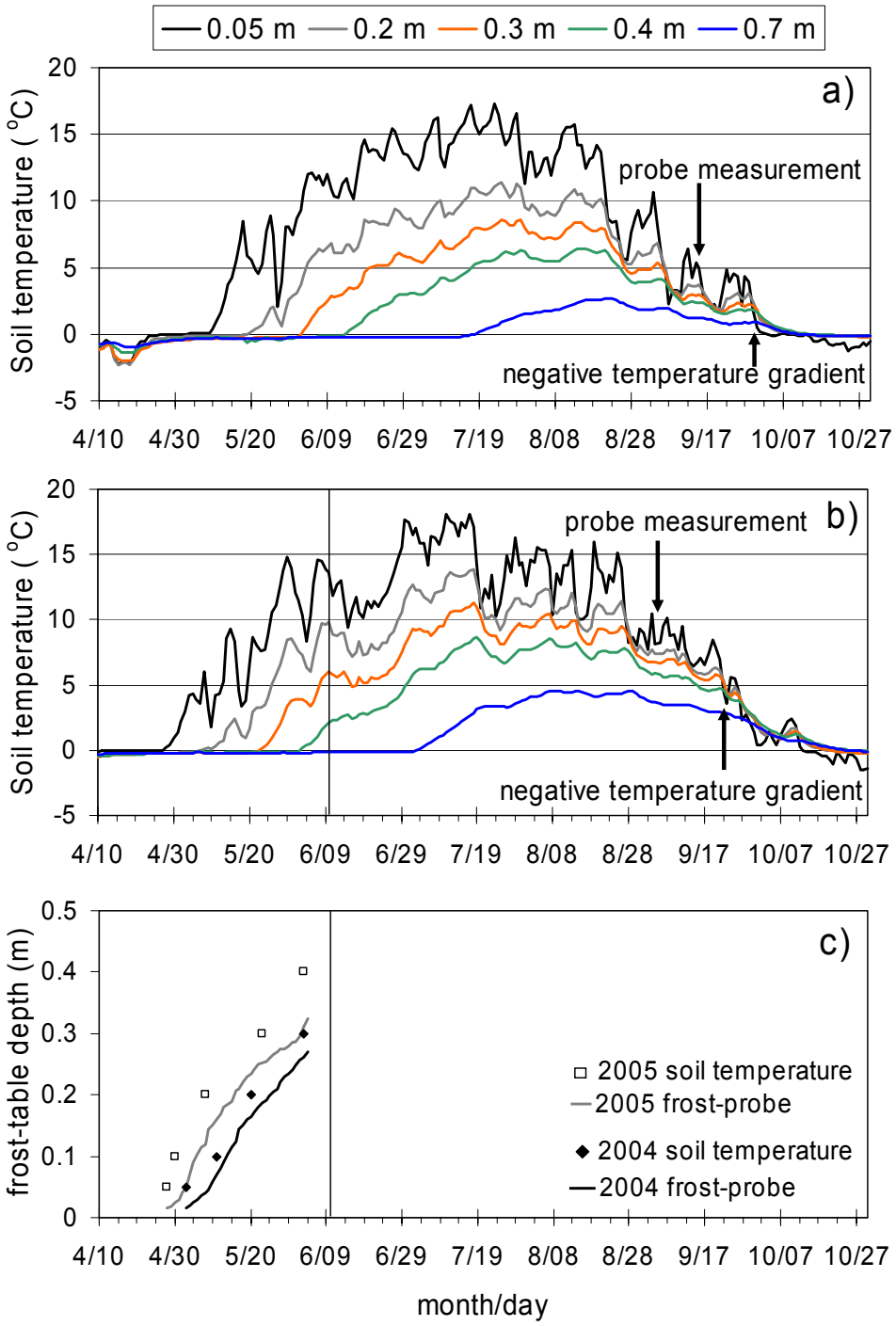

Figure 3-2 Average daily soil temperature of the Centre pit from 10 April to 1 November a) 2004 and b) 2005. c) The arrival of the thawing front at discrete depths, according to soil temperature data at the Centre pit (symbols), and the daily frost-table depth measured by the frost probe near the Centre pit (continuous line) during the spring field seasons of 2004 and 2005.

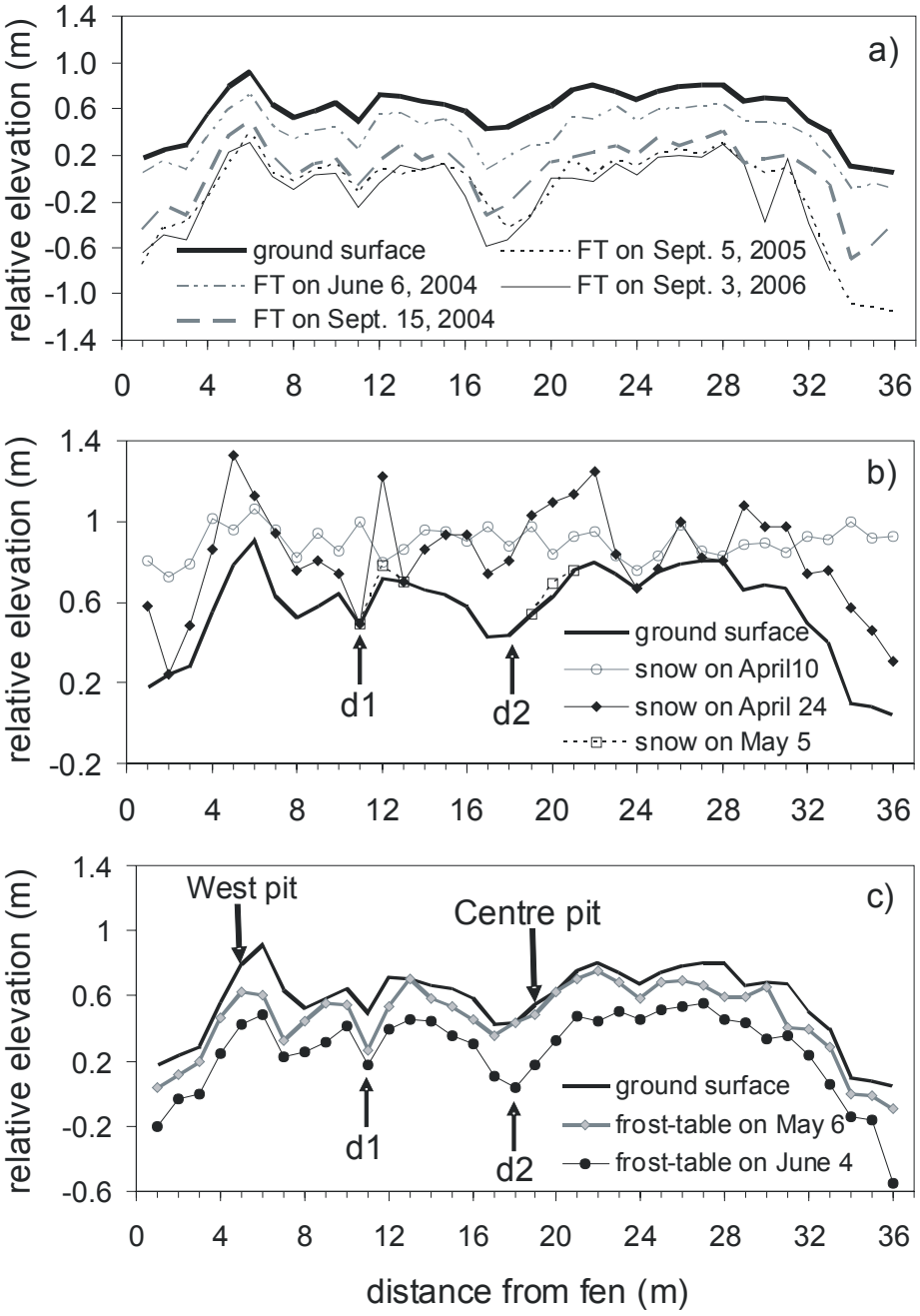

Figure 3-3 a) Seasonal and inter-annual variability of the frost-table (FT) elevation along T1 (see Fig. 3-1 for location). b) Elevation of the ground surface and snow surface on transect T1 in April and May 2005, and c) elevation of the ground surface and frost table in May and June 2005. Arrows with 1 and 2 indicate the depressions discussed in the text. West pit and Centre pit indicate the approximate location of the soil pits.

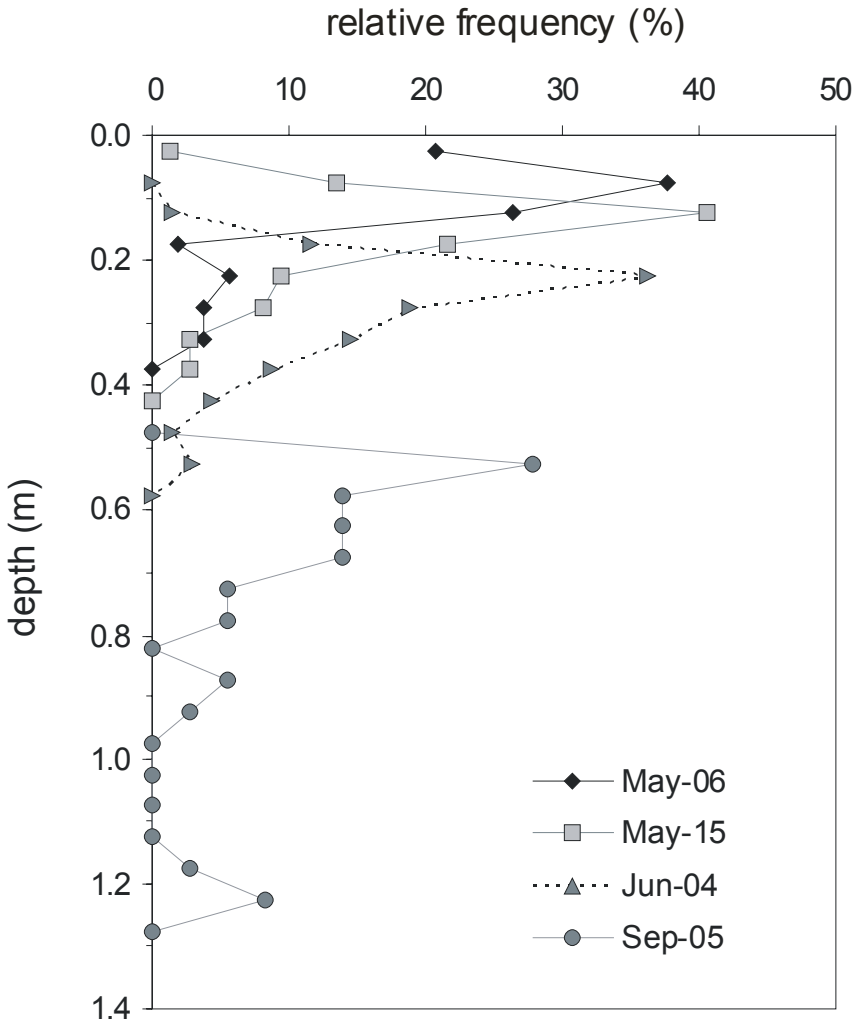

Figure 3-4 The distribution of frost-table depths measured at 40 to 74 points along T1, T2 and T3 on the peat plateau in 2005.

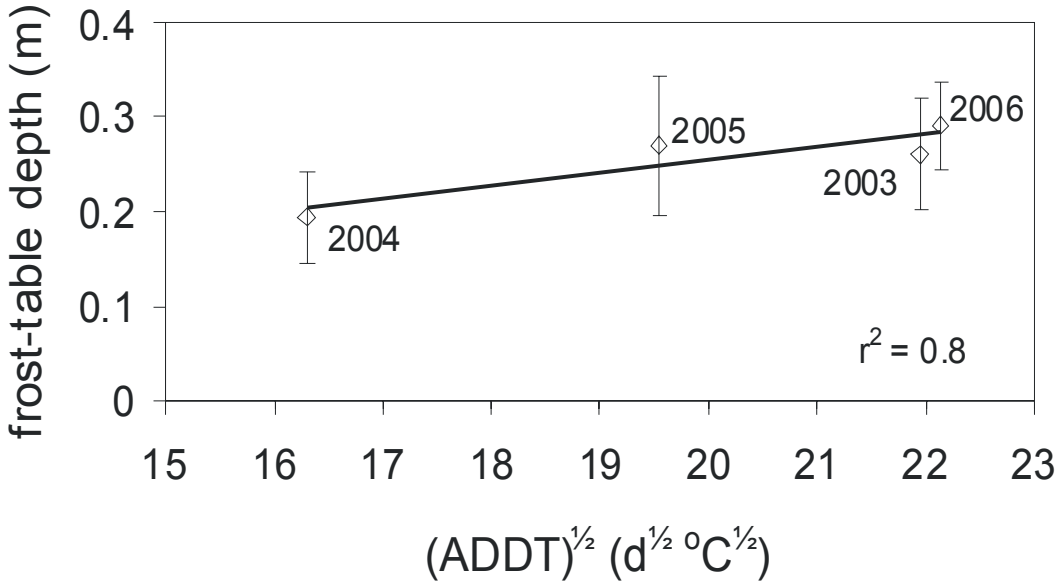

Figure 3-5 Mean frost-table depth at the end of spring versus the square root of accumulated degree days of thaw ($ADDT^{½}$) ($d^{½}\ {}^{o}C^{½}$), computed over the spring of 2003-2006. Bars indicate one standard deviation.

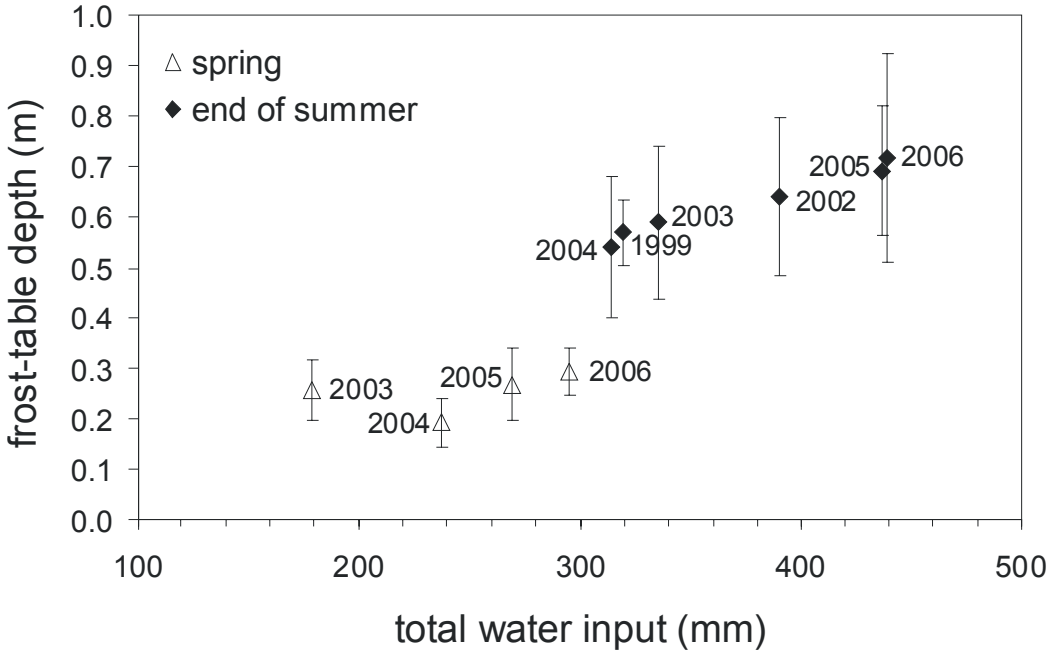

Figure 3-6 Mean frost-table depth at the end of spring and at the end of summer along T1, versus the total water input from the start of snowmelt to the end of spring in 2003-2006, and to the end of summer in 1999, 2002-2006. Bars indicate one standard deviation.

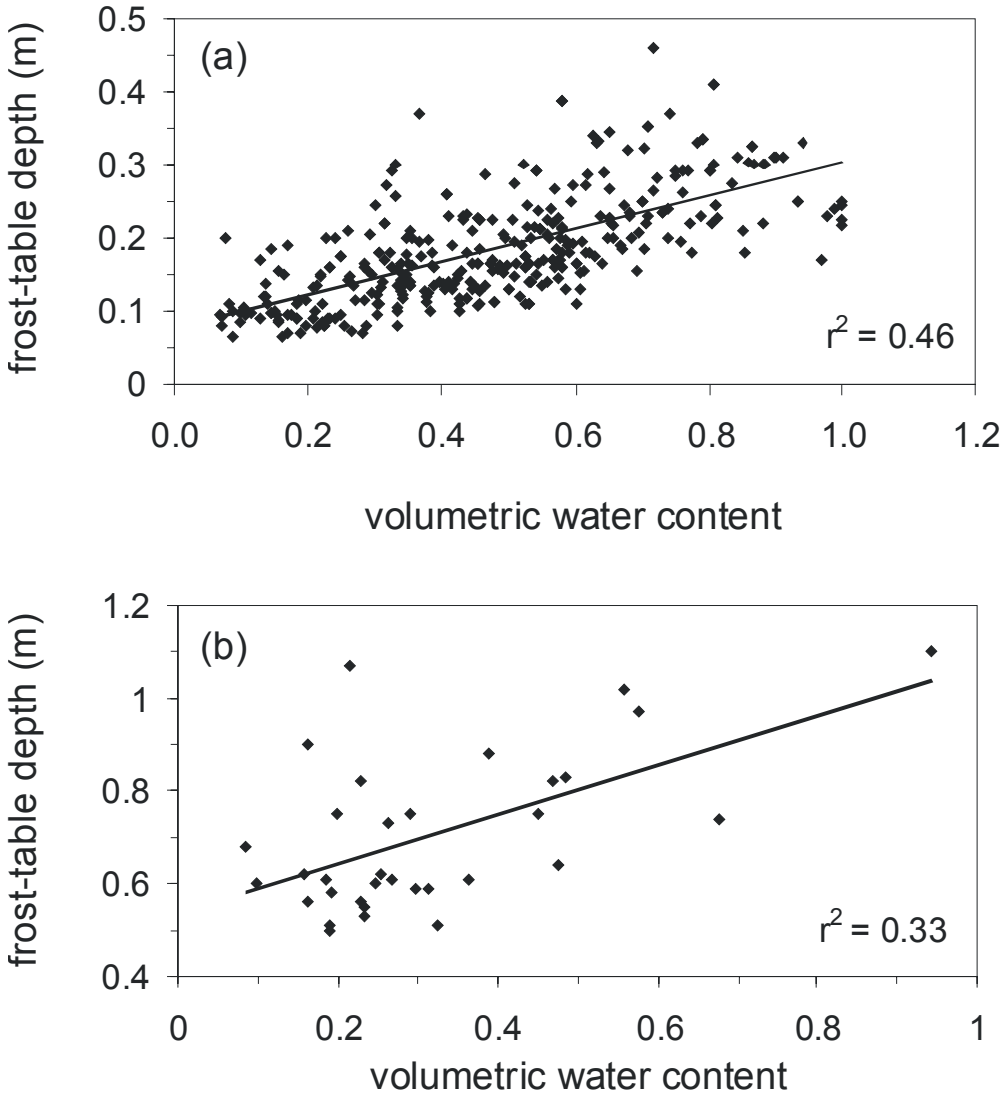

Figure 3-7 Frost-table depth versus volumetric water content measured across the peat plateau (a) at the 15 soil sampling points throughout May 2005 and (b) along transect T1 on 4 September, 2006.

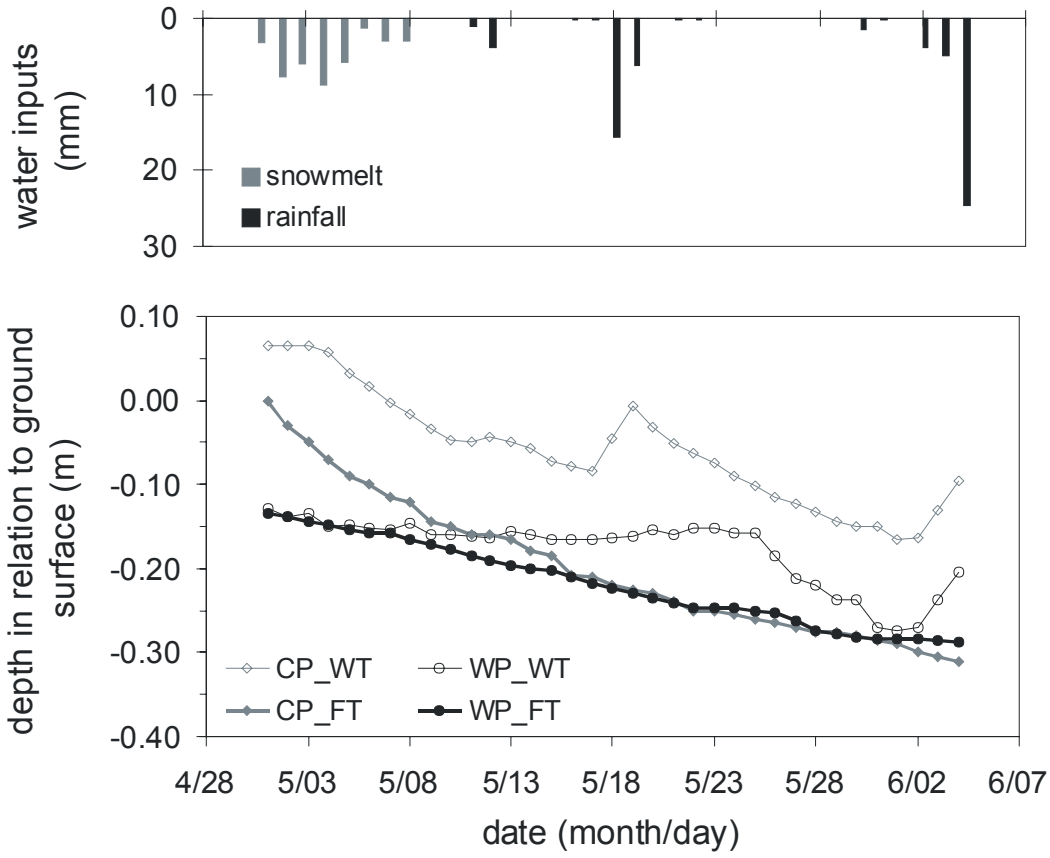

Figure 3-8 Daily snowmelt and rainfall plotted with the frost-table (FT) and water-table (WT) depths, measured daily at the Centre (CP) and West (WP) pits in 2005.

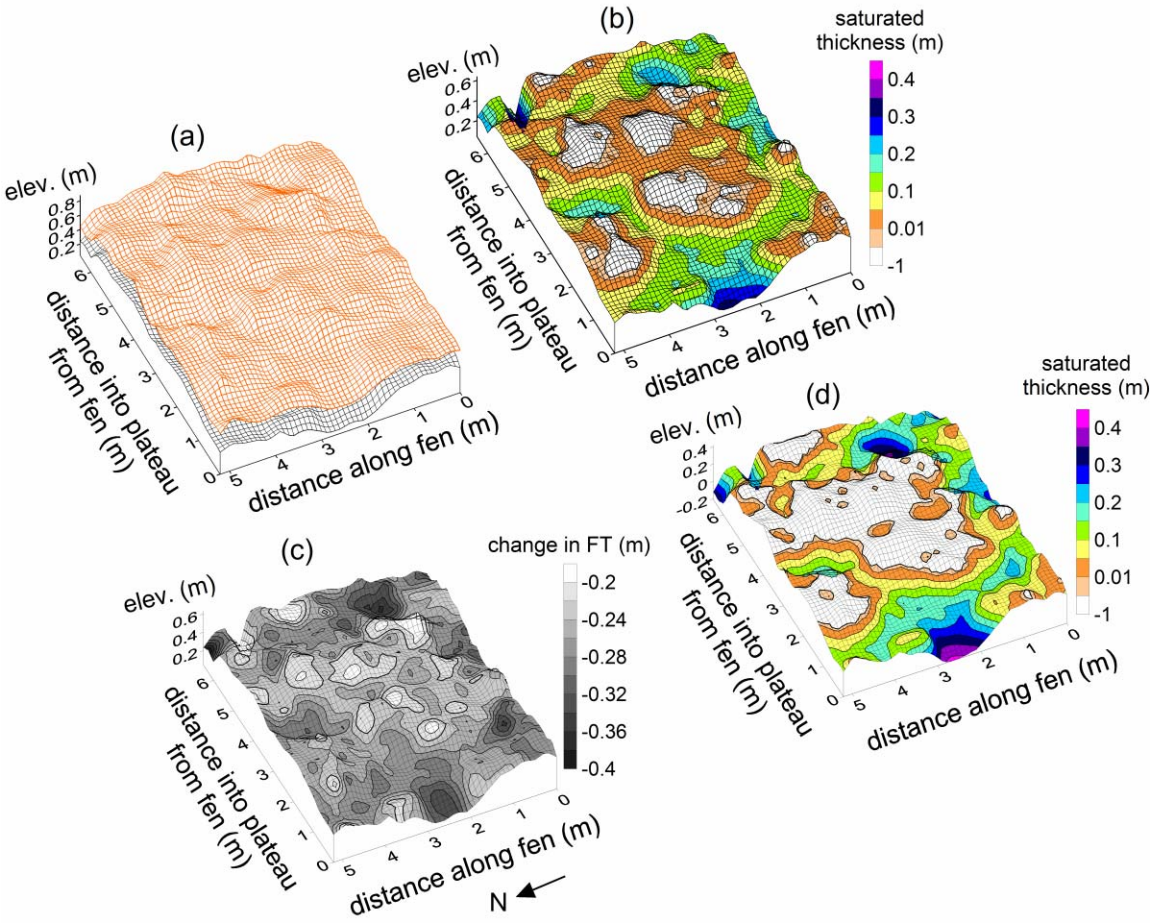

Figure 3-9 (a) Variability of the ground-surface (orange grid) and frost-table (black grid) elevation (elev.) on the peat plateau (see Fig. 3-1b for location). Note that both surface and frost-table topography were measured from the same datum. (b) Simulated thickness of the saturated zone (i.e. distance between the water table and the frost table) in relation to the frost-table elevation measured on 12 June, with a vertical water input of 15 mm; (c) simulated change in the frost-table (FT) (gray-scale contours) between 12 June and 11 July, overlaid on the original frost-table topography; and (d) simulated thickness of the saturated zone in relation to the frost-table elevation simulated on 11 July, with a vertical water input of 15 mm.

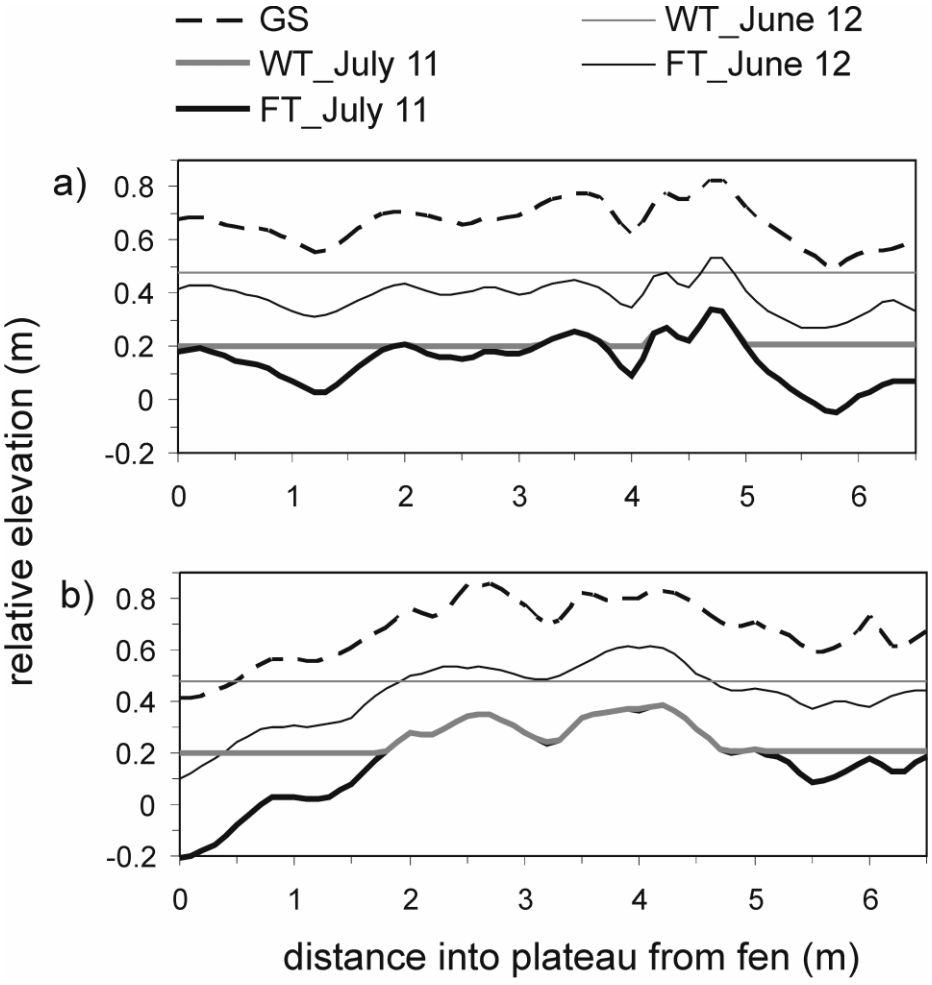

Figure 3-10 Cross-sections of the model domain (see Figure 3-9a) at a) 1.0 m and b) 2.6 m along the channel fen, showing the ground surface (GS), frost-table elevation (FT) measured on 12 June and simulated on 11 July, and the water-table elevation (WT) simulated by SFASH on 12 June and 11 July with a vertical water input of 15 mm. The frost table on 11 July was generated using SFASH coupled with a simple heat conduction algorithm. Note that the fen-plateau boundary is point 0 on the x-axis.

3.8 Tables

Table 3-1 Overview of the field measurements, including the spatial and temporal resolution and methodology.

Variables measured	Spatial resolution	Period of measurement and temporal resolution	Measurement method
Water table depth	Centre and West pit observation wells	2004-2005; half-hourly	pressure transducer
Soil temperature	Centre pit, 0.05-0.1 m depth interval	2003-2006; half-hourly	thermistor probes
Soil water content	Centre pit, 0.1 m depth interval 15 points, 0.05 m depth interval 1 m along transect T1, 0.2 m depth	2003-2006; half-hourly May 3-31, 2005; daily September 4, 2006	water content reflectometers *in situ* gravimetric measurements time domain reflectometry
Air temperature	meteorological station at plateau Fort Simpson airport	2003-2006; half-hourly 1999, 2002; daily	thermistor in a radiation shield
Rainfall	meteorological station at plateau Fort Simpson airport	2003-2006; half-hourly 1999, 2002; daily	tipping bucket rain gauge
Snow depth	1 m interval, transect T1 1 m interval, transect T2	1999, 2002-2006; daily 2004, 2005; daily	steel ruler
Snow water equivalent	5 m interval, transect T1 5 m interval, transect T2	1999, 2002-2006; daily 2004, 2005; daily	Eastern snow conference snow sampler and scale
Frost-table depth	2 m interval, transect T1 1 m interval, transect T1 1 m interval, transect T1, T2 and T3 Centre and West soil pits 15 soil sampling points 0.25 m interval in 5 m x 6.75 m grid	1999, 2002-2003* 2004-2006* May-June, '04,'05; daily April-June, '04, '05; daily May 3-31, 2005; daily June 12, 2006	graduated steel rod (frost probe)

* See Table 3-2 for measurement dates.

Table 3-2 Average daily frost-table depths measured on the peat plateau at the end of the spring and summer field seasons. Units expressed as meters below the ground surface. No measurements were made in the spring of 1999 and 2002.

Year	Day of measurement	Spring thaw depth (m)	Day of measurement	End-of-summer thaw depth (m)
1999	-	-	Sept. 18	0.57
2002	-	-	Aug. 26	0.64
2003	June 10	0.26	Aug. 26	0.60
2004	June 6	0.19	Sept. 15	0.55
2005	June 4	0.27	Sept. 5	0.69
2006	June 12	0.29	Sept. 3	0.72

Table 3-3 a) Geometric mean frost-table depths, standard deviations, and observed level of significance (*p*) for the difference between the two vegetation covers of moss and lichen. Units expressed as meters below the ground surface. Note: vegetation cover was not recorded in 2003. b) Mean volumetric water content (VWC), standard deviations, and observed level of *p* for the difference between the two vegetation covers at the 15 flagged sampling points during the spring thaw period of 2005, and at T1 on 4 September, 2006. "ns" means the data were not significantly different.

(a)	**June geometric mean thaw depths (m)**			**September geometric mean thaw depths (m)**		
	Moss	Lichen	*p*-value	Moss	Lichen	*p*-value
2004	0.21 ± 0.05	0.18 ± 0.05	= 0.05	0.62 ± 0.16	0.49 ± 0.07	< 0.01
2005	0.36 ± 0.06	0.27 ± 0.04	< 0.01	0.69 ± 0.16	0.57 ± 0.07	< 0.01
2006	0.30 ± 0.05	0.27 ± 0.04	= 0.02	0.81 ± 0.24	0.67 ± 0.11	< 0.02

(b)	**June VWC, 2005**			**September VWC, 2006**		
	Moss	Lichen	*p*-value	Moss	Lichen	*p*-value
	0.76 ± 0.17	0.49 ± 0.09	< 0.01	0.36 ± 0.23	0.29 ± 0.17	ns

3.9 Reference List

Aylsworth, J.M., Kettles, I.M. and Todd, B.J. 1993. Peatland distribution in the Fort Simpson area, Northwest Territories with a geophysical study of peatland-permafrost relationships at Antoine Lake. *Current Research, Geological Survey of Canada Paper* 93-1E: 141-148.

Bastien, J., Onclin, C. and Best, K. 2002. *Fort Simpson and Area Snow Surveys 2002*. NWRI internal report, unpublished data, Saskatoon, Canada.

Bayard, D., Stähli, M., Parriaux, A. and Flühler, H. 2005. The influence of seasonally frozen soil on the snowmelt runoff at two Alpine sites in southern Switzerland. *Journal of Hydrology* 309: 66-84.

Burgess, M.M. and Smith, S.L. 2000. Shallow ground temperatures. In *The physical environment of the Mackenzie Valley, Northwest Territories: a base line for the assessment of environmental change*, Dyke LD, Brooks GR (eds). Geological Survey of Canada Bulletin, 547: 89-103.

Buttle, J.M. and McDonald, D.J. 2002. Coupled vertical and lateral preferential flow on a forested slope. *Water Resources Research* 38(5): 1060, doi:10.1029/2001WR000773.

Carey, S.K. and Woo, M-K. 1998. The role of ground ice in active layer thaw. In *Proceedings, Seventh International Conference on Permafrost*, Yellowknife, Canada; pp. 127-131.

Carey, S.K. and Woo, M-K. 2001. Spatial variability of hillslope water balance, wolf creek basin, subarctic Yukon. *Hydrological Processes* 15: 3113-3132.

Carter, T. and Onclin, C. 1999. *Fort Simpson and Area Snow Surveys 1999*. NWRI internal report, unpublished data, Saskatoon, Canada.

Celia, M.A., Bouloutas, E.T. and Zarba, R.L. 1990. A general mass-conservative numerical solution for the unsaturated flow equation. *Water Resources Research* 26: 1483-1496.

Davis, J.C. 1973. *Statistics and Data Analysis in Geology*. Kansas Geological Survey, John Wiley and Sons, New York, N.Y.; 550 pp.

Dingman, S.L. 1973. Effects of permafrost on streamflow characteristics in the discontinuous permafrost zone of central Alaska. In *Permafrost: the North American contribution to the Second International Conference, Yakutsk, U.S.S.R*. Washington, National Academy of Sciences; pp. 447-453.

Dingman, S.L. 1975. *Hydrologic Effects of Frozen Ground: Literature Review and Synthesis*. CRREL Special Report 218, U.S. Army Corps of Engineers, Cold Regions Research and Engineering Laboratory, Hanover, NH.

Freer, J., McDonnell, J.J., Beven, K.J., Peters, N.E., Burns, D.A., Hooper, R.P., Aulenbach, B. and Kendall, C. 2002. The role of bedrock topography on subsurface storm flow. *Water Resources Research* 38: 1269, doi:10.1029/2001WR000872.

Glenn, M.S. and Woo M-K. 1987. Spring and summer hydrology of a valley-bottom wetland, Ellesmere Island, Northwest Territories, Canada. *Wetlands* 17: 321-329.

Goodison, B.E. 1978. Accuracy of snow samplers for measurement of shallow snowpacks: An Update. In *Proceedings of the 34th Eastern Snow Conference*. Hanover, New Hampshire; pp. 36-49.

Gray, J.T., Pilon, J. and Poitevin, J. 1988. A method to estimate active-layer thickness on the basis of correlations between terrain and climatic parameters as measured in northern Quebec. *Canadian Geotechnical Journal* 25: 607-616.

Hayashi, M., Goeller, N., Quinton, W.L. and Wright, N. 2007. A simple heat-conduction method for simulating frost table depth in hydrological models. *Hydrological Processes* 21: 2610-2622.

Heginbottom, J.A. and Radburn, L.K. 1992. Permafrost and ground ice conditions of Northwestern Canada. *Geological Survey of Canada, Map 1691A*, scale 1:1 000 000.

Hinkel, K.M. and Nelson, F.E. 2003. Spatial and temporal patterns of active layer thickness at Circumpolar Active layer Monitoring (CALM) sites in northern Alaska, 1995-2000. *Journal of Geophysical Research* 108(D2): 8168, doi: 10.1029/2001JD000927.

Hinkel, K. M., Outcalt, S.I. and Taylor, A.E. 1997. Seasonal patterns of coupled flow in the active layer at three sites in northwest North America. *Canadian Journal of Earth Science* 34(5): 667–678, doi:10.1139/e17-053.

Huyakorn, P.S. and Pinder, G.F. 1983. *Computational methods in subsurface flow*. Academic Press, San Diego, California; 473 pp.

Kane, D.L. and Chacho, E.F. 1990. Frozen ground effects on infiltration and runoff. In *Cold Regions Hydrology and Hydraulics*, W.L. Ryan and R.D. Crissman (eds). Technical Council on Cold Regions Engineering Monograph; pp. 259-300.

Kane, D.L., Hinkel, K.M., Goering, D.J., Hinzman, L.D. and Outcalt, S.I. 2001. Non-conductive heat transfer associated with frozen soils. *Global and Planetary Change* 29: 275-292.

Kellner, E. 2001. Surface energy exchange and hydrology of a poor *Sphagnum* mire. Acta Universitatis Upsaliensis, Kopieringshuset AB, Uppsala, 38 pp.

Iwata, Y., Hayashi, M. and Hirota, T. 2008. Comparison of snowmelt infiltration under different soil-freezing conditions influenced by snow cover. *Vadose Zone Journal* 7: 79-86, doi:10.2136/vzj2007.0089.

Lafleur, P.M., Hember, R.A., Admiral, S.W. and Roulet, N.T. 2005. Annual and seasonal variability in evapotranspiration and water table at a shrub-covered bog in southern Ontario, Canada. *Hydrological Processes* 19: 3533-3550.

Luetschg, M., Lehning, M. and Haeberli, W. 2008. A sensitivity study of factors influencing warm/thin permafrost in the Swiss Alps. *Journal of Glaciology* 54(187): 696-704.

Metcalfe, R.A. and Buttle, J.M. 1999. Semi-distributed water balance dynamics in a small boreal forest basin. *Journal of Hydrology* 226: 66-87.

Metcalfe, R.A. and Buttle, J.M. 2001. Soil partitioning and surface store controls on spring runoff from a boreal forest peatland basin in north-central Manitoba, Canada. *Hydrological Processes* 15: 2305-2324.

Meteorological Service of Canada (MSC) 2005. *National climate data archive of Canada.* Environment Canada: Dorval, Quebec.

National Wetlands Working Group (NWWG) 1988. *Wetlands of Canada: Ecological Land Classification Series, no. 24*. Sustainable Development Branch, Environment Canada, Ottawa, Ontario, and Polyscience Publications Inc., Montreal, Quebec; 452 pp.

Nelson, F.E., Hinkel, K.M., Shiklomanov, N.I., Mueller, G.R., Miller, L.L. and Walker, D.A. 1998. Active-layer thickness in north-central Alaska: systematic sampling, scale, and spatial autocorrelation. *Journal of Geophysical Research* 103: 28963-28973.

Nelson, F.E., Shiklomanov, N.I. and Mueller, G.R. 1999. Variability of active-layer thickness at multiple spatial scales, north-central Alaska, U.S.A. *Arctic, Antarctic, and Alpine Research* 31(2): 158-165.

Nelson, F.E., Shiklomanov, N.I., Mueller, G.R., Hinkel, K.M., Walker, D.A. and Bockheim, J.G. 1997. Estimating active-layer thickness over a large region: Kuparuk river basin, Alaska, U.S.A. *Arctic and Alpine Research* 29(4): 367-378.

Quinton, W.L., Carey, S.K. and Goeller, N.T. 2004. Snowmelt runoff from northern alpine tundra hillslopes: major processes and methods of simulation. *Hydrology and Earth System Sciences* 8(5): 877-890.

Quinton, W.L., Gray, D.M. and Marsh, P. 2000. Subsurface drainage from hummock-covered hillslope in the Arctic tundra. *Journal of Hydrology* 237: 113-125.

Quinton, W.L. and Hayashi, M. 2005. The flow and storage of water in the wetland-dominated central Mackenzie River basin: Recent advances and future directions. In: *Prediction in ungauged basins: Approaches for Canada's cold regions*, C. Spence, J.W. Pomeroy and A. Pietroniro (eds). Canadian Water Resources Association, Cambridge Ontario; pp. 45-66.

Quinton, W.L. and Marsh, P. 1999. A conceptual framework for runoff generation in a permafrost environment. *Hydrological Processes* 13: 2563-2581.

Romanovsky, V.E. and Osterkamp, T.E. 1997. Thawing of the active layer on the Coastal Plain of the Alaskan Arctic. *Permafrost and Periglacial Processes* 8: 1-22.

Rist, A. and Phillips, M. 2005. First results of field investigations on the hydrothermal processes within the active layer above alpine permafrost in steep terrain. *Norsk Geografisk Tidsskrift–Norwegian Journal of Geography* 59: 177–183.

Rouse, W.R. 2000. The energy and water balance of high-latitude wetlands: controls and extrapolation. *Global Change Biology* 6(1): 59-68.

Rouse, W.R. and Kershaw, K.A. 1971. The effects of burning on the heat and water regimes of lichen-dominated subarctic regimes. *Arctic and Alpine Research* 3(4): 291-304.

Rutter, N.W., Boydell, A.N., Savigny, K.W. and van Everdingen, R.O. 1973. *Terrain evaluation with respect to pipeline construction, Mackenzie pipeline construction: Southern part, Lat. 60^o to 64^{o}N*. Environmental-Social Committee Northern Pipelines, Task force on Northern oil development *Report N. 73-36*, Ottawa, Information Canada Cat. No. R72-10373; 135 pp.

Slaughter, C.W. and Kane, D.L. 1979. Hydrologic role of shallow organic soils in cold climates. In *Canadian hydrology symposium: Proceedings, 79- Cold climate hydrology*. National Research Council of Canada, Ottawa, Ontario; pp. 380-389.

Smith, M.W. 1975. Microclimate influences on ground temperatures and permafrost distribution, Mackenzie Delta, Northwest Territories. *Canadian Journal of Earth Sciences* 12, 1421–1438.

Spence, C. and Woo, M-K. 2003. Hydrology of subarctic Canadian shield: soil-filled valleys. *Journal of Hydrology* 279: 151-166.

Stadler, D., Bründl, M., Wunderli, H., Auckenthaler, A. and Flühler, H. 1996. Measurement of frost-induced snowmelt runoff in a forest soil. *Hydrological Processes* 10: 1293-1304.

Tromp-van Meerveld, H.J. and McDonnell, J.J. 2006. Threshold relations in subsurface stormflow: 2. The fill and spill hypothesis. *Water Resources Research* 42: W02411, doi:10.1029/2004WR003800.

Vitt, D.H. 2000. Peatlands: ecosystems dominated by bryophytes. *Bryophyte Biology*, J.R. Shaw J.R. and B.Goffinet (eds). Cambridge University Press, Cambridge; 312–343.

Weiler, M. and McDonnell, J. 2004. Virtual experiments: a new approach for improving process conceptualization in hillslope hydrology. *Journal of Hydrology* 285: 3-18.

Wigmosta, M.S. and Lettenmaier, D.P. 1999. A comparison of simplified methods for routing topographically driven subsurface flow. *Water Resources Research* 35: 255-264.

Woo, M-K. 1986. Permafrost hydrology in North America. *Atmosphere-Ocean* 24: 201-234.

Woo, M-K. and Steer, P. 1983. Slope hydrology as influenced by thawing of the active layer, Resolute, N.W.T. *Canadian Journal of Earth Sciences* 20(6): 978-986.

Woo, M-K. and Winter, T.C. 1993. The role of permafrost and seasonal frost in the hydrology of northern wetlands in North America. *Journal of Hydrology* 141: 5-31.

Wright, N., Quinton, W.L. and Hayashi, M. 2008. Hillslope runoff from an ice-cored peat plateau in a discontinuous permafrost basin, Northwest Territories, Canada. *Hydrological Processes* 22: 2816-2828, DOI: 10.1002/hyp.7005.

Young, K.L., Woo, M-K. and Edlund, S.A. 1997. Influence of local topography, soils, and vegetation on microclimate and hydrology at a High Arctic Site, Ellesmere Island, Canada. *Arctic and Alpine Research* 29(3): 270-284.

Preface to Chapter 4

While the previous two chapters were directly related to subsurface flow and runoff generation from a peat plateau, the following study is indirectly related to it. It is important to quantify the ground heat flux and understand what determines the presence of permafrost under current climate conditions, in order to predict future changes in runoff from permafrost slopes, as well as to elucidate the basin response to permafrost degradation. Though there are a growing number of studies on permafrost degradation, very few of these studies examine soil thaw in relation to the ground-surface energy balance and the factors controlling it. Given the recently reported increases in active layer thickness of permafrost landforms in northern latitudes, it seems appropriate to evaluate the factors controlling the ground heat flux of a peat plateau, as the previous chapter found the ground heat flux to be the primary mechanism of energy transfer for thawing frozen soil. The following chapter compares the annual surface energy balance and thermal regimes of a peat plateau and an adjacent permafrost-free wetland, for the purpose of identifying the site characteristics that control ground surface energy input rates, which impact runoff generation and the presence of permafrost on peat plateaus.

Chapter 4
Ground surface energetics and subsurface thermal regime of a perennially frozen peat plateau and a seasonally frozen bog

4.1 Introduction

Hydrological processes in northern latitudes are strongly influenced by the presence or absence of permafrost and peatlands (e.g. Slaughter and Kane, 1979; Woo and Winter, 1993; Quinton and Hayashi, 2005). Peatlands cover 1.1 million km^2, or 12% of the land surface in Canada (NWWG, 1988), most of which (97% by area) occur in the boreal (64%) and subarctic (33%) wetland regions (Tarnocai, 2006). Approximately 30% of peatlands in the High Boreal wetland region (defined by the National Wetlands Working Group, 1988) are underlain by permafrost (Zoltai, 1972; Seppälä, 1988; Aylsworth *et al*., 1993), and most commonly occur as tree-covered peat plateaus (Vitt *et al*., 1994). These permafrost peatlands are normally elevated 1 m above the surrounding seasonally-frozen bogs and fens, and can extend to several square kilometers in area (NWWG, 1988). The permafrost below peat plateaus is not a residual of the last glacial period, but is believed to have first developed about 4000 yr BP, during the period of climate cooling that followed the relatively warm middle Holocene (Zoltai and Tarnocai, 1975; Zoltai, 1993).

The ice-rich permafrost underlying these slopes confines most hydrological processes to a seasonally-frozen and thawed active layer. A significant portion of runoff from permafrost slopes is stored within the still-frozen part of the active layer early in the thaw season, and is slowly released as the active layer thaws (Woo and Heron, 1987;

Wright *et al*., 2008). Since flow through the active layer and the surface energy balance are linked by thawing of the impermeable frozen soil, their close coupling requires an understanding of the soil thaw rate in order to properly represent soil water flows in hydrological models (Woo, 1986; Wright *et al*., 2009). Thawing of the active layer occurs as a result of heat flux into the soil, which is the portion of net solar radiation transferred to the ground for thawing and warming of the soil and permafrost (Woo and Xia, 1996). The rate of downward thaw depends on the energy input at the surface and thermal diffusivity, which is strongly influenced by soil moisture conditions and vegetation cover (Rouse and Kershaw, 1971; Kane *et al*., 2001).

Very small changes in surface climate conditions can produce significant changes in permafrost temperatures (Lachenbruch and Marshall, 1986). Increases in shallow ground temperature and active layer thickness in the discontinuous permafrost zone has been observed in recent decades (Beilman and Robinson, 2003; Osterkamp, 2005), indicating degradation of warmer permafrost that is largely attributed to climate warming (Camill, 2005; Osterkamp, 2005). As ground ice can occupy a large proportion (up to 80%) of a peat plateau soil volume, permafrost thawing can trigger major changes in the surface topography through soil subsidence, and hydrology, which in turn affects the ground surface vegetation, nutrient and water cycling, and carbon and methane storage (Jorgenson *et al.,* 2001; Tarnocai, 2006; Turetsky *et al*., 2007).

To understand the potential impact of climate warming on permafrost peatlands, it is important to understand what controls the presence or absence of permafrost under current climate conditions. This study measures and compares the annual surface energy balance and thermal regimes of a peat plateau and an adjacent permafrost-free wetland,

for the purpose of identifying the site characteristics that control ground surface energy input rates, which impact runoff generation and the presence of permafrost on peat plateaus. More specifically, this study will: 1) quantify the partition of net radiation at the surface into sensible, latent and ground heat flux at the two sites during the spring thawing period; 2) determine the relative importance of short and long-wave contributions to the annual radiation budget, to discern the effects of canopy cover; 3) compare the annual soil thermal regime at the two sites, and examine the effects of soil moisture on the differences observed; and 4) relate soil thaw depth to energy supply at the ground surface, and how this varies seasonally.

4.2 Study Site

Field data were collected at Scotty Creek (61°18'N, 121°18'W), a 152 km^2 basin located in the lower Liard River valley, 50-km south of Fort Simpson, Northwest Territories, Canada (Figure 4-1a). The 1975-2005 climate data recorded at the Environment Canada station in Fort Simpson (169 m a.s.l) indicates the mean annual air temperature is -2.8 ^oC, which is 1.3 ^oC higher than the mean annual temperature during the preceding 30 years (1944-1974) (MSC, 2005). The mean annual precipitation for the same period (1975-2005) is 369 mm, 45% of which occurs between June and August; winter snowfall represents 44% of the total annual precipitation (MSC, 2005). The basin's snowpack generally begins to ablate in late March, and the snowmelt period usually lasts from two to six weeks depending on spring climatic conditions; during which time, the majority of the annual basin runoff occurs.

The National Wetlands Working Group (1988) indicates that the Fort Simpson peatlands are in the Continental High Boreal Wetland Region of Canada. Peat deposits in

the region have an average thickness of 2.4 m in bogs (though they vary in thickness from 0.5 m to 8 m), and are underlain by a mineral silt-sand layer ranging in thickness up to 1 m, which in turn covers a thick layer (averaging 6 m) of glaciolacustrine clay (Rutter *et al*., 1973; Aylesworth *et al*., 1993). Peat landforms in this region are typical of the discontinuous permafrost zone (Zoltai and Tarnocai, 1975), and include seasonally frozen channel fens and flat bogs, and raised frozen peat plateaus. This study focuses on field measurements made at a peat plateau and adjacent flat bog in the centre of the Scotty Creek peatland-complex located in the upper-reaches of Scotty Creek (61°18'48.9"N, 121°18'22.7"W; Figure 4-1b). Spatial analysis of a *ca.* 22 km^2 representative sample of this complex (see insert of Figure 4-1b) indicated that the ratio of peat plateaus to flat bogs is 43:37. The physical and hydrological characteristics of the peat plateau have been described in detail (Quinton and Hayashi, 2005; Wright *et al*., 2008); here we focus on the characteristics that distinguish the plateau from the bog.

The ground surface of the plateau rises 0.9 m above the surrounding permafrost-free terrain. Permafrost thickness has not been measured at the study plateau, but is 5-10 m under other peat-covered sites near Fort Simpson (Burgess and Smith, 2000). The base of the active layer measured over four consecutive years (2003-2006) extends to an average depth of 0.64 m ± 0.18 m, though peat in wet depressions has been observed to thaw to depths greater than 1 m. The plateau supports a sparse tree canopy (1 stem m^{-2}) composed predominantly of relatively short (mean height was 3.1 ± 2.2 m; maximum height was 9.3 m) black spruce trees (*Picea mariana*), and a few Jack pine (*Pinus banksiana*) seedlings. The average leaf area index (LAI) across the peat plateau was 1.45, measured on September 17, 2004 using a TRAC instrument (Tracing Radiation and

Architecture of Canopies; Leblanc *et al*., 2002). Shrubs occupy 56% of the understorey, of which Labrador tea (*Ledum groenlandicum*) is the dominant. The ground cover is dominated by lichen (mostly *Cladina* spp.), covering 65% of the forest floor, while the remaining 35% is occupied by moss (mostly *Sphagnum* spp.).

The bog is a seasonally-frozen, wetland; its water table remains near the ground surface throughout the year. The bog surface is relatively fixed, and is completely covered by moss (predominantly *Sphagnum fuscum* and *Pleurozium schreberi*). Ericacous shrubs, such as leatherleaf (*Chamaedaphne calyculata*), bog birch (*Betula glandulosa*) and northern bog-laurel (*Kalmia polifolia*), grow on slightly raised hummocks (up to 30-cm above the water table in summer). The bog has a few stunted and scattered black spruce and tamarack (*Larix laricina*), and is surrounded on three sides by peat plateaus.

4.3 Methods

4.3.1 Surface energy balance equation

The energy balance of the snow-free plateau and bog ground surfaces was computed daily during the 2005 spring field season, from 27 April to 4 June. The energy balance of the ground surface is expressed as:

$$Q^* = K\downarrow - K\uparrow + L\downarrow - L\uparrow = Qg + Qe + Qh + Qa + Qp \qquad (4.1)$$

where net all-wave radiation (Q^*), incoming (↓) and outgoing (↑) solar radiation (K) and longwave radiation (L), ground heat flux (Qg), and the turbulent fluxes of latent (Qe) and sensible heat (Qh) all have units of W m^{-2}. There was insufficient data to quantify the advection of energy from the lateral (subsurface or overland) flow of water (Qa). In a previous study, the vertical infiltration of water during the spring rain events of 2005

were found to have little effect on soil thawing rates (Wright *et al*., 2009), and therefore, the energy from rain infiltration (*Qp*) was considered negligible. *Qh* was solved as a residual of the energy balance equation, and the other terms in Eq. (4.1) were measured or estimated following the methods described in the sections below.

4.3.2 Site instrumentation

Similar instrumentation was installed on two meteorological stations, one located at the plateau, approximately 10 m from its western edge, and the other at the bog, approximately 100 m from its western edge (also the eastern edge of the plateau) (Figure 4-2). Net radiation and upward and downward-directed short and long wave radiation were measured at the meteorological stations (Kipp & Zonen, CNR1), 2 m above a moss-covered ground surface at the plateau, and 1.5 m above a moss and sedge-covered ground surface at the bog. Wind speed at 2.7 m (plateau) and 2.2 m (bog) (Met One 014A), and relative humidity and air temperature at 2 m (Vaisala, HMP45C) were also measured at the meteorological stations. Soil temperature sensors (Campbell Scientific 107B) were vertically attached to a wooden dowel and installed next to the bog meteorological station at depths of 0.1 and 0.3 m. The plateau had two existing instrumented soil pits, both located within 5 m on either side of the meteorological station. The Centre soil pit was used in this study, because it had a greater number of temperature and moisture sensors. The Centre pit was instrumented with thermistor probes (Campbell Scientific 107B) at 0.05, 0.1, 0.15, 0.2, 0.25, 0.3, 0.4, 0.5, 0.6, and 0.7 m depths; water content reflectometers (Campbell Scientific CS615) at 0.1, 0.2, 0.3 and 0.4 m depths; and a heat flux plate (Campbell Scientific, HFT3) at 0.05 m depth. The water content reflectometers (WCR) were calibrated against the water content of 17 peat samples (sample volume = 82 cm^3)

that were collected from the face of the soil pit at the time of installation, and the heat flux plate was calibrated following the results of Hayashi *et al*. (2007, p. 2616-2617). The 17 peat samples used to calibrate the WCR sensors at the plateau, and 19 peat samples (sample volume = 162 cm^3) collected at 0.05-m depth intervals to a depth of 0.4 m at the bog soil pit, were used to measure soil porosity and bulk density in the laboratory following the approach of Quinton *et al*. (2000). Snow depth and snow water equivalent (SWE) measurements commenced at the peak of the snow-accumulation season, and were made daily at both the bog and plateau soil pits, using a steel ruler and an Eastern Snow Conference snow sampler (ESC-30) (Goodison, 1978) and scale (calibrated to ± 3 mm). Lowering of the snow surface during the winter months (October-April) was monitored with a sonic ranging sensor (Campbell Scientific, SR50) located on the meteorological station at the peat plateau. The distance to the snow surface measured from the SR50 sensor was converted to snow depth via manual snow depth measurements made daily at the meteorological tower in the spring of 2005. Rainfall was measured using tipping-bucket rain gauges (0.2-m diameter, 0.35 m height, with a 0.26 mm bucket tip) located at the plateau and bog meteorological stations. Two PVC (polyvinyl chloride) observation wells located at the Centre pit (0.1 m inner diameter, 0.7 m depth) and near the bog meteorological station (0.05 m inner diameter, 1.5 m depth), were instrumented with Global Water WL15 pressure transducers that measured the elevation of the water table every minute, and averaged and recorded these measurements every 30 minutes. The water table depth at each of the wells was also measured manually with a water level sounder and ruler on a daily basis during the spring field campaign, to ensure the accuracy of the transducer measurements. All other sensors were connected to

Campbell Scientific, CR10X dataloggers, programmed to measure every minute and averaged and recorded every 30 minutes.

The plateau radiometer was moved to the bog weather station for a 24-hr period (23 August, 12:00 to 24 August, 12:00, 2008), in order to cross-reference it with the bog radiometer; which were set at a logging interval of 10-minute average. When the 24-hour data were compared, the difference between the Plateau sensor and Bog sensor was insignificant for both shortwave (K↓bog = 0.9968· K↓plateau in W m^{-2}, r^2 = 0.99) and longwave (L↓bog = 0.9949· L↓plateau in W m^{-2}, r^2 = 0.99) radiometers, giving confidence in the comparison of radiation terms at the two land covers. Ground surface temperature was estimated from long-wave radiation (L) measured by the radiometers and the Stefan-Boltzmann equation (Oke, 1987):

$$\sigma\varepsilon T_s^4 = L\uparrow + (1- \varepsilon)\, L\downarrow \qquad (4.2)$$

where σ is the Stefan-Boltzmann constant and ε is surface emissivity, assumed to be 0.98. The overall accuracy of measuring surface temperature from the radiometer and Eq. (4.2) is expected to be within 2 ^{o}C (Hayashi *et al*., 2007). This was validated by comparing the daily mean surface temperature computed from the plateau sensor using Eq. (4.2), with that measured by an infrared thermocouple (IRT) sensor (Apogee Instruments, IRTS-P) located 1.5 m above the Centre pit, during the winter months of 2005 (October 2004 to April 2005) when the difference in surface temperature between the bog and plateau was the greatest. The average difference in daily mean surface temperature during this period was 1 ^{o}C (the radiometer was higher) with a standard deviation of 2.4 ^{o}C. The IRT sensor had an instrumental accuracy of 0.3 ^{o}C, according to the manufacture's specification.

4.3.3 Latent heat flux estimation

During the spring field season (27 April- 4 June), direct measurements of evapotranspiration (*ET*, in mm day^{-1}) were used to determine the latent heat flux (*Qe*) from the plateau and bog. At each of the land covers, *ET* was measured daily from 5 identical evaporation pans (translucent plastic pails of 0.19 m diameter and depth) and 10 soil lysimeters (0.19 m diameter; same as the evaporation pans), following the methodology described in Wright *et al*. (2008). In summary, daily evaporation from pools was obtained by measuring the volume of water required to restore the water level in the evaporation pans to a fixed mark. The daily rate of evapotranspiration from the moss and lichen surfaces at the plateau, and the moss surface at the bog, was computed from the daily change in the weight of the soil-filled lysimeters, measured gravimetrically. The total daily *ET* for the plateau was computed as a weighted average based on the measured evaporation and percent cover of moss, lichen and meltwater pools on the plateau. The total daily *ET* computation for the bog was similar to that at the plateau, where it was computed as a weighted average based on the measured evaporation and percent cover of moss and pools, which was estimated weekly from the relative proportion of the two ground cover types measured in a 1 × 1 m grid, every metre along a 68-m transect that traversed the bog.

For the 11 days when the lysimeter data were unreliable due to rainfall, *ET* from the plateau and bog was estimated using the Priestley and Taylor (1972) method. For these computations, all meteorological variables were supplied by the measurements made at the meteorological stations, and the ground heat flux was computed from the calorimetric method described in *4.3.4*. Direct measurements of evapotranspiration from

the pans and lysimeters were plotted against equilibrium evaporation to determine the dimensionless coefficient, α for the bog and plateau ground surfaces.

4.3.4 Ground heat flux estimation

Ground heat flux (*Qg*) into the plateau and bog soil column is comprised of three terms:

$$Qg = Qi + Qs + Qc \tag{4.3}$$

where *Qi* is the latent heat used to melt ice, *Qs* is the sensible heat storage in the soil column, and *Qc* is the heat conducted into and out of the bottom of the soil column. A fixed soil column thickness of 0.7 m was used, because the deepest temperature sensor at the plateau was at 0.7 m; the bog soil column was set to the same thickness, in order to make a direct comparison of plateau and bog *Qg*. Ground heat flux at the bog was computed daily from the calorimetric method (Woo and Xia, 1996) during spring (27 April to 4 June), and a numerical simulation of heat conduction (see Appendix 2) during the summer (to 31 August) of 2005. The calorimetric method was also used to compute daily *Qg* at the plateau, but only until the frost table at the Centre pit reached a depth of 0.5 m (12 June, 2005), after which time *Qg* was estimated from the heat flux plate. The calorimetric method was not used to compute plateau *Qg* for the entire study period, because extrapolating the water content data at 0.4 m (deepest WCR) to depths below 0.5 m was considered unreliable. Hayashi *et al*. (2007) gives an extensive description of the calorimetric method used to compute ground heat flux (*Qg*) at the peat plateau, as well as the *Qg* totals for the plateau from 27 April to 12 June, 2005. Therefore, the following gives a brief overview of the methodology, focusing on the calorimetric computation and the one-dimensional simulation of *Qg* at the bog.

Daily values of Qi were computed from the daily rate of change in frost table depth (Δz) and the latent heat required to thaw the frozen soil (λ) (Woo and Xia, 1996):

$$Qi = \rho \lambda f_{ice} \Delta z \tag{4.4}$$

where ρ is the density of ice and f_{ice} is the fraction of ice in the soil. This method assumes that the frost table, or zero-degree isotherm, coincides with the upper surface of the frozen, water- (and ice-) saturated soil. This was verified for both land-covers by comparing the depth to the zero-degree isotherm, interpolated from the soil temperature data at the instrumented soil pits, with the thickness of the thawed soil layer measured at the same soil pits using a frost probe, which clearly detected the top of the frozen layer. The water table depth at the bog fluctuates between 0.05 and 0.1 m during the summer months, suggesting that the bog soil column is likely saturated at depths below 0.1 m prior to ground thaw in spring. The f_{ice} of saturated soil was determined by subtracting the volumetric liquid water content (unfrozen VWC) from the depth-derived soil porosity (see 4.3.2 for methods). The frozen bog soil was assumed to have an unfrozen VWC of 0.2, based on the WCR data at the plateau soil pit, which showed the water content was close to 0.2 at all depths while the soil was frozen (Hayashi *et al.*, 2007). A moss-covered frozen soil core extracted from the peat plateau prior to ground thaw in 2003 was reported by Hayashi *et al.* (2007, Fig. 4(a)) to have a total volumetric moisture content (total VWC) of 0.8 at depths below 0.1 m, indicating saturation. Given that the bog soil and moss-covered frozen soil core were both saturated at depths below 0.1-m depth, it seemed reasonable to assume that the upper 0.1 m of bog soil had a similar total VWC as the moss-covered frozen soil core (0.6). Thus, the f_{ice} of unsaturated soil at the bog was

determined from the depth profile of the volumetric fraction of ice measured for the moss-covered frozen soil core.

To calculate *Qs*, the soil was divided into computational layers representing the depth of the soil temperature sensors. Daily values of *Qs* were calculated from the daily rate of temperature change and the specific heat of the soil (Hayashi *et al.*, 2007; Eq. (14)). The volumetric heat capacity (*C*) of the soil layers was computed from the fractional components of peat, water, and air (de Vries, 1963). Table 4-1 presents an overview of the soil physical and thermal properties of the upper 0.5 m of the bog and plateau, used in the computation of *Qs*. At the plateau, the fractional component of liquid water content (f_{water}) was measured from the WCR sensors; however, the bog had no WCR sensors and had to be estimated as follows. The f_{water} of the thawed, saturated portion of the bog soil layers was assumed to equal the average porosity of the saturated layer, where the latter was derived from the single-valued function of porosity with respect to depth measured at the bog soil pit at the time of instrument installation. The f_{water} for unsaturated bog soil layers was estimated from daily volumetric liquid water content measurements made gravimetrically at 0.05-m depth increments to the water table at 10 sampling locations, using 162-cm^3 soil sample tins. The depth-dependant daily average values of volumetric liquid water content measured at the 10 sampling locations were used for days in which the volumetric liquid water content were not measured, due to rainfall. In order to estimate the f_{water} in bog soil layers that were partially saturated, the volumetric liquid water content (unfrozen VWC) measured from the 0.1-m deep WCR sensor at the plateau soil pit was compared with water-table (WT) depth during the spring (to June 4), when the plateau WT was within the upper 0.15-m soil layer; this depth was

chosen because the bog WT depth did not drop below 0.12 m during spring and summer. There was a relatively good correlation between the unfrozen VWC and water-table depth at the plateau [unfrozenVWC=(-1.994·WTdepth)+0.7976, r^2=0.95]; this relationship was used to determine the unfrozen VWC of the partially saturated bog soil layers, using the daily water table depth measurements made at the bog.

Daily values of *Qc* in the plateau were computed from the conductivity and thermal gradient method (Hayashi *et al*., 2007, p. 2614). Daily values of bog *Qc* were also computed from the conductivity and temperature gradient between 0.5 and 0.7-m depths, using soil temperatures and the thermal conductivity (λ) simulated from a one-dimensional heat transport model that was used to compute ground heat flux into the bog surface during the summer period. One-dimensional heat transport into the bog ground surface was simulated using an explicit-in-time finite difference method to numerically compute the Fourier's equation (see Appendix 2 for methodology). The model was calibrated by varying the thermal diffusivity (*D*) to fit the average daily soil temperature data recorded at 0.1 and 0.3-m depths at the bog soil pit. Statistical analysis of the modeled results follows the methods of Willmott (1982). From the best-fit value of thermal diffusivity, thermal conductivity was back-calculated from an independent estimate of heat capacity (*C)*. *Qg* was then computed from the product of the gradient at the surface (calculated for z = 0 and 0.3 m) and thermal conductivity.

4.4 Results

4.4.1 Spring surface energy balance

Mean daily fluxes of the individual energy balance terms [Eq. (4.1)] computed during the spring field season, from 27 April to 4 June, are shown in Figure 4-3. During

this time, the total net radiation (Q^*) at the ground surface was 26% greater at the bog than at the plateau (Table 4-2). Total ground heat flux *(Qg)* at the plateau (74.3 MJ m^{-2}) and bog (73.9 MJ m^{-2}) were very similar during spring, though the ratio of Qg/Q^* was 25% greater at the plateau than at the bog (Table 4-2). Mean daily evapotranspiration (*ET*) from the bog (2.9 mm day^{-1}) was almost double that from the plateau ground surface (1.5 mm day^{-1}). By 4 June, the cumulative *ET* at the bog was 113 mm, compared to 57 mm at the plateau, which is reflected in the large difference in the latent heat flux (*Qe*) at the two sites (Table 4-2). *ET* was greater at the bog than the plateau, because the bog had a relatively unlimited availability of moisture at the surface (Figure 4-4), greater net all-wave radiation, and a daily average wind speed that was 67% greater than at the plateau. While the latent heat flux (*Qe*) was the largest fraction (60%) of Q^* at the bog, the sensible heat flux (*Qh*) was largest (42%) at the plateau; thus the daily average Bowen ratios (β) were larger at the plateau (1.1) than at the bog (0.4) (Table 4-2).

4.4.2 Uncertainty in the energy balance calculation

The accuracy for daily totals of net radiation is ± 10%, according to the manufactures specification. The difference in daily radiation flux totals at the bog and plateau are relatively insignificant as described in section 4.3.2. The accuracy of *Qe* is dependant on the field measurement and computation of *ET*. The potential error in measuring evapotranspiration, taken to be equal to the areally weighted, mean daily standard error of the five pool evaporation pans and the ten soil lysimeters, was 0.15 mm day^{-1}, or 9% of the mean daily evapotranspiration for the 28 days in which *ET* was measured on the plateau in 2005, and 0.5 mm day^{-1}, or 15% of the mean daily evapotranspiration for the 28 days in which *ET* was measured on the bog. For those days

in which *ET* had to be estimated from the Priestley and Taylor (1972) method, errors could be as high as 15% (Shuttleworth, 1993).

The calorimetric method is sensitive to estimates of soil water content for the computation of *Qs*, and ice content for the computation of *Qi* (Halliwell and Rouse, 1987). However, the cumulative total *Qg* on the plateau from 27 April to 12 June, 2005 was 96 MJ m^{-2} using the calorimetric method and 98 MJ m^{-2} using the heat flux plate; indicating that we can treat the calorimetric data with a reasonable degree of confidence. Based on the day-to-day variations of the two computations, the accuracy of *Qg* at the plateau is estimated to be ± 19%. However, bog *Qg* may be underestimated by as much as 50%, because *Qs* could not be computed until the bog soil temperature at 0.3 m rose above 0^{o}C (on 21 May), resulting in 24 days during the spring computation period, in which *Qs* was computed for the plateau, but not the bog. Likewise, *Qc* values may also be underestimated given that the deepest soil thermistor at the bog was 0.3 m, and therefore, the temperature at 0.5 and 0.7-m depths had to be simulated from the heat transport model (Appendix 2). However, the error is likely minor given that *Qc* computed for the soil layer above this totalled only 0.03 MJ m^{-2} during the 24 missing days in 2005, or 0.005% of the total *Qc* computed over the same time period.

Based on the error estimates of individual energy balance components, and noting that some errors may cancel each other over the entire period, we expect that the computed sensible heat flux, *Qh* in Table 4-2 may have an error margin of 10-20% at the plateau and 20-30% at the bog, although this only provides a rough estimate.

4.4.3 Annual net radiation balance

To further examine the differences in radiation input and determine the relative importance of short and long-wave contributions to the plateau and bog ground surface, the 2004-2005 annual radiation balance was computed, and divided into the soil freezing period, from 1 October 2004 to 26 April 2005, and the soil thawing period, from 27 April to 30 September, 2005. The large day-to-day variability of Q^* at both sites during the soil thawing period (Figure 4-5a) mirrored that of incoming shortwave radiation ($K\downarrow$), which experienced annual maximum average values in May and June (Figure 4-5b). During the soil thawing period, incoming ($\downarrow$) and outgoing ($\uparrow$) longwave radiation (L) was less than 5% greater at the plateau than at the bog; while during the same time period, the bog surface received 25% more incoming shortwave ($K\downarrow$) and reflected ($K\uparrow$) 70% more shortwave radiation than the plateau (Table 4-3a). Thus, the total net radiation (Q^*) at the ground surface was 17% greater at the bog (1440 MJ m^{-2}) than at the plateau (1232 MJ m^{-2}) (Table 4-3a). So while the plateau had greater $L\downarrow$ to its ground surface, the canopy restricted enough atmospheric $K\downarrow$ to the surface through shading, to reduce Q^* at the plateau surface below that received at the bog surface.

During the soil freezing period, incoming shortwave radiation ($K\downarrow$) was significantly reduced at both surfaces (Figure 4-5b), due to fewer daylight hours (e.g. Figure 4-6), and net longwave radiation (L^*) to the surface was enhanced (Table 4-3b). During this period, the bog surface received 40% more $K\downarrow$ than the plateau surface, but reflected ($K\uparrow$) 86% more shortwave radiation. Thus, the plateau surface received 10% more net shortwave radiation (K^*) than the bog in winter (Table 4-3b). The plateau surface also received 23% more net longwave radiation (L^*) than the bog surface (Table 4-3b); the difference in L^* between the two land covers was greatest between February

13 and March 9, during which time $L\downarrow$ was greater at the plateau surface (Figure 4-5c). The greater amount of K^* and L^* at the plateau ground surface, meant it received 72% more Q^* (199 MJ m^{-2}) than the bog surface (116 MJ m^{-2}) during the soil freezing period (Table 4-3b). The difference in total annual net all wave radiation at the bog and plateau from October 2004 to October 2005 was relatively small (125 MJ m^{-2}); Q^* was 8.7% greater at the bog than at the plateau.

To examine the effects of the tree canopy on direct and diffuse radiation, and how the effects change with solar angle, average half-hourly radiation flux densities at the plateau and open bog were compared for four 24-hour periods: a cloudless (11 June) and cloudy (completely overcast) day (14 June) during the soil thawing/summer period, and a cloudless (9 November) and cloudy day (12 November) during the soil freezing/winter period (Figure 4-6). At both surfaces, incoming solar radiation ($K\downarrow$) decreased with both increased cloud cover and decreased solar elevation. The difference in radiation fluxes at the two ground surfaces was greater on clear days (Figure 4-6 a, c) than on cloudy days (Figure 4-6 b, d). Outgoing longwave radiation ($L\uparrow$) at both surfaces (Figure 4-6) was greater during the soil thawing/summer period than the soil freezing/winter period. $L\uparrow$ was greater at the plateau than at the bog during both the cloudless and cloudy days of summer (Figure 4-6), likely because the plateau surface temperature was higher than the bog during this period (Figure 4-7). This was also true for the clear and cloudy days of winter; however, the difference in $L\uparrow$ was much greater for the snow-covered bog and plateau surfaces in winter than for the snow-free surfaces in summer. The total outgoing flux of longwave radiation ($L\uparrow$) was greater than the incoming flux ($L\downarrow$) in summer (Figure 4-6), resulting in a net longwave (L*) deficit, which was on average, greater at

the bog than at the plateau. The opposite was true in winter, though the difference in $L\uparrow$ compared to $L\downarrow$ was much less on cloudy days (e.g. 12 November) than on clear days (e.g. 9 November) (Figure 4-6), which resulted in a net gain in longwave radiation received at both surfaces.

4.4.4 Annual air and soil thermal regime

Figure 4-8 shows the air, ground surface and soil temperatures at the plateau and bog from October 2004 to October 2005, to illustrate their thermal regimes. Average daily air temperatures were similar at the two snow-covered ground surfaces during the frozen/winter period of 1 October to 26 April (-13.9 ^{o}C at the bog and -13.1 ^{o}C at the plateau), and at the two snow-free surfaces during the unfrozen/summer period of 27 April to 30 September (11.6 ^{o}C at the bog and 11.9 ^{o}C at the plateau). On clear-sky days, the air above the bog was cooler than the air above the plateau during the daytime, while at night air temperatures at the two landcovers were similar during summer, and colder at the bog during winter (Figure 4-7).

The bog surface was warmer than the air in summer and colder in winter, while the plateau surface was warmer than the air in both summer and winter. The average daily temperature of the snow-free ground surface was similar at the bog (13.8 ^{o}C) and plateau (13.9 ^{o}C) (Figure 4-8). On clear-sky days in summer (e.g. 11 June), the surface of the bog was warmer at night, compared to the plateau surface, and cooler during the day. The same was true on cloudy-sky days in summer (e.g. 14 June); the bog surface temperature was warmer in the evening, relative to the plateau surface, and cooler during the day (Figure 4-7). The same pattern was observed for clear (e.g. 9 November) and cloudy-sky (e.g. 12 November) days during winter (October-April). The average snow-

surface temperature at the plateau (-12.7 ^{o}C) was 1.7 ^{o}C warmer than at the bog (-14.4 ^{o}C). However, this temperature difference is likely to be much less (approximately 0.7 ^{o}C) given the accuracy of the method [Eq. (4.2)] used to determine ground surface temperature during winter (see *4.3.2*) The snow-surface temperature is likely influenced by air temperature, given that the difference in air and surface temperature was 0.4-0.5 ^{o}C at both the plateau and bog during this period.

While the plateau had greater surface temperatures, the bog had much warmer soil temperatures during both the frozen and unfrozen periods. While the soil was frozen (October-April), its average temperature at 0.1-m depth in the bog (-0.12 ^{o}C) was 1.7 ^{o}C higher than in the plateau (-1.8 ^{o}C); a similar difference in the average temperature at 0.3-m was observed at the two sites (0.74 ^{o}C in the bog and -0.92 ^{o}C in the plateau). In the thawed state, the average soil temperature difference at 0.1-m in the bog and plateau was 1.4 ^{o}C (11.4 ^{o}C in the bog compared to 10 ^{o}C in the plateau); while the temperature difference at 0.3-m depth was 5.6 ^{o}C (11.4 ^{o}C in the bog and 5.8 ^{o}C in the plateau).

The effect of snow cover is often cited as the principal source of the temperature difference between the air and the ground (e.g. Gold and Lachenbruch, 1973). The difference in surface and soil temperatures at the bog and plateau may be due to differences in the timing and amount of snow accumulation at the two land-covers. The plateau experienced very cold air temperatures while the snow pack was still relatively thin in early winter (October-December) (Figure 4-9); unfortunately, we lack snow data for the bog during this period to compare to the plateau. Peak snow depth measured at the two soil pits on 10 April was 0.84 m at the bog and 0.79 m at the plateau.

Soil water content controls the amount of latent heat released with freezing, and thus affects the rate of soil freezing, which in turn influences the timing of soil thaw in the following spring. With a greater volume of water (as indicated by the high water table, Figure 4-4), the bog had a higher heat capacity than the plateau (Table 4-1) and soil temperatures remained isothermal at or near 0 ^{o}C (referred to as the "zero-curtain") for a longer period of time; thus, it took longer for the bog to freeze. For example, the temperature at 0.1-m depth in 2004 dropped below 0 ^{o}C on 4 October at the plateau and nearly a month later (1 November) at the bog (Figure 4-8). The difference in the timing of soil freezing was even greater at 0.3 m-depth, with the temperature at this depth dropping below 0 ^{o}C on 13 October in the plateau, and on 27 January in the bog (Figure 4-8), but remaining isothermal at or near 0 ^{o}C for approximately a month at the plateau (October-November), and five months at the bog (December-May) (Figure 4-8). The bog was able to off-set the freezing process for a much longer period, because the higher water content meant that the bog soil released 5 times the amount of latent heat than the plateau, based on the difference in unfrozen moisture content before and after freezing at each landcover.

4.4.5 Evaluation of the heat transport model in computing bog soil temperature and thermal conductivity

The accuracy of the estimated ground heat flux primarily depends on the accuracy of the thermal conductivity (λ, 0.5 W m^{-1} K^{-1}) estimate, which was found from the best-fit value of thermal diffusivity (D, 0.12 x 10^{-6} m^{2} s^{-1}) and an independent estimate of heat capacity (C, 4.13 x 10^{6} MJ m^{-3} K^{-1}). The forward-differencing method (Appendix 2) did reasonably well in simulating bog soil temperatures (Figure 4-10), giving confidence in

the use of the best-fit value of thermal diffusivity in computing bog *Qc* and *Qs* from the thermal gradient method. Based on the percent difference of measured and modeled soil temperatures, we estimate the error of thermal diffusivity to be about ± 2.4%. The volumetric heat capacity is controlled by water content, and therefore, any error in this measurement will reduce the accuracy of the heat capacity estimate. Based on the methods used to determine the water content of the bog (section 4.3.4.), we estimate a potential error of ± 5% for *C*. Given the accuracy estimated for *D* and *C*, errors for λ are approximately ± 8%, or a value between 0.46-0.54 W m^{-1} K^{-1}.

4.4.6 Ground heat flux estimation

The differences in the volume of liquid and frozen water, soil thaw rate and temperature gradient between the bog and plateau, produce different partitioning of the ground heat flux (*Qg*) into ice melt (*Qi*), soil warming (Q_S), and heat conduction (*Qc*) components (Table 4-4**)**. During the spring computation period (27 April- 4 June), *Qg* was dominated by *Qi*, which accounted for 88% of total *Qg* at the plateau, and 66% at the bog. The plateau required 34% more energy to melt ice (*Qi*) than the bog (Table 4-4). This was largely due to the greater volume of ice that had thawed at the plateau during this time, as the thaw depth at the plateau was 0.4 m on 4 June, while the thaw depth at the bog was 0.3 m prior to becoming frost-free on 21 May. During the same time period, *Qs* at the bog (20.5 MJ m^{-2}) was more than double that at the plateau (7.6 MJ m^{-2}), and comprised 28% of total *Qg* at the bog, and 10% at the plateau. The greater *Qs* at the bog was largely due to the relatively high heat capacity (*C*) of the bog soil (Table 4-1), owing to its high moisture content. *Qc* values were small in comparison to *Qi* and *Qs* values

(Table 4-4), and comprised a relatively small percentage of total *Qg* at the bog (6%) and the plateau (2%).

During the spring computation period (to 4 June), total *Qg* at the plateau (74.3 MJ m^{-2}) and bog (73.9 MJ m^{-2}) were very similar. However, there was a reversal in the magnitude of *Qg* at the bog shortly after the disappearance of ice (Figure 4-11), so that in the months following, the plateau continued to have high *Qg* due to the presence of ice, while *Qg* at the bog was used only to warm the unfrozen peat. As a result, *Qg* at the plateau totalled 171 MJ m^{-2} by August 31, while *Qg* at the bog totalled 111 MJ m^{-2} (Figure 4-11), despite the higher Q^* input to the bog (870 MJ m^{-2} versus 764 MJ m^{-2} at the plateau). From 27 April to 31 August, cumulative ground heat flux (*Qg*) was 15% of cumulative Q^* at the plateau, and 8% of cumulative Q^* at the bog. The total annual ground heat flux of the plateau from October 2004 to October 2005, estimated from the heat flux plate at the Centre pit, was 7.6 MJ m^{-2}.

4.5 Discussion and Conclusion

The tree canopy and differences in soil moisture and albedo were largely responsible for the different energy and thermal regimes observed at the peat plateau and bog. Trees have a low albedo, and are thus, efficient absorbers of incoming shortwave radiation (Gryning *et al*. 2001). Likewise, at low solar elevation angles the canopy shades the surface, which effectively reduces the shortwave radiation received at the plateau surface by 25% in summer and 40% in winter. However, trees have a higher radiating temperature than the sky and clouds above, which enhances the incoming longwave radiation received at the surface (Wilson and Petzold, 1973), resulting in a net gain of longwave radiation to the plateau surface of 19% in summer and 23% in winter,

compared to the bog surface. The greater net all wave radiation (72%) recieved at the plateau snow surface in winter was largely due to the significantly lower surface albedo at the plateau relative to the bog (Table 4-3). The considerably lower soil temperatures at the plateau, compared to the bog, were attributed primarily to differences in soil moisture rather than shading of the surface by the tree canopy, given the very similar air and surface temperatures measured at the two sites during the snow-free period. The difference in snow-surface temperatures may also be due to the greater loss of radiative energy in the bog, which results in sufficient cooling of the snow surface in winter (Wilson and Petzold, 1973). Other studies (e.g. Moore, 1987; Luetschg and Haeberli, 2005) suggest that snow depth is the dominant factor controlling soil temperature and the depth of freezing in peatlands. Unfortunately, we lack sufficient data to make this conclusion at our site.

It should be noted that the effects of daily interception, absorption and emittance of radiation by trees on reducing or enhancing radiation received at the ground surface depend on the tree species, height of the tree crowns, and canopy distribution and morphology (Lafleur and Adams, 1986). The *Picea mariana* stands of peat plateaus in the High Boreal wetland region are characterised by a low canopy density, low leaf area index, and an open structure, with highly clumped shoots on narrow tree crowns. This enables a high proportion of solar radiation to reach the ground surface compared to stands of other species (Baldocchi *et al*., 2000) or of the same species with greater canopy densities (e.g. Petzold, 1981; Davis *et al*., 1997). Absorption of solar radiation by trunks and branches of a denser canopy would lead to considerably greater longwave flux being emitted to the surface; this difference is more noticeable during the snow-covered than

the snow-free period (Jackson, 1960). Likewise, the ratio of *Qg* to *Q** is largely controlled by LAI and stem area, which both influence shading of the surface, and by surface albedo (Eugster *et al*., 2000). Radiation inputs were the largest energy source for soil thaw, and though the plateau canopy reduced the amount of *Q** received at the ground surface in summer, soil thaw was not inhibited by it. In a denser, more closed canopy, shading may play a more important role in reducing surface temperatures (Camill and Clark, 1998), which would result in slower soil thaw rates and shallower active layers compared to low canopy density black spruce, such as that found at the plateau. The difference in crown density and tree height would therefore have a significant impact on the rate of active layer thaw and the thermal degradation of permafrost, and should therefore be examined in future studies.

The ground heat flux (*Qg*) determines the presence or absence of permafrost. Cumulative *Qg* during the soil thawing/summer period was 54% greater at the plateau than at the bog, largely because the plateau has a much steeper soil temperature gradient than the bog, which is only seasonally frozen, and the bog releases a large fraction of net-all wave radiation (*Q**) as latent heat of evaporation (*Qe*). Despite this, the net annual input of heat to the plateau ground surface from October 2004 to October 2005 was positive (7.6 MJ m^{-2}). A net annual non-positive ground heat flux is assumed necessary for the maintenance and growth of permafrost (Yu *et al*., 2002; Cheng *et al*., 2004). The net annual ground heat flux and annual average soil temperatures at the base of the active layer need to be examined over multiple years, to determine if the plateau is able to support and maintain permafrost under current climate conditions and to predict future

changes in permafrost. These results would have important implications for runoff from the slope, and the water, nutrient and carbon cycling of the basin.

4.6 Figures

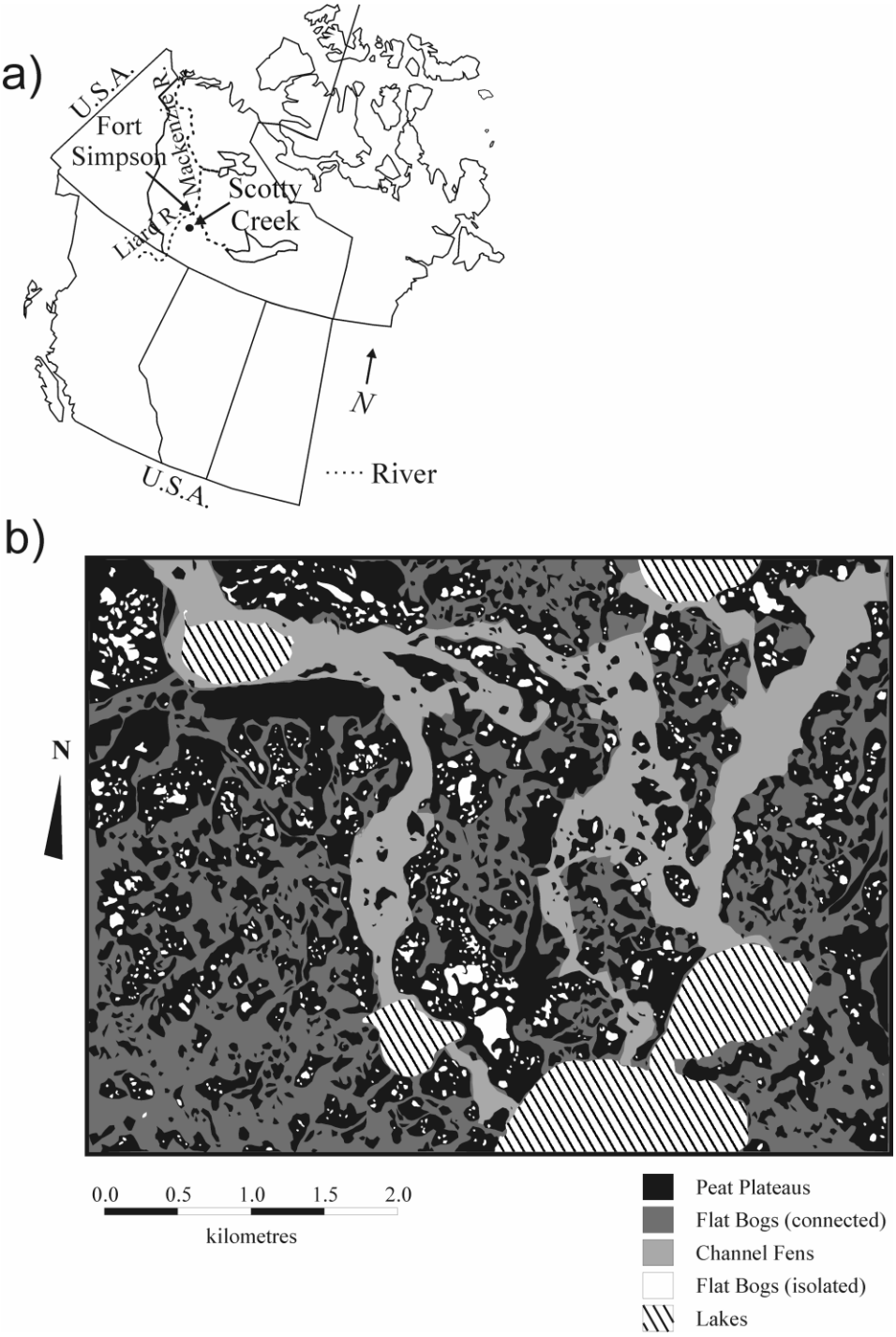

Figure 4-1 a) The location of Scotty Creek within north-western Canada. b) The different land covers of the 22 km^2 peatland complex located in the Scotty Creek basin.

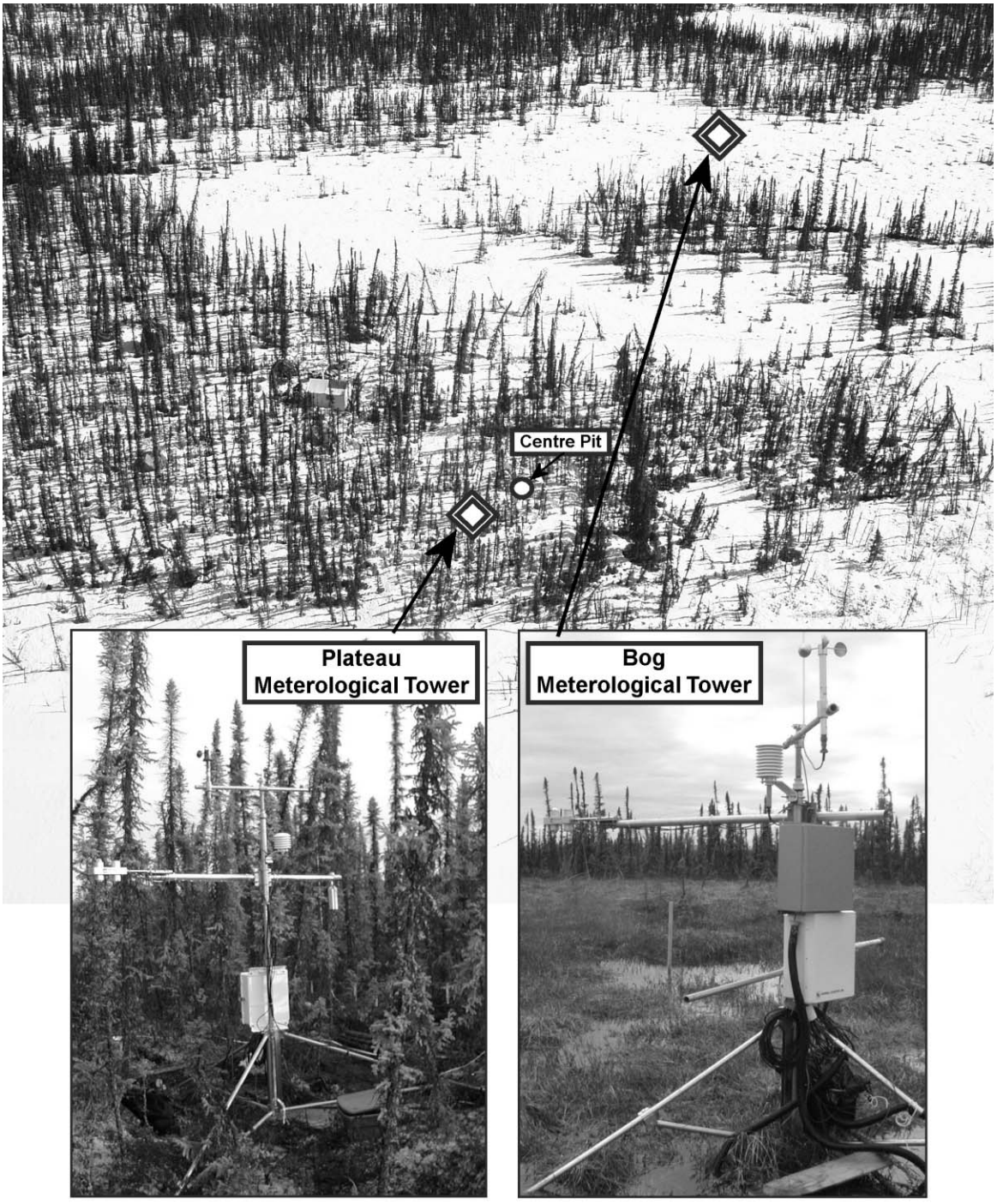

Figure 4-2 Location and instrumentation of the meteorological towers at the peat plateau and flat bog, and the location of Centre soil pit at the peat plateau.

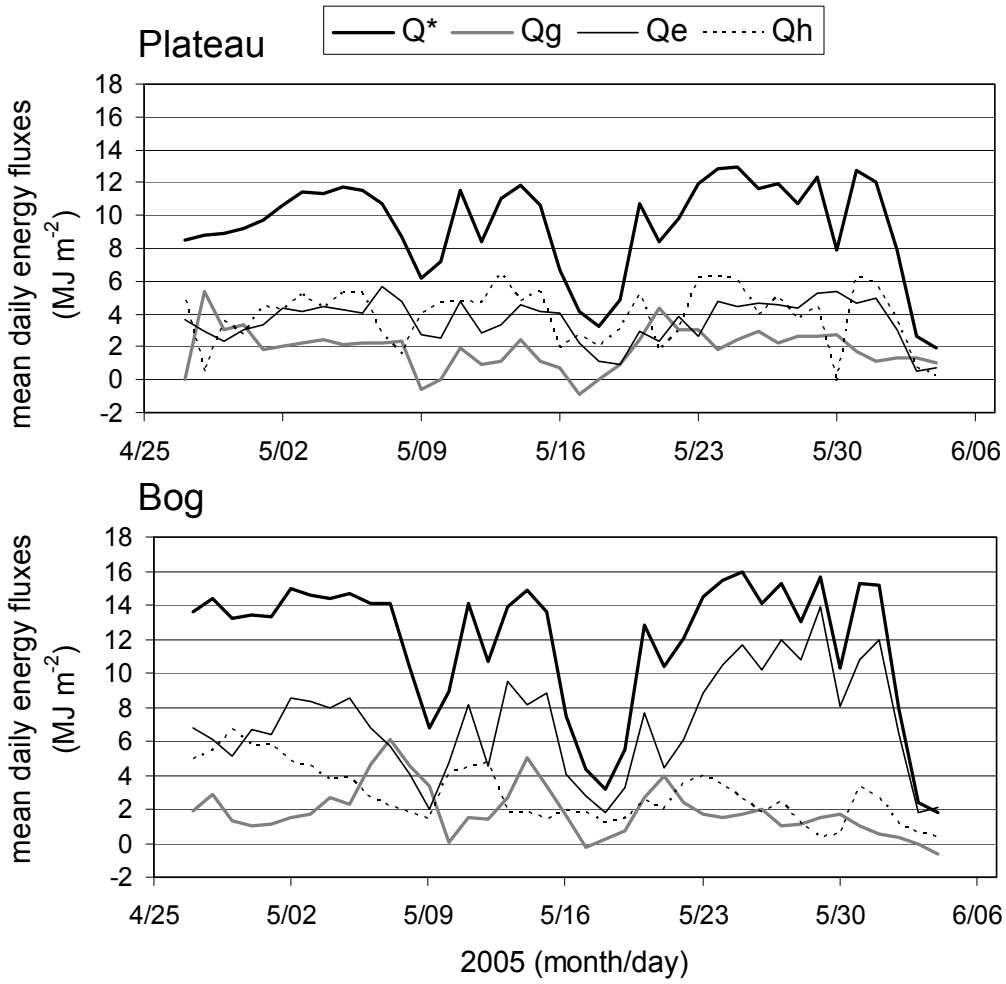

Figure 4-3 Mean daily energy fluxes of the plateau and bog, computed for the 2005 spring field season, from 27 April to 4 June. *Q** represents net all-wave radiation, *Qh*, the sensible heat flux, *Qg*, the ground heat flux and *Qe*, the evaporative latent heat flux. Units were converted from W m^{-2} to MJ m^{-2}.

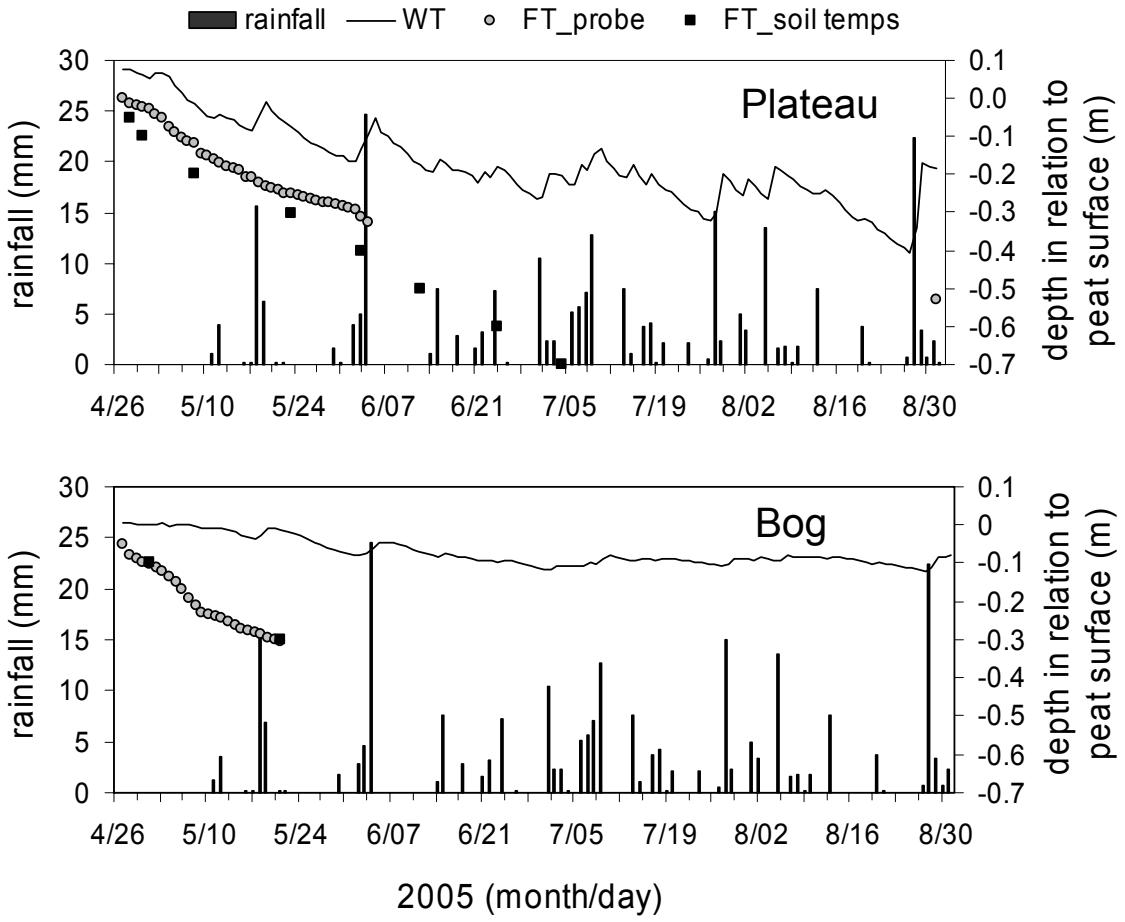

Figure 4-4 Daily rainfall (mm), and water-table (WT) and frost-table (FT) depths (m) measured in relation to the peat surface at the plateau and bog, from 27 April to 31 August, 2005. For comparison, the FT depth (or thawing front depth) according to the soil temperature data at the soil pits (FT_soil temps) is shown with the FT depth measured daily by a frost probe next to the soil pits (FT_probe).

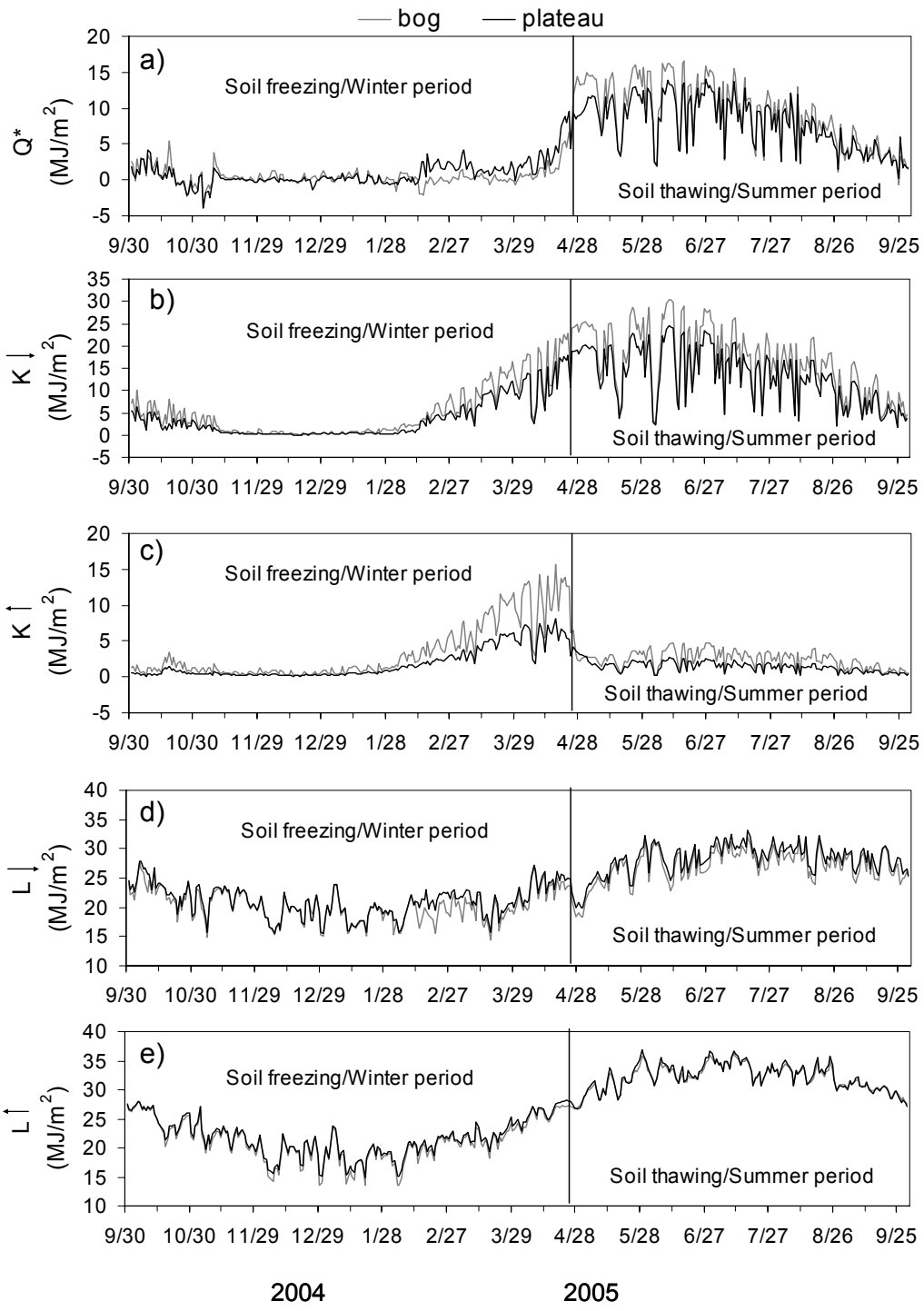

Figure 4-5 Mean daily a) net radiation (Q^*), and b) incoming shortwave ($K\downarrow$), c) outgoing shortwave ($K\uparrow$), d) incoming longwave ($L\downarrow$), and e) outgoing longwave ($L\uparrow$) radiation at the bog and plateau from 1 October 2004 to 30 September 2005. Units were converted from W m^{-2} to MJ m^{-2}. Note that the fluxes have different y-axis scales, in order to better illustrate differences.

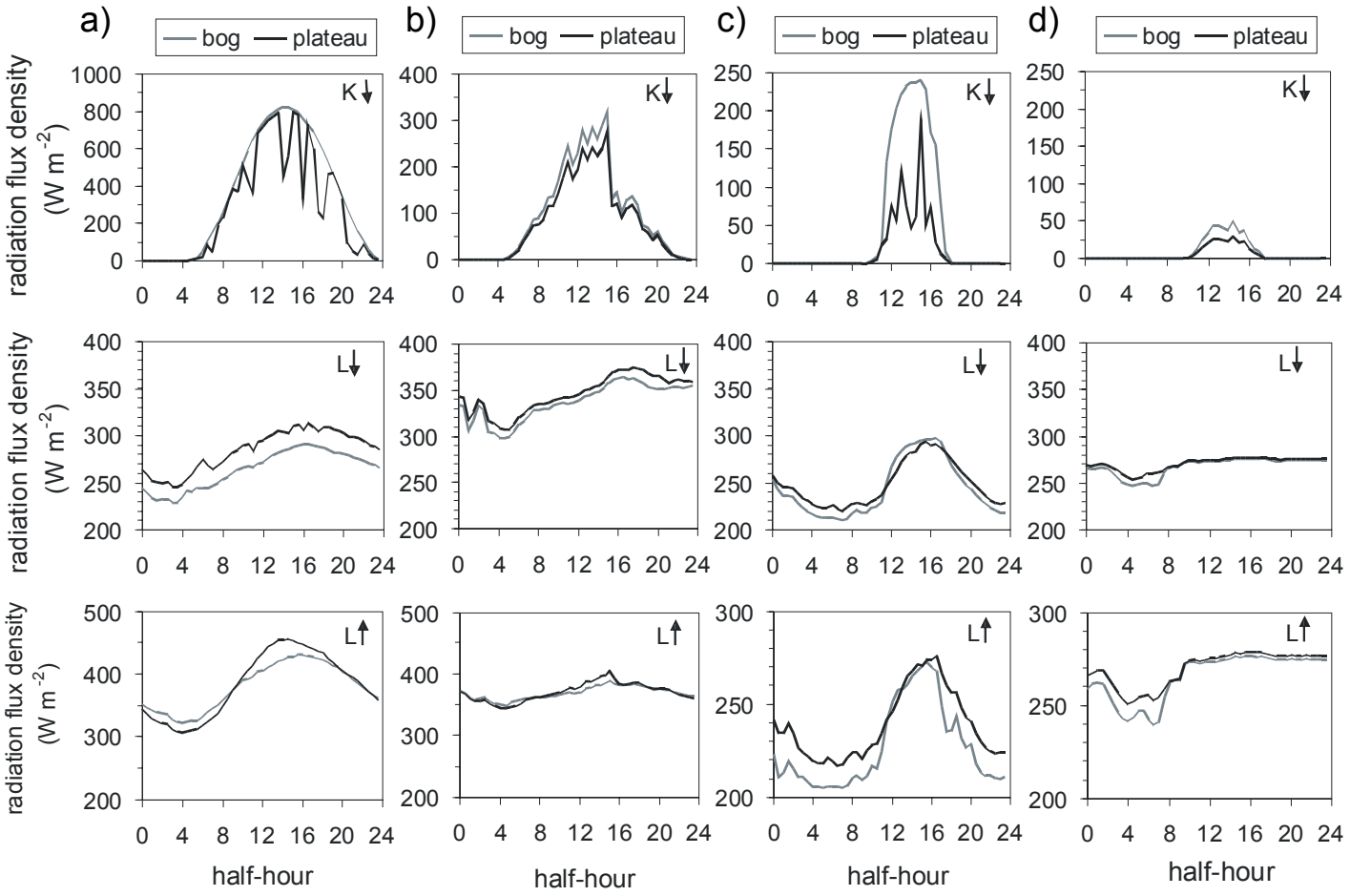

Figure 4-6 Half-hourly radiation flux densities of incoming shortwave radiation (K↓), and incoming (L↓) and outgoing longwave radiation (L↑) for a snow-free bog and plateau surface on a) 11 June (a cloudless day) and b) 14 June (a cloudy day), 2005, and a snow-covered bog and plateau surface on c) 9 November (a cloudless day) and d) 12 November, 2004. Note that the fluxes have different y-axis scales, in order to better illustrate differences.

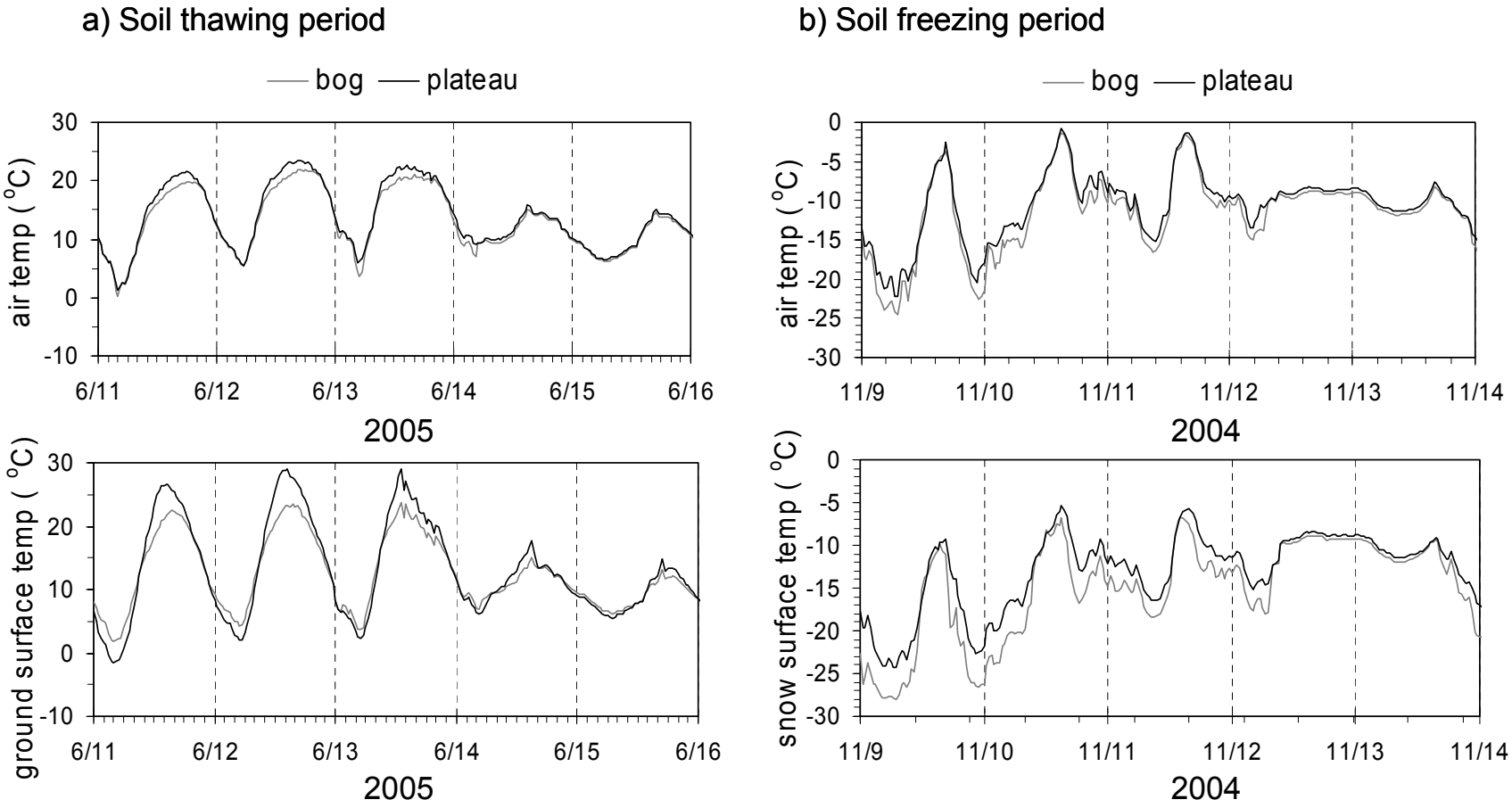

Figure 4-7 Air and surface temperature of the bog and plateau over 5 days during the a) soil thawing period (summer/snow-free ground surface), b) and soil freezing period (winter/snow-covered ground surface).

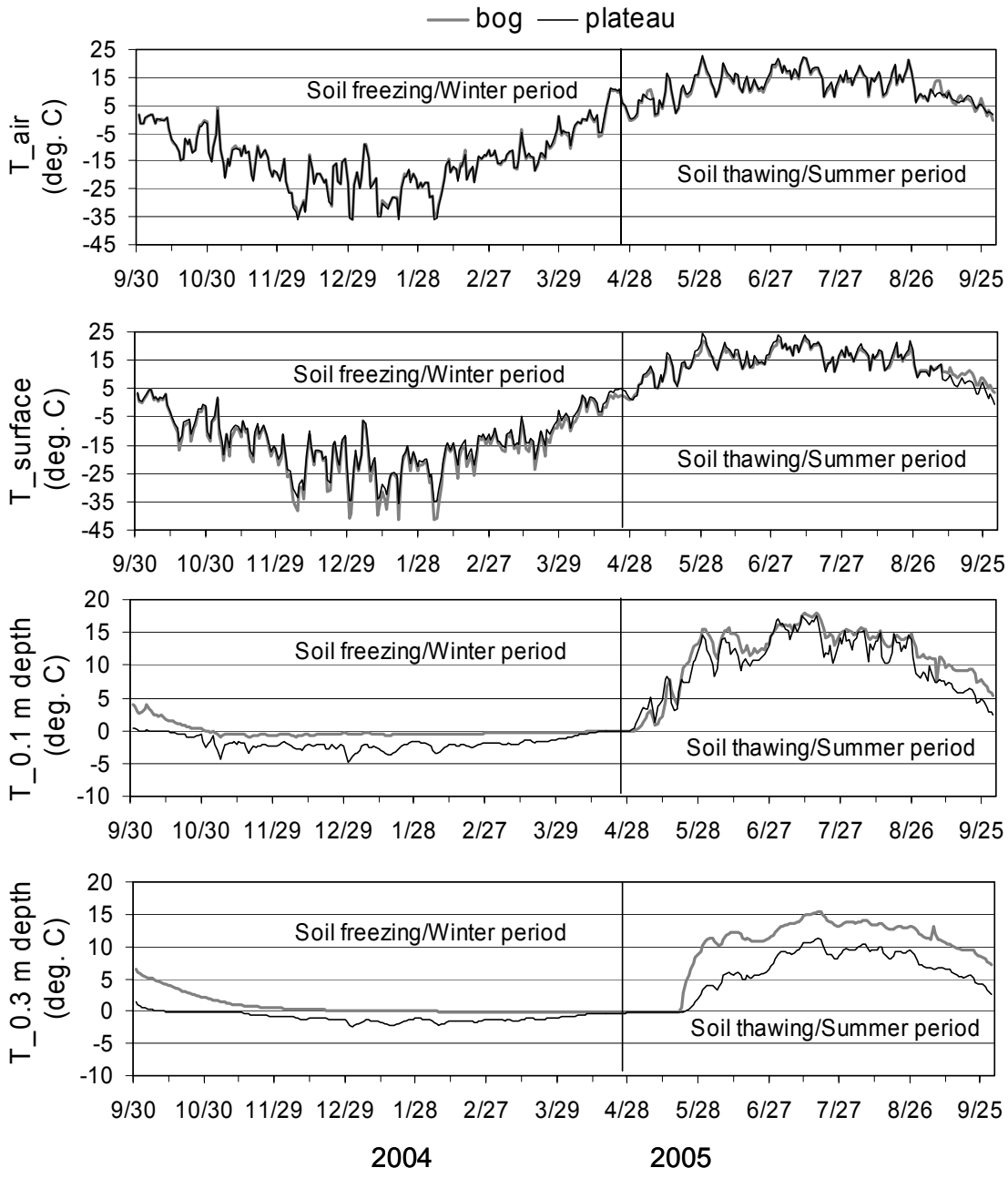

Figure 4-8 Temperature (^{o}C) of the air (T_air), ground surface (T_surface) and soil at depths of 0.1 m (T_0.1) and 0.3 m (T_0.3) at the plateau and bog from 1 October 2004 to 30 September 2005. Note that T_0.1 and T_0.3 have a different y-axis to T_air and T_surface, in order to better illustrate the temperature at these depths. Note that for the most part, the surface is snow-covered during the winter period and snow-free during the summer period.

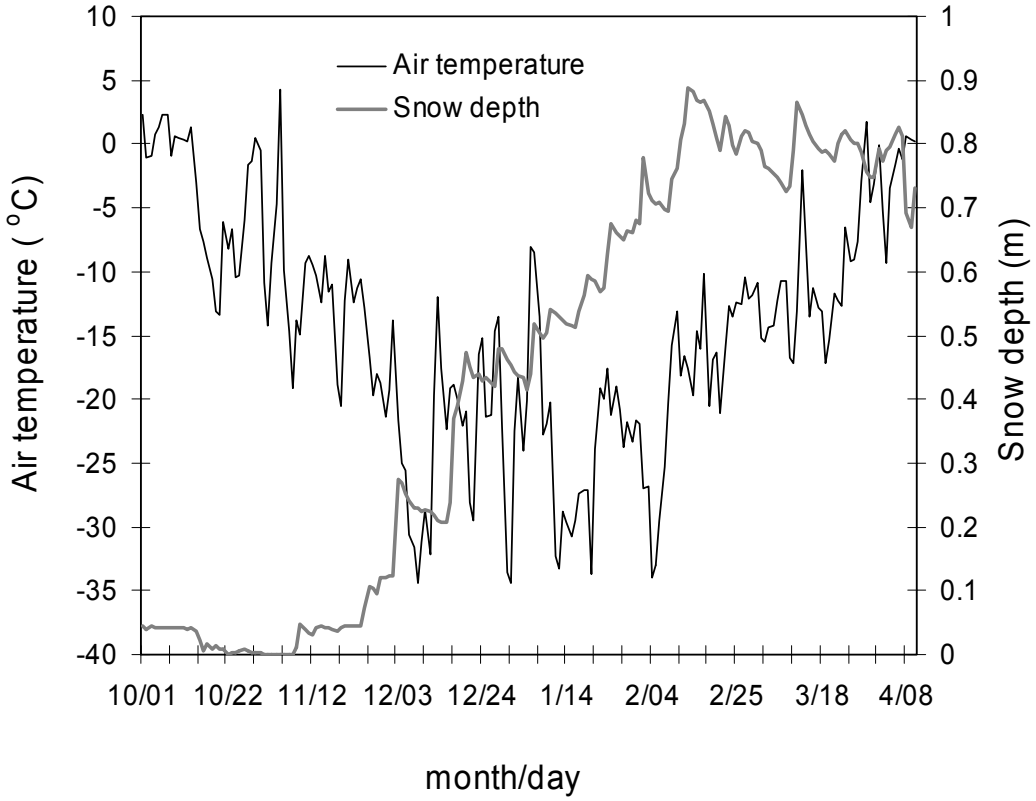

Figure 4-9 Mean daily air temperature and snow depth measured at the peat plateau meteorological tower from 1 October to 10 April (when the height of snow depth occurred).

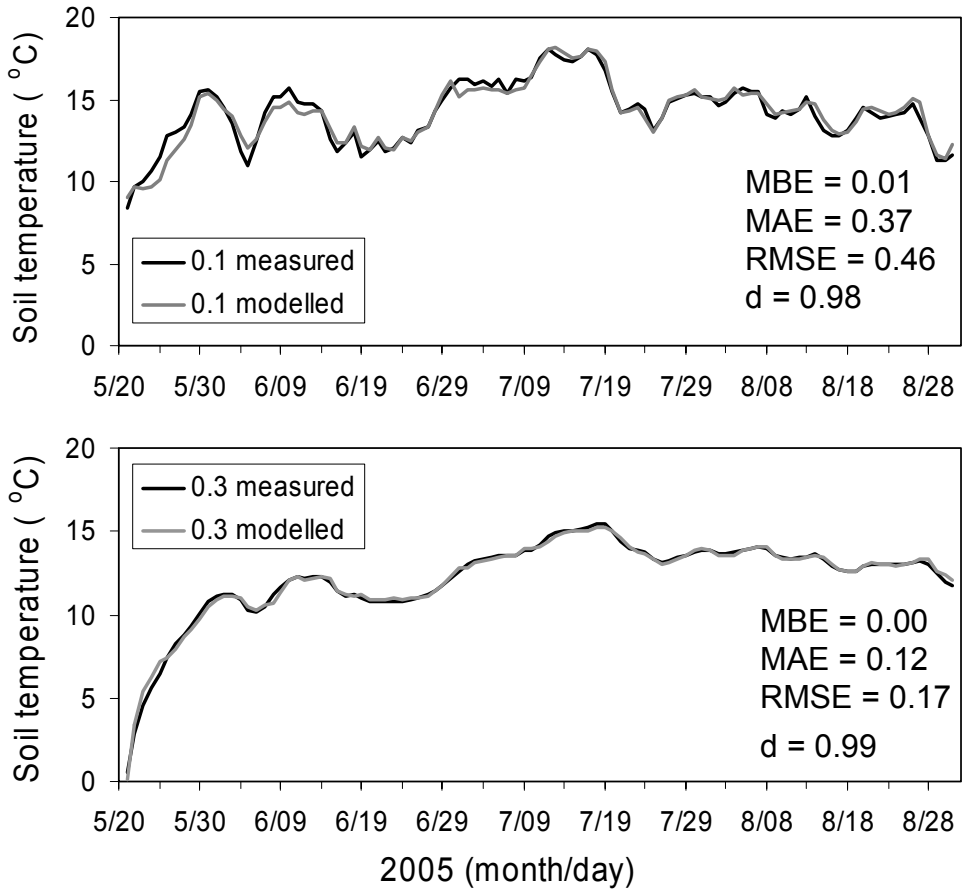

Figure 4-10 Measured and modelled bog soil temperatures at 0.1 and 0.3 m depth from 21 May (when the bog soil pit became frost-free) to 31 August, 2005. Comparative statistics are shown, where perfect agreement between observed and modeled data would result in zero values for mean bias error (MBE), mean absolute error (MAE), and root mean squared error (RMSE), and a value of 1.0 for the index of agreement (d). Units are degrees Celsius, with the exception of d, which is dimensionless.

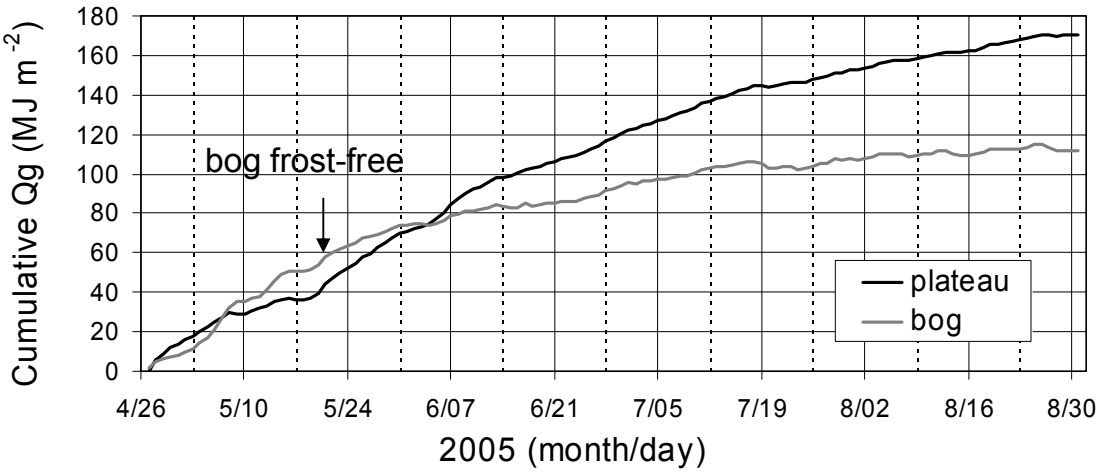

Figure 4-11 Cumulative daily total ground heat flux (*Qg*) computed for the plateau and bog from 27 April to 31 August, 2005. Units were converted from W m^{-2} to MJ m^{-2}. Note that plateau *Qg* was measured from the soil heat flux plate from 13 June to 31 August, 2005.

4.7 Tables

Table 4-1 Soil physical and thermal properties of the upper 0.5 m of the bog and plateau, measured and estimated (after de Vries, 1963) for use in the computation of ground heat flux. Note that the soil column at both land covers was not completely saturated.

Terrain type	Depth (m)	Bulk density (kg m^{-3})	Total porosity	Heat capacity (MJ m^{-3} K^{-1})	Thermal conductivity (W m^{-1} K^{-1})
Plateau	0 - 0.5	135	0.88	3.2[+]	0.37[+]
Bog	0 - 0.5	65	0.94	4.1	0.5[±]

[+] from Hayashi *et al*., 2007

± computed from the best-fit thermal diffusivity value, estimated from the numerical heat conduction model and the heat capacity

Table 4-2 Energy balance of the plateau and bog, computed from 27 April to 4 June 2005. *Q** is net radiation, *Qg* the ground heat flux, *Qe* the latent heat flux, *Qh* the sensible heat flux, and *β* the Bowen ratio (*Qh*/*Qe*). Values were converted from W m^{-2} to MJ m^{-2}. Flux ratios and *β* are unit-less.

Terrain type	Q*	Qg	Qe	Qh	Qg/Q*	Qe/Q*	Qh/Q*	*β*
Plateau	366 ± 37	74 ±14	140 ± 13	152 ± 30	0.20	0.38	0.42	1.1
Bog	461 ± 46	74 ± 37	276 ± 41	111 ± 33	0.16	0.60	0.24	0.4

Table 4-3 Cumulative total and mean daily incoming (↓), outgoing (↑) and net (*) shortwave (*K*), longwave (*L*) and all wave (*Q*) radiation fluxes, and surface albedo (α) at the plateau and bog ground surface, computed for the period of a) soil thawing, from 27 April to 30 September, 2005, and b) soil freezing, from 1 October 2004 to 26 April 2005. Values were converted from W m^{-2} to MJ m^{-2} for the cumulative total fluxes and the mean daily fluxes. The accuracy for the total cumulative fluxes is approximately ± 10%.

a) Soil thawing period Terrain type		K↓	K↑	L↓	L↑	K*	L*	Q*	α
Plateau	total cumulative	2088	226	4424	5053	1861	-629	1232	0.11
	mean daily	13.3	1.4	28.2	32.2	11.9	-4.0	7.8	
Bog	total cumulative	2605	385	4246	5025	2220	-780	1440	0.15
	mean daily	16.6	2.5	27.0	32.0	14.1	-5.0	9.2	
b) Soil freezing period Terrain type		K↓	K↑	L↓	L↑	K*	L*	Q*	α
Plateau	total cumulative	747	387	4375	4537	361	-161	199	0.52
	mean daily	3.6	1.9	21.0	21.8	1.7	-0.8	1.0	
Bog	total cumulative	1048	721	4219	4430	326	-211	116	0.69
	mean daily	5.0	3.5	20.3	21.3	1.6	-1.0	0.6	

Table 4-4 Depth and rate of soil thaw (according to temperature data at the soil pits), cumulative total of the latent heat used to melt ice (*Qi*), the sensible heat storage in the soil column (*Qs*), the heat conducted into and out of the bottom of the soil column (*Qc*), ground heat flux (*Qg*), and average *Qi/Qg* and *Qs/Qg,* computed from 27 April to 4 June, 2005.

Terrain type	Thaw depth (m)	Thaw rate (m day^{-1})	Qi (MJ m^{-2})	Qs (MJ m^{-2})	Qc (MJ m^{-2})	Qg (MJ m^{-2})	Qi/Qg	Qs/Qg
Plateau	0.41	0.011	65.3	7.6	1.5	74.4	0.88	0.10
Bog	0.30	0.011	48.7	20.5	4.7	73.9	0.66	0.28

4.8 Reference List

Aylsworth, J.M., Kettles, I.M. and Todd, B.J., 1993. Peatland distribution in the Fort Simpson area, Northwest Territories with a geophysical study of peatland-permafrost relationships at Antoine Lake. In *Current Research, Part E*. Geological Survey of Canada Paper 93-1E: 141-148.

Baldocchi, D., Kelliher, F.M., Black, T.A. and Jarvis, P. 2000. Climate and vegetation controls on boreal zone energy exchange. *Global Change Biology* 6 (1): 69-83.

Beilman, D.W. and Robinson, S.D. 2003. Peatland permafrost thaw and landform type along a climatic gradient. In *Permafrost*, M. Phillips, S.M. Springman, and L.U. Arenson (eds). Swets and Zeilinger, Liesse; pp. 61-64.

Burgess, M.M. and Smith, S.L. 2000. Shallow ground temperatures. In The physical environment of the Mackenzie Valley, Northwest Territories: a base line for the assessment of environmental change, Dyke LD, Brooks GR (eds). Geological Survey of Canada Bulletin 547: 89-103.

Camill, P. and Clark, J.S. 1998. Climate change disequilibrium of boreal permafrost peatlands caused by local processes. *The American Naturalist* 151(3):207-222.

Camill, P. 2005. Permafrost thaw accelerates in boreal peatlands during late-20th century climate warming. *Climatic Change* 68: 135-152.

Cheng, G., Zhang, J., Sheng, Y. and Chen, J. 2004. Principle for thermal insulation for permafrost protection. *Cold Regions Science and Technology* 40: 71-79.

Davis, R.E., Hardy, J.P., Ni., W., Woodcock, C., McKenzie, J.C., Jordan, R. and Li, X. 1997. Variation of snow cover ablation in the boreal forest – a sensitivity study on the effects of conifer canopy. *Journal of Geophysical Research* 102(D24): 29389-29395.

de Vries, D.A. 1963. Thermal properties of soil. In *Physics of the Plant Environment*, W.R. van Wijk (ed.). North-Holland, Amsterdam; pp. 210-235.

Eugster, W., Rouse, W.R., Pielkesr, R.A., McFadden, J.P., Baldocchi, D.D., Kittel, T.G.F., Chapin III, F.S., Liston, G.E., Vidale, P.L., Vaganov, E. and Chambers, S. 2000. Land-atmosphere energy exchange in Arctic tundra and boreal forest: available data and feedback to climate. *Global Change Biology* 6(1): 84-115.

Gold, L.W. and Lachenbruch, A.H. 1973. Thermal conditions in permafrost: A review of North American literature. *2nd International Conference on Permafrost, North American Contribution*, National Academy of Sciences, Washington, D.C.; 3-23.

Goodison, B.E. 1978. Accuracy of snow samplers for measurement of shallow snowpacks: An Update. In *Proceedings of the 34th Eastern Snow Conference*. Hanover, New Hampshire; pp. 36-49.

Gryning, S-E., Batchvarova, E. and De Bruin, H.A.R. 2001. Energy balance of a sparse coniferous high-latitude forest under winter conditions. *Boundary-Layer Meteorology* 99: 465-488.

Halliwell, D.H. and Rouse, W.R. 1987. Soil heat flux in permafrost: characteristics and accuracy of measurement. *Journal of Climatology* 7: 571-584.

Hayashi, M., Goeller, N., Quinton, W.L. and Wright, N. 2007. A simple heat-conduction method for simulating frost table depth in hydrological models. *Hydrological Processes* 21: 2610-2622

Jackson, C.I. 1960. Estimates of total radiation and albedo in subarctic Canada. *Archives for Meteorology and Geophysics and Bioclimatology, Series B* 10: 193-199.

Jorgenson, M.T., Racine, C.H., Walter, J.C. and Osterkamp, T.E. 2001. Permafrost degradation and ecological changes associated with a warming climate in central Alaska. *Climate Change* 48: 551–579.

Kane, D.L., Hinkel, K.M., Goering, D.J., Hinzman, L.D. and Outcalt, S.I. 2001. Non-conductive heat transfer associated with frozen soils. *Global and Planetary Change* 29: 275-292.

Lachenbruch, A.H. and Marshall, B.V. 1986. Changing climate: geothermal evidence from permafrost in the Alaskan Arctic. *Science* 234: 689-696.

Lafleur P. and Adams, P. 1986. The radiation budget of a subarctic woodland canopy. *Arctic* 39(2): 172-176.

Leblanc, S.G., Chen, J.M. and Kwong, M. 2002. *Tracing Radiation and Architecture of Canopies*, TRAC manual Version 2.1. Natural Resources Canada, Centre for Remote Sensing, Ontario, Canada. 25 pp.

Luetschg, M. and Haeberli, W. 2005. Permafrost evolution in the Swiss Alps in a changing climate and the role of the snow cover. *Norwegian Journal of Geography* 59: 78-83.

Meteorological Service of Canada (MSC) 2005. *National climate data archive of Canada.* Environment Canada: Dorval, Quebec.

Moore, T.R. 1987. Thermal regime of peatlands in subarctic eastern Canada. *Canadian Journal of Earth Sciences* 24: 1352-1359.

National Wetlands Working Group (NWWG) 1988. *Wetlands of Canada: Ecological Land Classification Series, no. 24*. Sustainable Development Branch, Environment Canada, Ottawa, Ontario, and Polyscience Publications Inc., Montreal, Quebec. 452 pp.

Oke, T.R. 1987. Boundary Layer Climates. Routledge, New York. 435 pp.

Osterkamp, T. E. 2005. The recent warming of permafrost in Alaska. *Global and Planetary Change* 49 (3-4): 187-202.

Petzold, D.E. 1981. The radiation balance of melting snow in open boreal forest. *Arctic and Alpine Research* 13(3): 287-293.

Priestley, C.H.B and Taylor, R.J. 1972. On the assessment of surface heat flux and evaporation using large-scale parameters. *Monthly Weather Review* 100(2): 81-92.

Quinton, W.L., Gray, D.M. and Marsh, P. 2000. Subsurface drainage from hummock-covered hillslope in the Arctic tundra. *Journal of Hydrology* 237: 113-125.

Quinton, W.L. and Hayashi, M. 2005. The flow and storage of water in the wetland-dominated central Mackenzie River basin: Recent advances and future directions. In *Prediction in ungauged basins: Approaches for Canada's cold regions*, C. Spence, J.W. Pomeroy and A. Pietroniro (eds). Canadian Water Resources Association, Cambridge Ontario; pp. 45-66.

Rouse, W.R. and Kershaw, K.A. 1971. The effects of burning on the heat and water regimes of lichen-dominated subarctic regimes. *Arctic and Alpine Research* 3(4): 291-304.

Rutter, N.W., Boydell, A.N., Savigny, K.W. and van Everdingen, R.O. 1973. *Terrain evaluation with respect to pipeline construction, Mackenzie pipeline construction: Southern part, Lat. 60^o to 64^{o}N*. Environmental-Social Committee Northern Pipelines, Task force on Northern oil development *Report N. 73-36*, 135 pp., Ottawa, Information Canada Cat. No. R72-10373.

Seppälä, M. 1988. Palsas and related forms. In *Advances in Periglacial Geomorphology*, M.J. Clark (ed.). Wiley, Chichester; pp. 247-278.

Shuttleworth, W. J. 1993. Evaporation. In *Handbook of Hydrology*, Maidment DR (ed). McGraw-Hill, New York; 4.1-4.53.

Slaughter, C.W. and Kane, D.L 1979. Hydrologic role of shallow organic soils in cold climates. In *Canadian hydrology symposium: Proceedings, 79- Cold climate hydrology*, pp. 380-389, National Research Council of Canada, Ottawa, Ontario.

Tarnocai, C. 2006. The effect of climate change on carbon in Canadian peatlands. *Global and Planetary Change* 53: 222-232.

Turetsky, M.R., Wieder, R.K., Vitt, D.H., Evans, R.J. and Scott, K.D. 2007. The disappearance of relict permafrost in boreal north America: Effects on peatland carbon storage and fluxes. *Global Change Biology* 13: 1922–1934.

Vitt, D.H., Halsey, L.A. and Zoltai, S.C. 1994. The bog landforms of Continental Western Canada in relation to climate and permafrost patterns. *Arctic and Alpine Research* 26(1): 1-13.

Willmott, C. J. 1982. Some comments on the evaluation of model performance. *Bulletin of the American Meteorological Society* 63: 1309-1313.

Wilson R.G. and Petzold, D.E. 1973. A solar radiation for sub-arctic woodlands. *Journal of Applied Meteorology* 12: 1259-1266.

Woo, M-K. 1986. Permafrost hydrology in North America. *Atmosphere-Ocean* 24: 201-234.

Woo, M-K. and Heron, R. 1987. Effects of forests on wetland runoff during spring. In *Forest Hydrology and Watershed Management*, Swanson RH, Bernier PY and Woodard PD (eds). IAHS Publication No. 167, IAHS Press, Wallingford; 297-307.

Woo, M-K. and Winter, T.C. 1993. The role of permafrost and seasonal frost in the hydrology of northern wetlands in North America. *Journal of Hydrology* 141: 5-31.

Woo, M-K. and Xia, Z. 1996. Effects of hydrology on the thermal conditions of the active layer. *Nordic Hydrology* 27: 429-448.

Wright, N., Hayashi, M. and Quinton, W.L. 2009. Spatial and temporal variations in active-layer thawing and their implication on runoff generation in peat-covered permafrost terrain. *Water Resources Research*, 45, W05414, doi:10.1029/2008WR006880.

Wright, N., Quinton, W.L. and Hayashi, M. 2008. Hillslope runoff from an ice-cored peat plateau in a discontinuous permafrost basin, Northwest Territories, Canada. *Hydrological Processes* 22: 2816-2828. DOI: 10.1002/hyp.7005.

Yu, S., Jianming, Z., Yongzhi, L. and Jingman, W. 2002. Thermal regime in the embankment of Qinghai-Tibetan Highway in permafrost regions. *Cold Regions Science and Technology* 35: 35-44.

Zoltai, S.C. 1972. Palsas and peat plateaus in central Manitoba and Saskatchewan. *Canadian Journal of Forest Research* 2: 291-302.

Zoltai, S.C. 1993. Cyclic development of permafrost in the peatlands of northwestern Alberta, Canada. *Arctic and Alpine Research* 25: 240-246.

Zoltai, S.C. and Tarnocai, C. 1975. Perennially frozen peatlands in the western Arctic and Subarctic of Canada. *Canadian Journal of Earth Sciences* 12:28-43.

Chapter 5
Conclusions and Future Research Recommendations

5.1 Synthesis and Conclusions

Effective modelling of runoff from wetland-dominated basins in the discontinuous permafrost zone requires an understanding of the physical processes that control runoff generation from peat plateaus, as they are an often dominant land-cover of these basins, provide a major source of water for basin runoff, control basin drainage by affecting flow pathways between wetlands, and are degrading and disappearing from these basins, in response to climate warming. The research presented in this dissertation provides original contributions in the areas of slope-scale runoff generation, soil moisture and soil thaw feedback processes, and vegetation and moisture effects on ground-surface energetics, soil thaw, and the maintenance of permafrost. The first study (Chapter 2) presents one of the few attempts to quantify subsurface runoff from a peat-covered permafrost slope, and is unique in that the amount of water from the melt of ground ice was quantified. The study also demonstrates the utility of the Dupuit-Forchheimer approximation in accurately estimating the timing and magnitude of runoff from peat plateaus. The second study (Chapter 3) provides new scientific insights into the effects of the spatial and temporal variability of soil thaw on subsurface flow on a peat plateau, and demonstrated the usefulness of a simple numerical model of coupled water and heat flow in investigating the complex interplay between subsurface flow and active layer thawing. While the previous two studies are directly related to subsurface flow and runoff generation from a peat plateau, the last study (Chapter 4) is indirectly related. This study

provides a unique comparison of the annual surface energy balance and thermal regimes of a treed permafrost plateau and an adjacent permafrost-free bog, and demonstrates tree canopy, soil moisture and albedo effects on the ground heat flux, and thus gives insight into their effect on soil thaw rates and permafrost maintenance on peat plateaus.

These studies provide valuable energy and water balance data for an understudied and important ecosystem (based on their wide distribution), and can be compared to other peat-covered permafrost slopes across the circumpolar region in order to assess the effects of climate and vegetation on hydrological processes. This is important since there is evidence relating to increased soil temperatures, active-layer thickness and permafrost degradation in northern latitudes. The results of this research provide important insight into the effect these changes might have on future runoff production from peat-covered permafrost slopes and the basins in which they occupy.

The timing and magnitude of runoff from peat-covered permafrost slopes is dependant on the amount of water input (and the amount of water already in storage), the saturated hydraulic conductivity of the soil, and the spatial and temporal variability of thaw depths, given their control on the soil storage capacity. Though soil thaw depths are highly variable across the slope, their distribution is not random. The latter is controlled by soil moisture through its strong influence on thermal conduction, and by canopy cover and ground-cover type (i.e. moss or lichen) through their strong influence on the surface radiation balance and soil moisture. Changes to the soil water budget could therefore have important consequences for subsurface flow from plateaus, which in turn would affect basin drainage.

Increased soil moisture in areas where water converges to frost table depressions often results in ponding during spring, which may expand laterally with time, causing ground surface subsidence and tree fall. The removal of trees from the plateau would have a significant impact on the surface energy balance, by increasing the amount of annual shortwave radiation and reducing the amount of longwave radiation received at the surface. The resulting net increase in energy inputs to the surface would enhance soil thaw rates, which is likely to cause an increase in soil moisture from ice melt. However, the actual amount of ice melt needed to cause a positive feedback on soil thawing rates is dependant on antecedent soil moisture conditions and the ground ice content. The presence of permafrost that is ice-saturated (i.e. has excess ice) is a critical control on the potential increase in active-layer thickness, owing to latent heat effects, and can retard the rate of permafrost degradation. For example, with 50% excess ice, the upper 10 cm of permafrost must be thawed for the active layer to deepen by 5 cm (Mackay, 1970).

Tree fall has also been observed to cause enhanced soil moisture (Iwahana *et al*., 2005). A change in the soil water budget is likely to result in a change in ground surface vegetation from lichen to *Sphagnum* moss, resulting in changes to evapotranspiration and soil thaw rates. However, tree fall and permafrost thaw will not happen uniformly across the slope, given the high spatial variability in thaw depths, so that water is retained in areas with deeper thaw. This has the potential of reducing the magnitude of runoff from the plateau, as the storage capacity within individual depressions increases and the saturated connectivity needed for lateral drainage decreases. Less runoff from the plateau would result in more water going to soil storage, which could further enhance soil thaw rates, but may also result in a shift of net energy partitioning in summer from sensible to

latent heat fluxes. Greater soil water storage and a reduction in runoff from plateaus will likely result in lower basin runoff in the future.

Presently, gauging stations in the southwest/central Northwest Territories, a region dominated by sporadic and discontinuous permafrost, are showing significant increases in mean annual flow, particularly in winter (St. Jacques and Sauchyn, 2009). These increased winter base flows have largely been attributed to increased soil and ground water inputs due to permafrost melting (St. Jacques and Sauchyn, 2009); though increased precipitation may also be a contributing factor (Zhang *et al*., 2000; Woo and Thorne, 2003). This signifies the importance of understanding soil moisture and soil thaw feedbacks on peat plateaus to predict future runoff from these basins.

5.2 Future research needs

A number of remaining research challenges have emerged from the present work.

i.) This study focused on examining the hydrology of a single peat plateau, and thus the question exists as to how representative this plateau is to others in the basin. For example, canopy density and tree height are important controlling factors of net radiation below the canopy. The differences in these forest characteristics can result in large changes in the timing and rate of ablation and melt, active layer thaw (Metcalfe and Buttle, 1995; Hardy *et al*., 1997), and thus runoff generation. Future studies require an examination of the spatial distribution of canopy density over a larger scale, and its effects on radiation inputs and soil thaw. Likewise, the role of *Sphagnum* in controlling the soil moisture and soil thaw distribution on peat plateaus should be further examined.

ii.) The high-resolution mapping of the frost table and use of a simple coupled heat and water flow model provided new insight into the spatial and temporal feedback

between soil thawing and subsurface flow. To further advance our understanding of flow processes in the active layer, depth-dependant hydraulic conductivity and improved parameterization of water storage and redistribution needs to be incorporated into the model. Models such as this could provide an effective tool for exploring critical thresholds of permafrost thaw, as well as exploring suitable means to scale up runoff from a single plateau to a population of plateaus, which is needed to parameterize basin runoff models. For example, the results of this research show that the frost-table topography controls runoff, and therefore the spatial distribution of runoff rates must be controlled by the distribution of frost-table depths. This suggests that the distribution of plateau subsurface runoff could be derived from readily obtainable frost-table data, in order to derive the range of flow contributions from a population of plateaus. However, though the depth of the frost table may be a good indicator of runoff, as it is the lowest boundary of the saturated layer; runoff is also controlled by water input, antecedent moisture conditions and the saturated hydraulic conductivity-depth distribution. Model simulations could help to determine the conditions in which it can be assumed that the runoff distribution is the same as the frost-table distribution, for the purpose of up-scaling runoff. To begin with, future simulations should explore the depth distribution of saturated hydraulic conductivity and examine its effect on subsurface flow and runoff over a range of rainfall and antecedent moisture conditions.

iii.) The aim of this research was to improve understanding of the physical processes governing runoff generation from peat-covered permafrost slopes, in order to guide development of a runoff model for wetland-dominated basins in the discontinuous permafrost zone. Despite the inability of this study to develop such a model, a significant

contribution has been made in its pursuit. Modelling basin runoff, however, requires an improved understanding of the cycling of water within the other major land-cover types of the basin (e.g. flat bog and channel fen), the hydrological connectivity between these cover-types and peat plateaus, and how these processes vary between snowmelt and freeze-up, as the moisture supply and degree of thaw vary. Likewise, the hydrological function and the position of the land-covers within the basin also need to be considered when further elucidating the hydrological response of basins to permafrost thaw and degradation (Rouse, 2000; Metcalfe and Buttle, 2001).

iv.) This research presents one of very few studies that have examined the radiation and energy budgets of a peat plateau, which is critical for understanding the peatland-permafrost relationship and the potential impact of climate warming on permafrost peatlands. One interesting result of this research is that the plateau has a positive annual ground heat flux. The inter-annual variations in soil temperature and ground heat flux of the peat plateau are currently being examined as part of an ongoing study to determine how the positive net energy balance affects soil thaw rates and the presence of permafrost on the peat plateau.

5.3 Reference List

Hardy, J., Davis, R., Jordan, R., Li, X., Woodcock, C., Ni, W., and McKenzie, J. 1997. Snow ablation modeling at the stand scale in a boreal jack pine forest. *Journal of Geophysical Research* 102 (N24): 29,397-29,406.

Iwahana G.T., Machimura T., Kobayashi Y., Fedorov A.N., Konstantinov P.Y. and Fukuda M., 2005. Influence of forest clear-cutting on the thermal and hydrological regime of the active layer near Yakutsk, eastern Siberia. J. *Geophys. Res*., 110, G02004, doi:10.1029/2005JG00039.

Mackay, J.R. 1970. Disturbances to the tundra and forest environment of the western Arctic. *Canadian Geotechnical Journal* 7: 420-432.

Metcalfe, R.A. and Buttle, J.M. 1995. Controls on canopy structure on snowmelt rates in the boreal forest. *Proceedings of the 52nd annual Eastern Snow Conferences*, 249-257.

Metcalfe, R.A. and Buttle, J.M. 2001. Soil partitioning and surface store controls on spring runoff from a boreal forest peatland basin in north-central Manitoba, Canada. *Hydrological Processes* 15: 2305-2324.

Rouse, W.R. 2000. The energy and water balance of high-latitude wetlands: controls and extrapolation. *Global Change Biology* 6(1): 59-68.

St. Jacques, J-M. and Sauchyn, D.J. 2009. Increasing winter baseflow and mean annual streamflow from possible permafrost thawing in the Northwest Territories, Canada. *Geophysical Research Letters* 36, L01401, doi: 10.1029/2008GL035822.

Woo, M.-K. and Thorne, R. 2003. Streamflow in the Mackenzie Basin, Canada. *Arctic* 56: 328-340.

Zhang, X., Vincent, L.A., Hogg, W.D. and Niitsoo, A. 2000. Temperature and precipitation trends in Canada during the 20th Century. *Atmosphere-Ocean* 38: 395-429.

Appendices

Appendix 1: Dupuit-Forchheimer approximation of hillslope flow

Hillslope flow in a uniform material bounded by an impermeable sloping surface (e.g. permafrost table) can be modeled using the Dupuit-Forchheimer approximation (Childs, 1971). When the flow is driven by constant recharge flux r (m s^{-1}), the flow equation is given by (McEnroe, 1993, Eq. 9)

$$rx = Ky\left(\tan\beta - \frac{dy}{dx}\right)\cos^2\beta \tag{1.A1}$$

where K (m s^{-1}) is hydraulic conductivity, y (m) is the saturated thickness (i.e. vertical distance between the water table and the impermeable boundary), β is the slope angle, and x (m) is the horizontal distance from the top of the slope (i.e. drainage divide). Suppose that two water table wells are located on a slope transect at x_1 and x_2. Integrating Eq. (1.A1) from $x = x_1$ to $x = x_2$ yields:

$$\frac{r(x_2^{\,2} - x_1^{\,2})}{2\cos^2\beta} = K\tan\beta\int_{x1}^{x2} y(x)dx - K\frac{y_2^{\,2} - y_1^{\,2}}{2}. \tag{1.A2}$$

This can be written as:

$$\frac{rx_m}{\cos^2\beta} = K\tan\beta y_m - \frac{K(y_2^{\,2} - y_1^{\,2})}{2(x_2 - x_1)} \tag{1.A3}$$

where $x_m = \frac{x_1 + x_2}{2}$ and $y_m = \frac{1}{x_2 - x_1}\int_{x1}^{x2} y(x)dx$ represent the mean values of x and y, respectively, in the interval $x_1 < x < x_2$. To simplify Eq. (1.A3), we approximate y_m by an arithmetic mean of the two end values, $y_m \cong (y_1 + y_2) / 2$, and recall the definition of the slope angle,

$$\tan\beta = (\zeta_{f2} - \zeta_{f1}) / (x_1 - x_2) \tag{1.A4}$$

where ζ_{f1} and ζ_{f2} are the elevation of the frost table (m) at x_1 and x_2, respectively. It follows from Eq. (1.A3) that:

$$\begin{aligned} \frac{rx_m}{\cos^2\beta} &= K\frac{(\zeta_{f1} - \zeta_{f2})(y_2 + y_1)}{2(x_2 - x_1)} - \frac{K(y_2 - y_1)(y_2 + y_1)}{2(x_2 - x_1)} \\ &= K\frac{y_2 + y_1}{2}\frac{(\zeta_{f1} + y_1) - (\zeta_{f2} + y_2)}{x_2 - x_1} \end{aligned} \tag{1.A5}$$

Noting that water-table elevation h (m) is given by $h = \zeta_f + y$, and that $\cos^2\beta \cong 1$ for gentle slopes (e.g. $\beta < 5$ °), such as the slope of the peat plateau, Eq. (1.A5) reduces to:

$$r = -\frac{Ky_m}{x_m}\frac{h_2 - h_1}{x_2 - x_1} \tag{1.A6}$$

This equation can be used to estimate the rate of water input to a hillslope from the water-table elevation (i.e. hydraulic head) measured in two wells on the hillslope.

References

Childs, E.C. 1971. Drainage of groundwater resting on a sloping bed. *Water Resources Research* 7: 1256-1263.

McEnroe, B.M. 1993. Maximum saturated depth over landfill liner. *Journal of Environmental Engineering* 109: 262-270.

Appendix 2: One-dimensional sensible heat transport into and out of the bog soil column

The one-dimensional conduction of heat through a soil body in non-steady state conditions is described by combining the Fourier equation with the continuity equation (Hillel, 1998; p.314):

$$\frac{\partial T}{\partial t} = -D\frac{\partial^2 T}{\partial z^2} \tag{2.A1}$$

where $\frac{\partial T}{\partial t}$ is the time rate of temperature change (K s^{-1}), $\frac{\partial^2 T}{\partial z^2}$ is the temperature gradient in the vertical direction representing soil depth (z = 0 being the soil surface), and D is the thermal diffusivity of the soil (m^2 s^{-1}) equal to the soil thermal conductivity divided by the soil heat capacity (λ/C).

The Taylor series was used to find a one dimensional numerical approximation of the first and second derivatives that appear in Fourier's conductivity Eq. (2.A1). The approximation for the first derivative following Ames (1992) is

$$\frac{\partial T}{\partial t}(z_i, t_n) = \frac{T_i^{n+1} - T_i^n}{\Delta t} + e \tag{2.A2}$$

where depth (z) is determined at points z_i = iΔz, t_n = nΔt, for $0 \le i \le NZ$, $0 \le n \le NT$ (where NZ is the number of discrete depth points and NT is the number of discrete time points). The numerical solution of $T(z_i, t_n)$ at $z = z_i$, $t = t_n$ is denoted as T_i^n, using the subscript for the spatial step and the superscript for the time step. The value e is the error in this approximation equal to:

$$e = -\frac{\Delta t}{\alpha}\frac{\partial^2 T}{\partial t^2}(z,t) - \frac{\Delta t^2}{6}\frac{\partial^3 T}{\partial t^3}(x,t)\ldots. \tag{2.A3}$$

The approximation for the second derivative following Ames (1992) is

$$\frac{\partial^2 T}{\partial t^2}(z_i, t_n) = \frac{T_{i-1}^n - 2T_i^n + T_{i+1}^n}{\Delta z^2} + e. \quad (2.A4)$$

The forward-differencing approximation to Fourier's conductivity Eq. (2.A1), in a non-steady temperature regime is therefore

$$\frac{T_i^{n+1} - T_i^n}{\Delta t} = \alpha \frac{[T_{i-1}^n - 2T_i^n + T_{i+1}^n]}{\Delta z^2} \quad (2.A5)$$

(Ames, 1992). Rearranging this equation to calculate the new value T_i^{n+1} from the three current values gives:

$$T_t^{n+1} = T_i^n + r[T_{i-1}^n - 2T_i^n + T_{i+1}^n] \quad (2.A6)$$

where $r = \alpha \frac{\Delta t}{\Delta z^2}$. In other words, the temperature regime at the next time step and at a depth point *i*, is proportional to the summation of the temperatures at the current time step.

To model heat transport at the bog, specified temperature boundaries were applied to the top and bottom of the model. The upper boundary condition was set over time to be dependant on input values of mean half-hourly ground surface temperature. The lower boundary temperatures were approximated by choosing the boundary deep enough in the soil (5 m) that the temperatures would not measurably change during the modelling period. The lower boundary temperatures were set to an arbitrary temperature of 1 ^{o}C.

The model was run at a time-step (Δt) of 1800 s and the depth-step (Δz) was set to 0.025 m to satisfy the stability criterion ($D^*\Delta t/(\Delta z)^2 < 0.5$). Model output was half-hourly.

References

Ames, W.F., 1992. *Numerical Methods for Partial Differential Equations, 3rd ed*. Academic Press, San Diego. 451 pp.

Hillel, D. 1998. *Environmental Soil Physics*. Academic Press, New York. 771 pp.